

Search for double beta decay of ^{130}Te to the 0^+ states of ^{130}Xe with the CUORE experiment

PhD Candidate
G. Fantini^{1,2}

Advisors
C. Bucci²
C.Tomei³

¹ Gran Sasso Science Institute, L'Aquila I-67100, Italy

² INFN - Laboratori Nazionali del Gran Sasso, Assergi (L'Aquila), I-67100, Italy

³ INFN - Sezione di Roma, Roma, I-00185, Italy

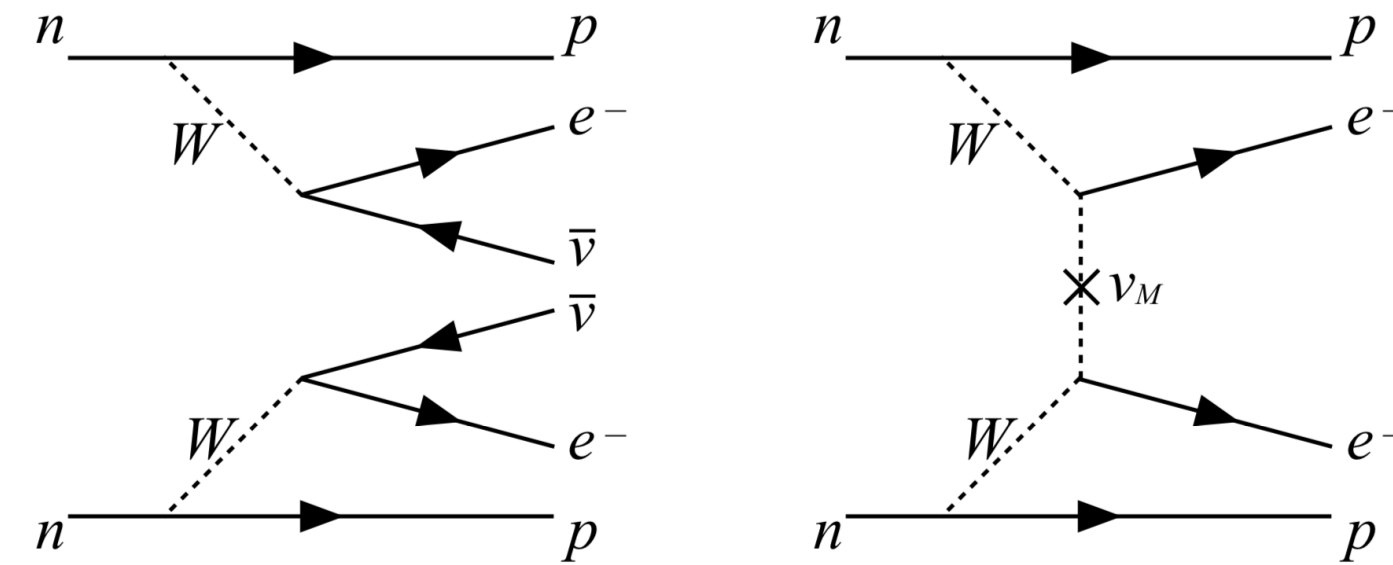
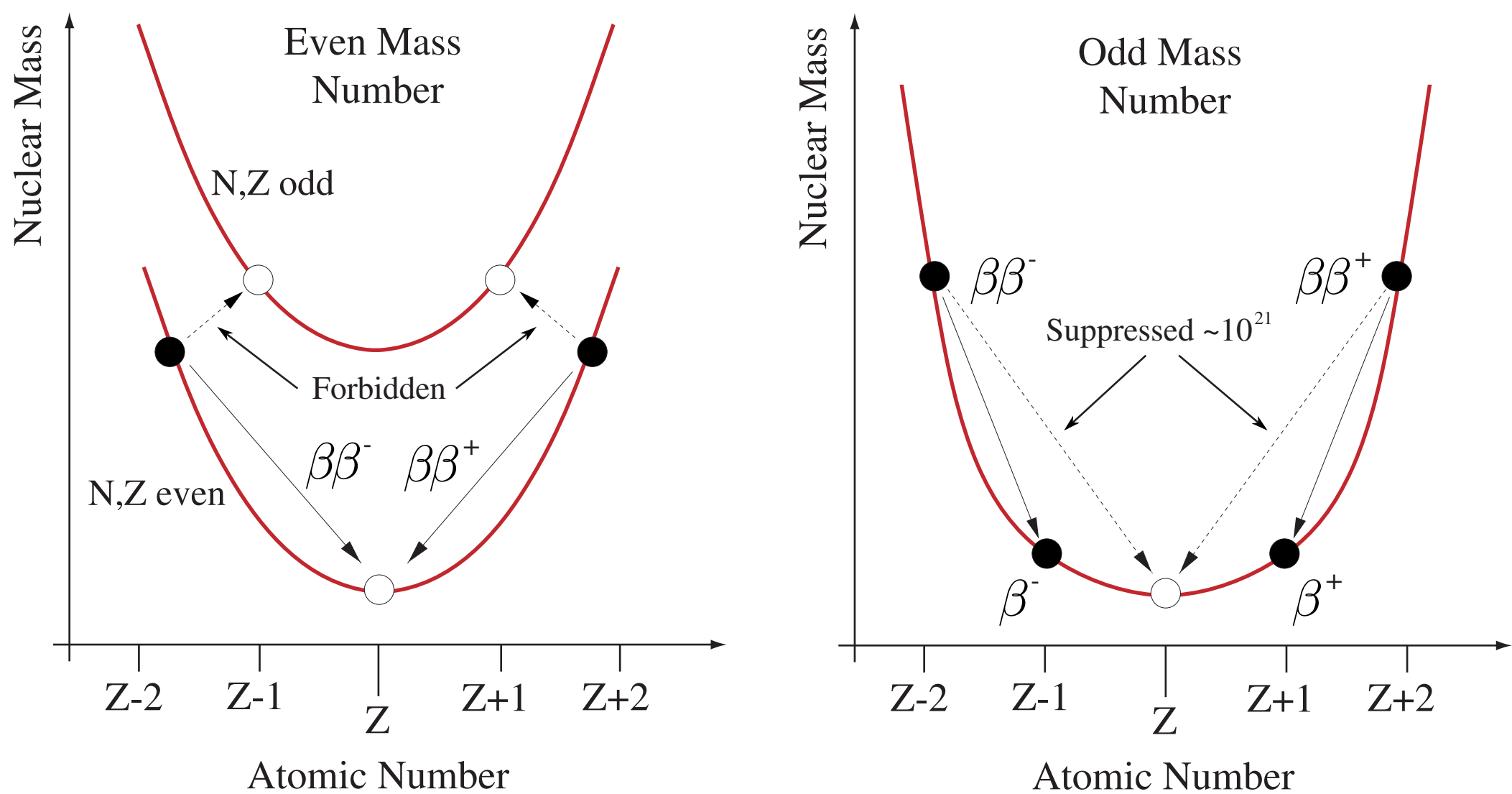
Outline

- Introduction
- The CUORE experiment
 - Operating principles
 - Data processing
 - Detector characterization
- Ground state $0\nu\beta\beta$ decay search
- Excited state searches

Introduction

Double Beta Decay

$$(A, Z) \rightarrow (A, Z+2) + 2e^- (+X)$$



$$X = 2\bar{\nu}_e$$

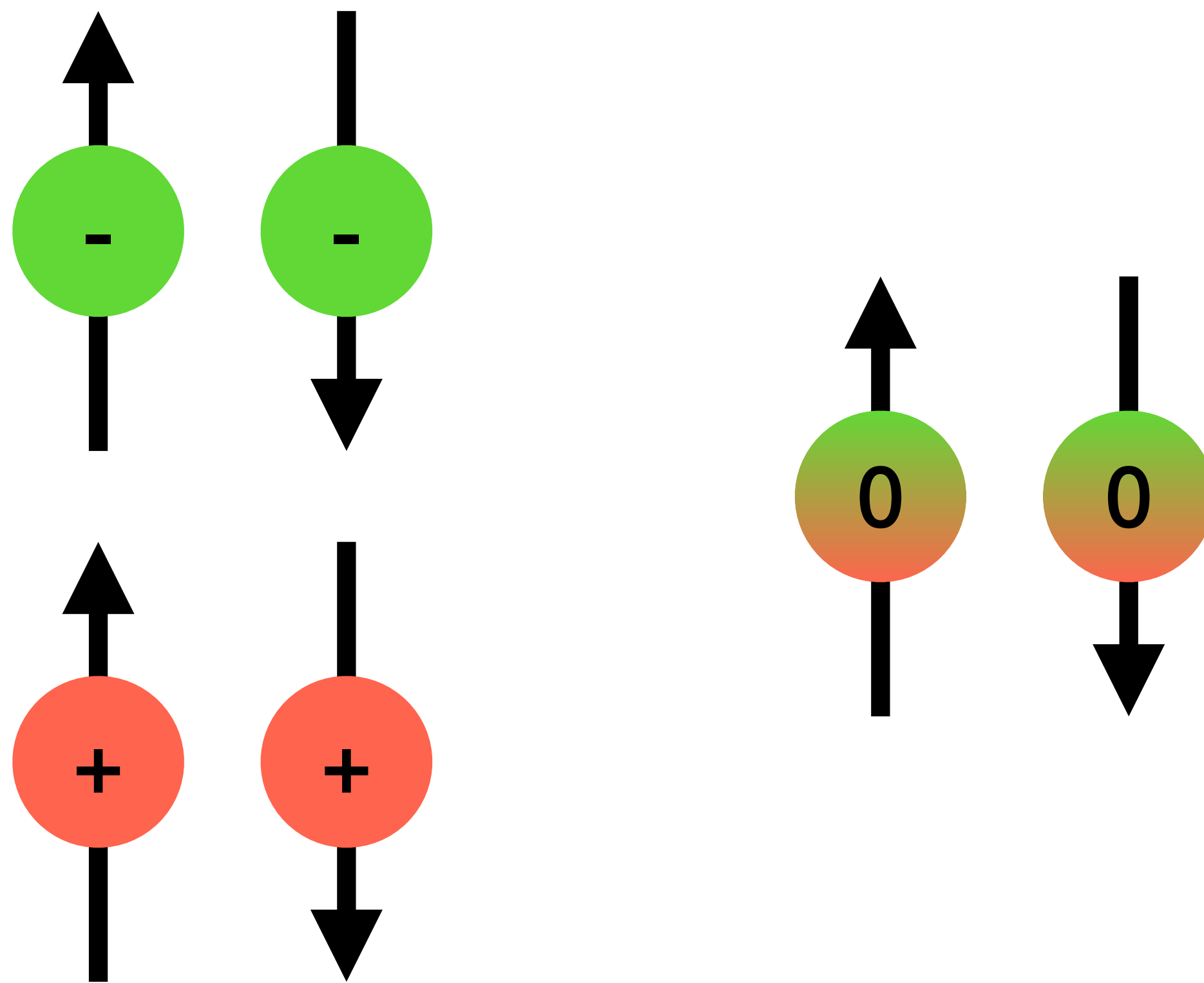
- Allowed within the Standard Model
- 2nd order process
- observed in 12 isotopes

$$X = \emptyset$$

- Beyond Standard Model
- Majorana nature of neutrinos
- Lepton number violation

Introduction

Majorana neutrinos



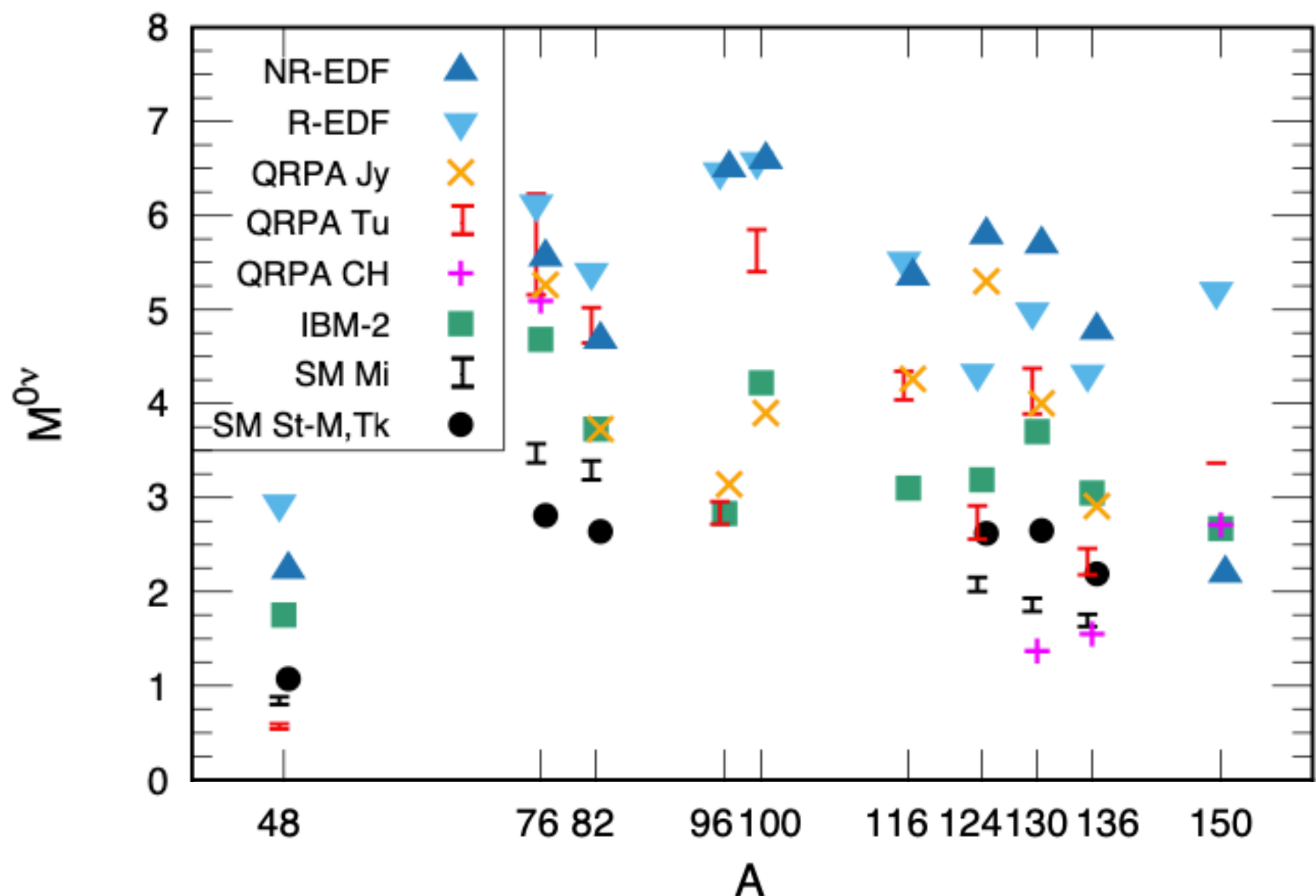
Majorana

- Vanishing internal quantum numbers (lepton number)
- Their own anti-particles
- Neutrino mass generation mechanism
- Mediate neutrino-less double beta decay
- Leptogenesis

Introduction

Neutrinoless Double Beta Decay

$$\langle m_{\beta\beta} \rangle = \left| \sum_i U_{ei}^2 m_i \right|$$

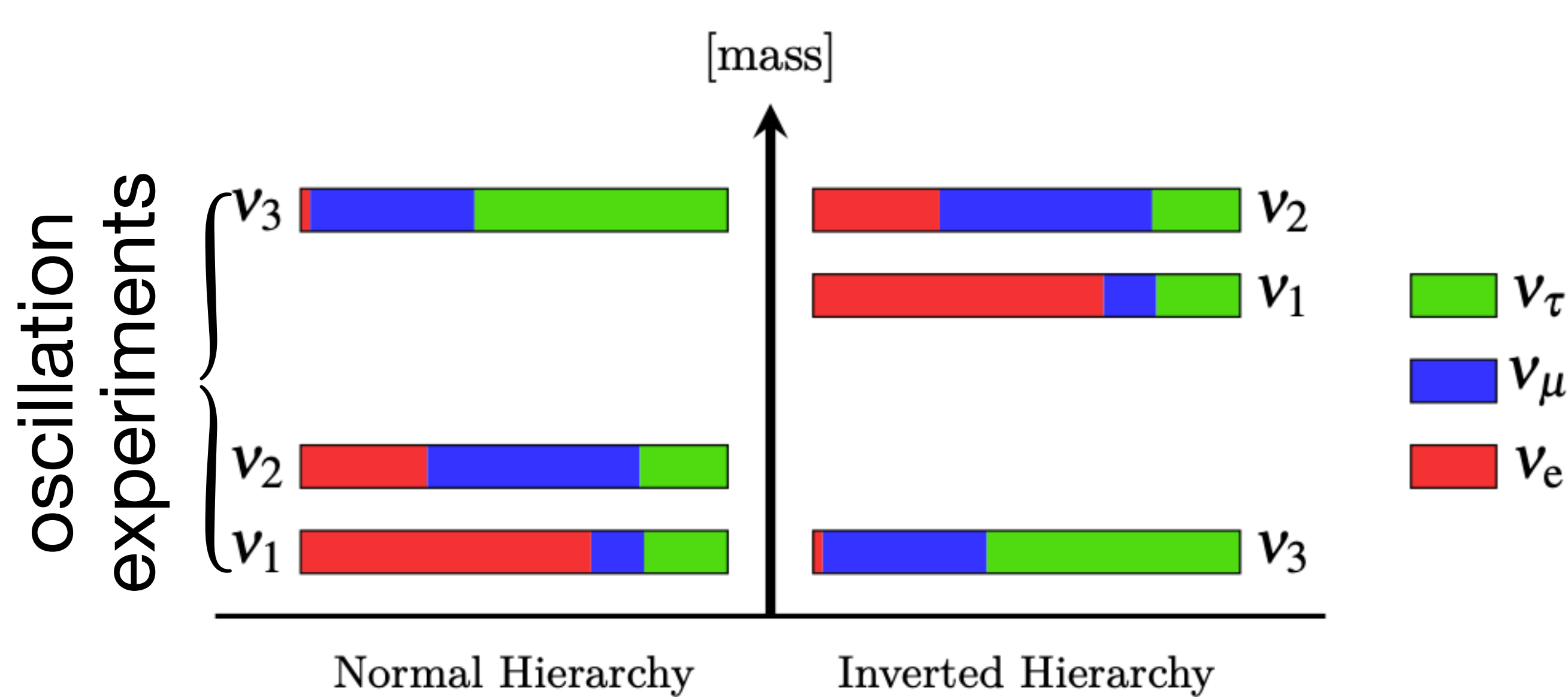


$$\Gamma_{0\nu} = G_{0\nu} g_A^4 |M_{0\nu}|^2 \frac{\langle m_{\beta\beta} \rangle^2}{m_e^2}$$

- $G_{0\nu}$ phase space factor
(well known, small uncertainty)
- Nuclear Matrix Element (NME)
(model dependence, large uncertainty)
- Effective Majorana mass
(unknown)

[J.Engel, J.Menéndez, Rep. Prog. Phys. 80, 4 (2017)]

Introduction



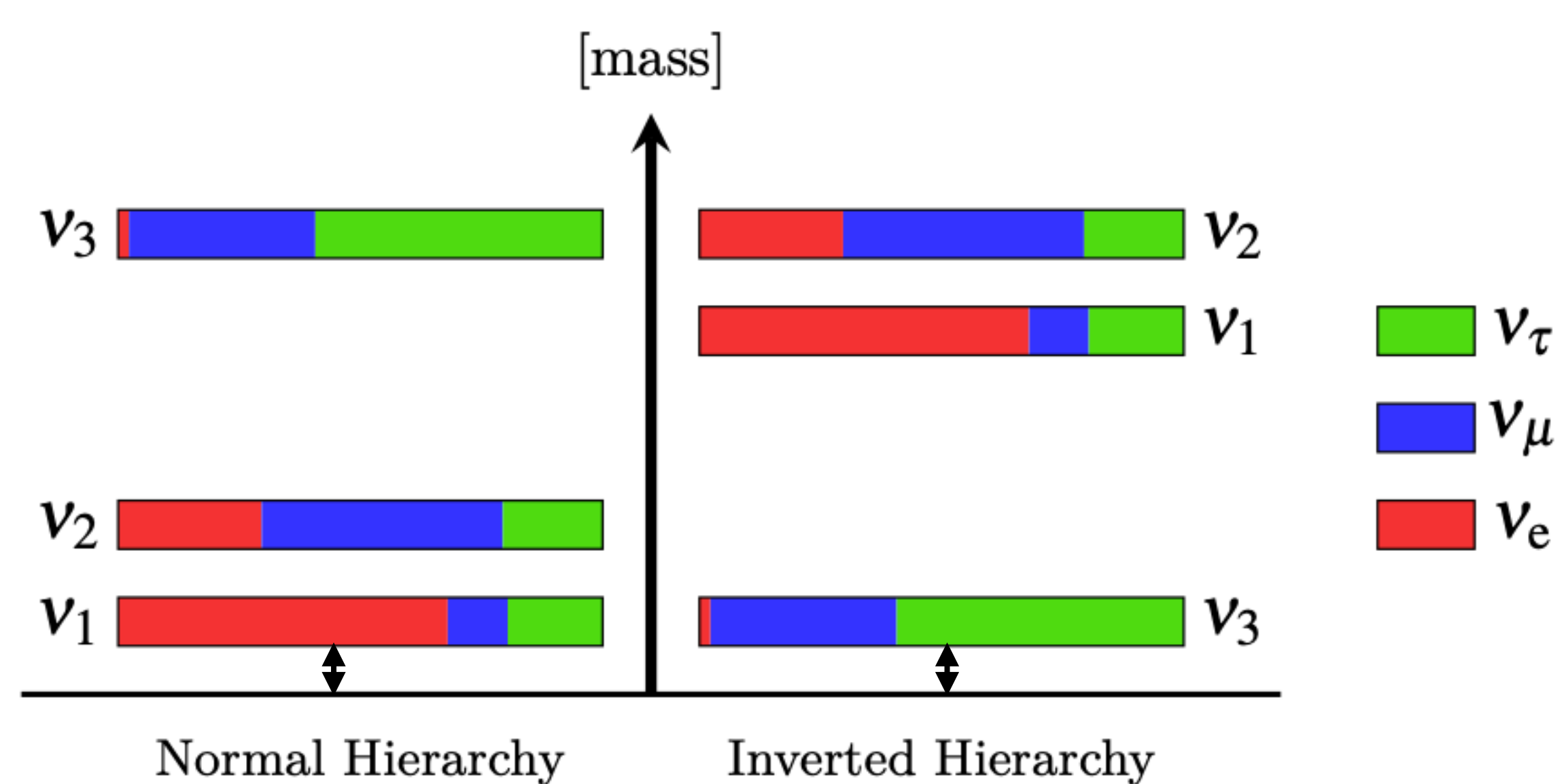
[G. Fantini, A. Gallo Rosso, F. Vissani, V. Zema, Adv. Ser. Direct. High Energy Phys. 28 (2018) 37-119]

$$\nu_{f,L} = \sum_{j=1}^3 U_{l,j} \nu_{j,L}$$

- Pontecorvo-Maki-Nakagawa-Sakata mixing matrix
- 3 mixing angles
- 1 (Dirac) / 3 (Majorana) CP violating phases

Introduction

cosmology
 β decay
 $0\nu\beta\beta$



[G. Fantini, A. Gallo Rosso, F. Vissani, V. Zema, Adv. Ser. Direct. High Energy Phys. 28 (2018) 37-119]

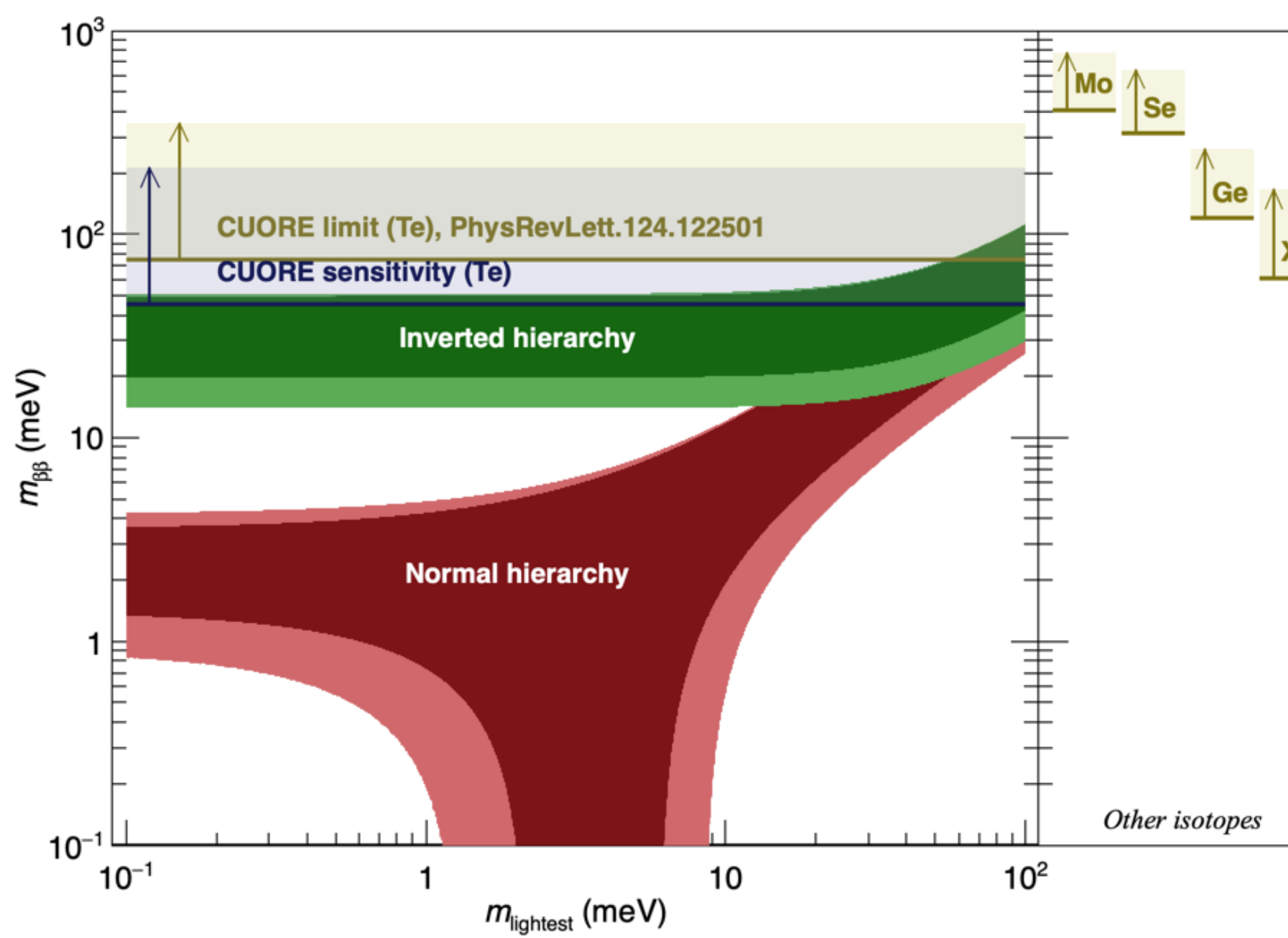
$$\nu_{f,L} = \sum_{j=1}^3 U_{l,j} \nu_{j,L}$$

- Pontecorvo-Maki-Nakagawa-Sakata mixing matrix
- 3 mixing angles
- 1 (Dirac) / 3 (Majorana) CP violating phases

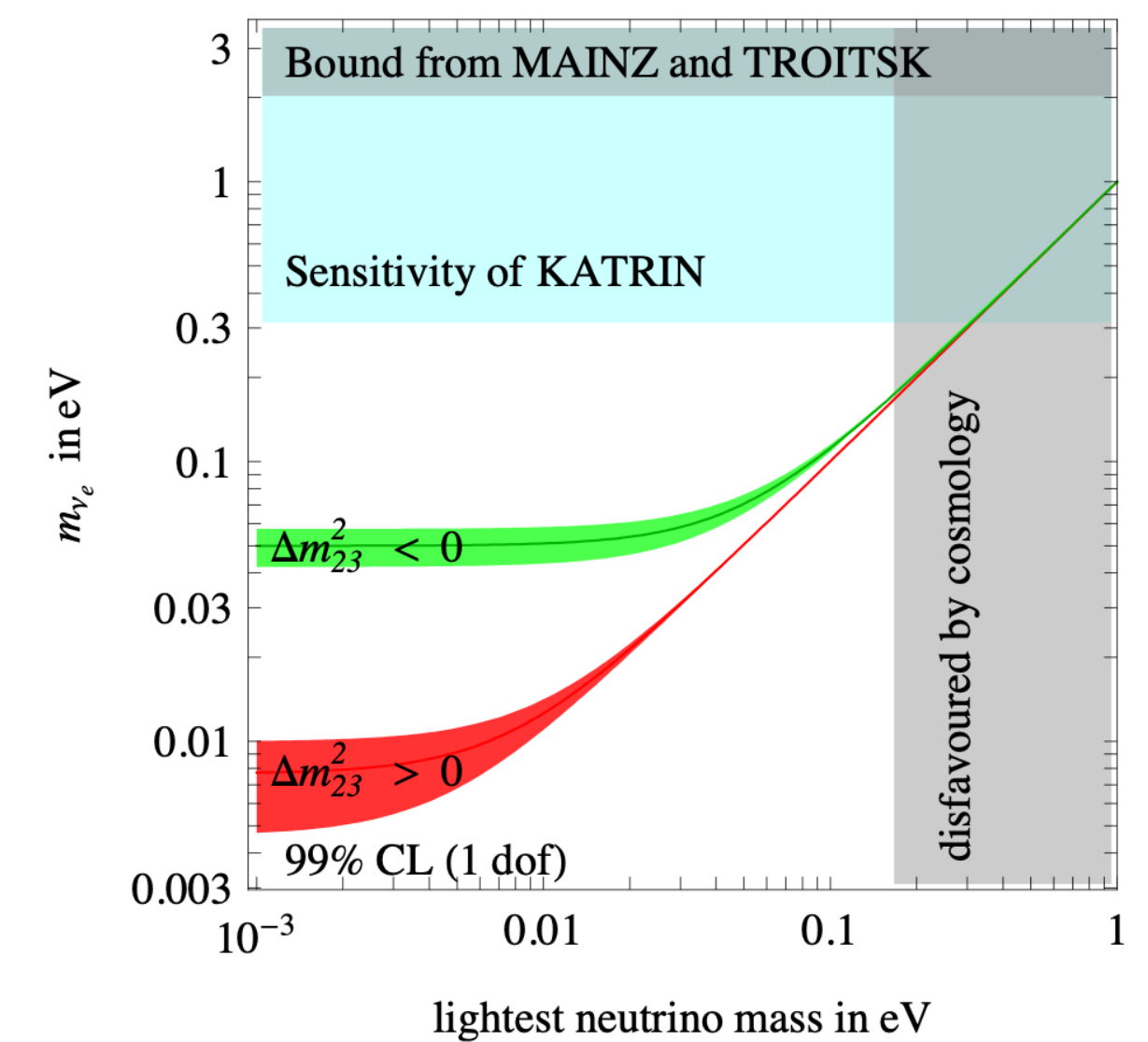
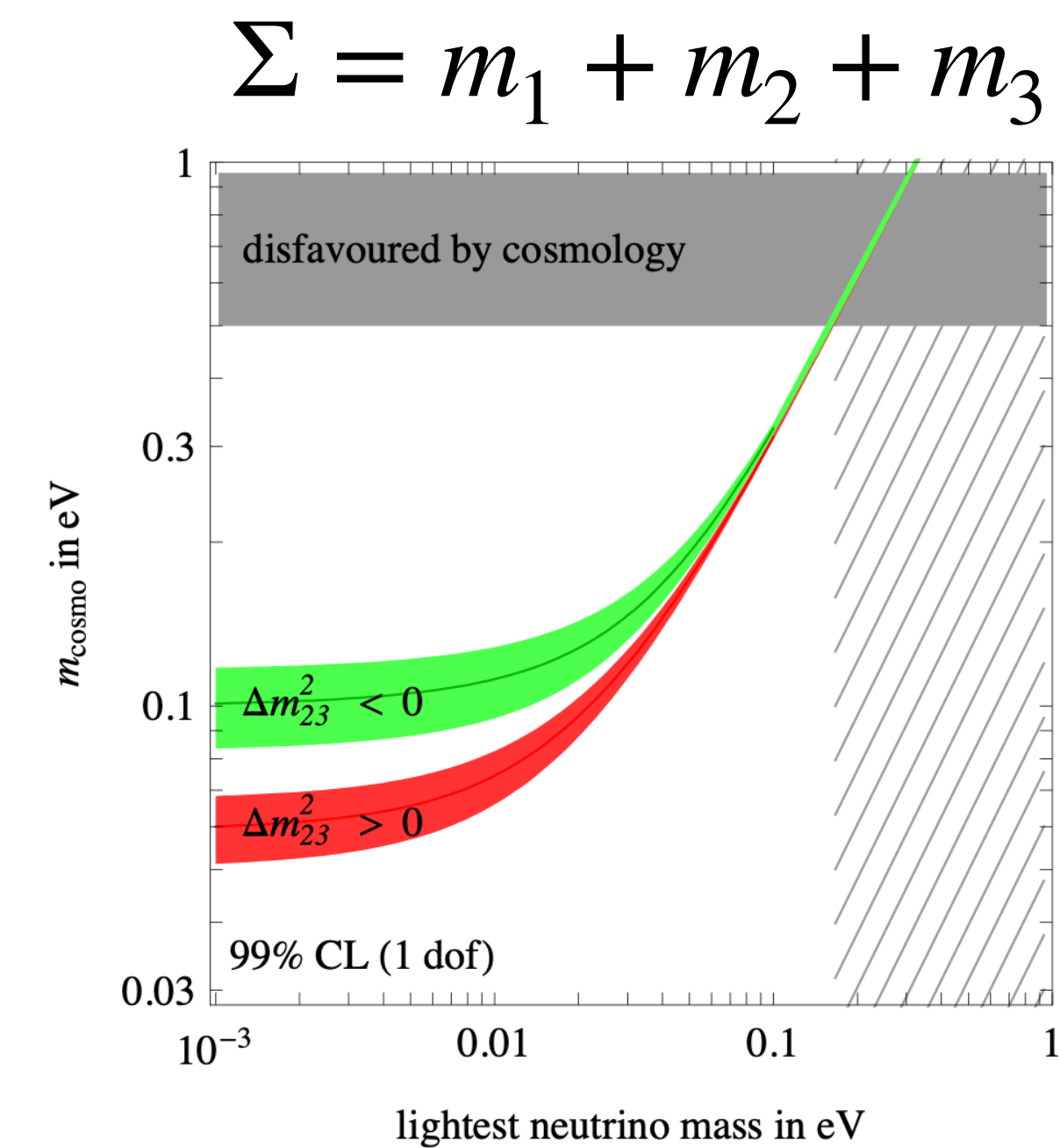
Introduction

$$\langle m_{\beta\beta} \rangle = \left| \sum_i U_{ei}^2 m_i \right|$$

$$\Gamma_{0\nu} = G_{0\nu} g_A^4 |M_{0\nu}|^2 \frac{\langle m_{\beta\beta} \rangle^2}{m_e^2}$$



- Neutrino-less double beta decay
- Cosmology
- Beta decay endpoint



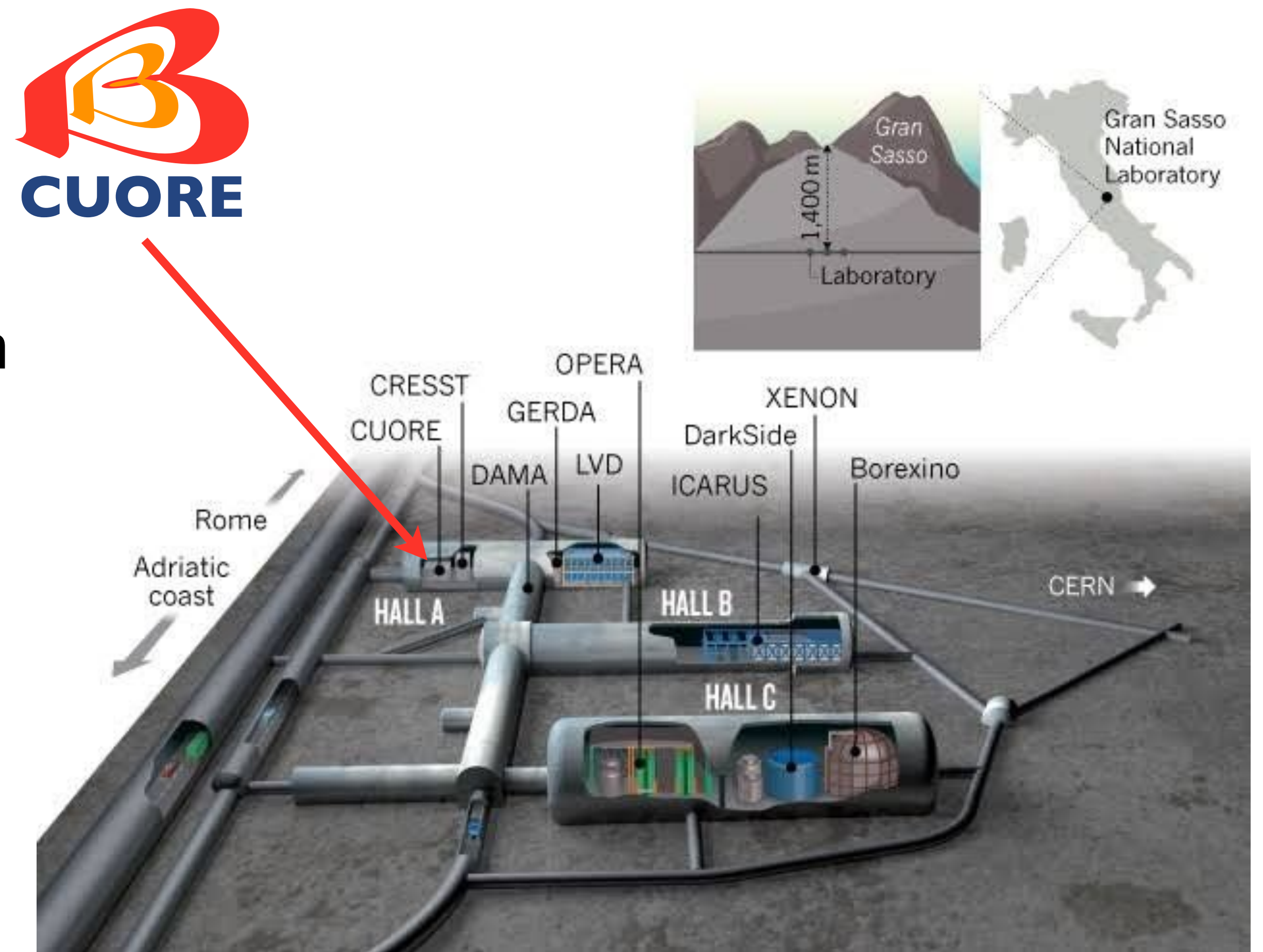


The CUORE experiment



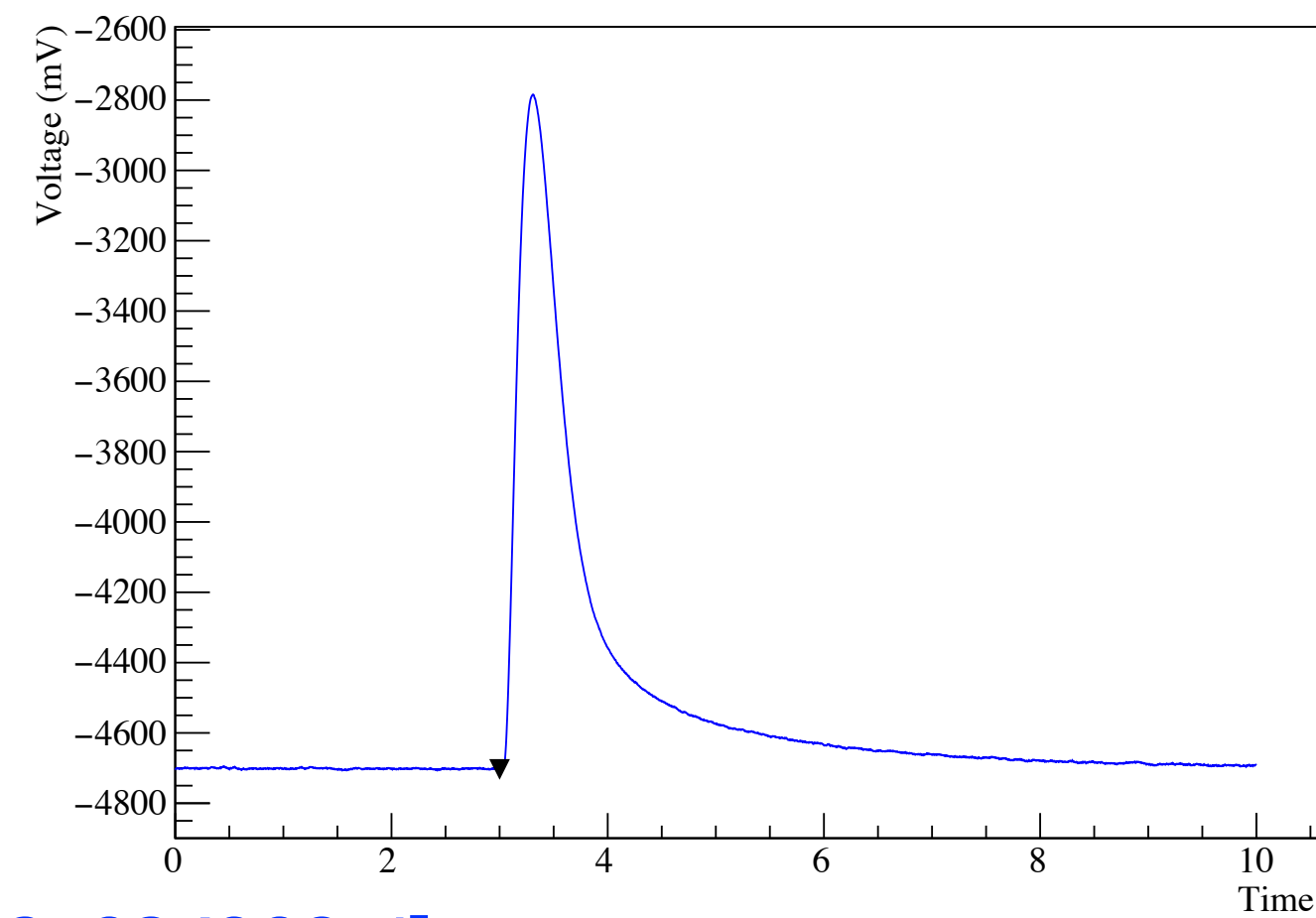
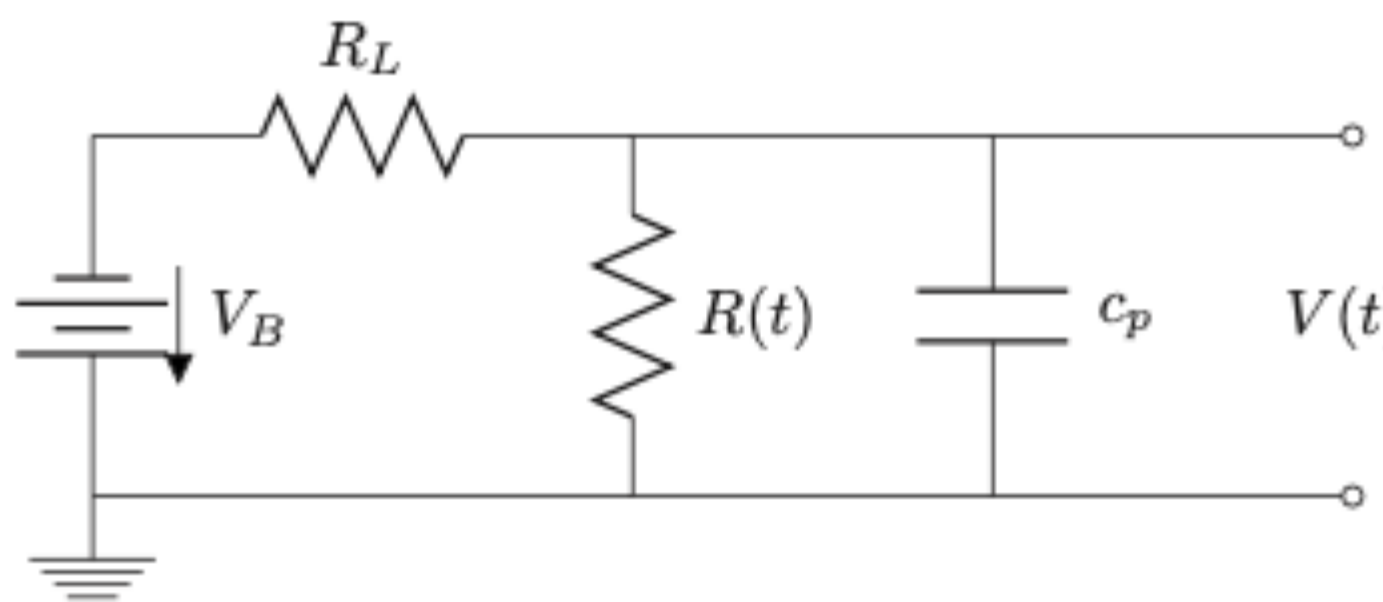
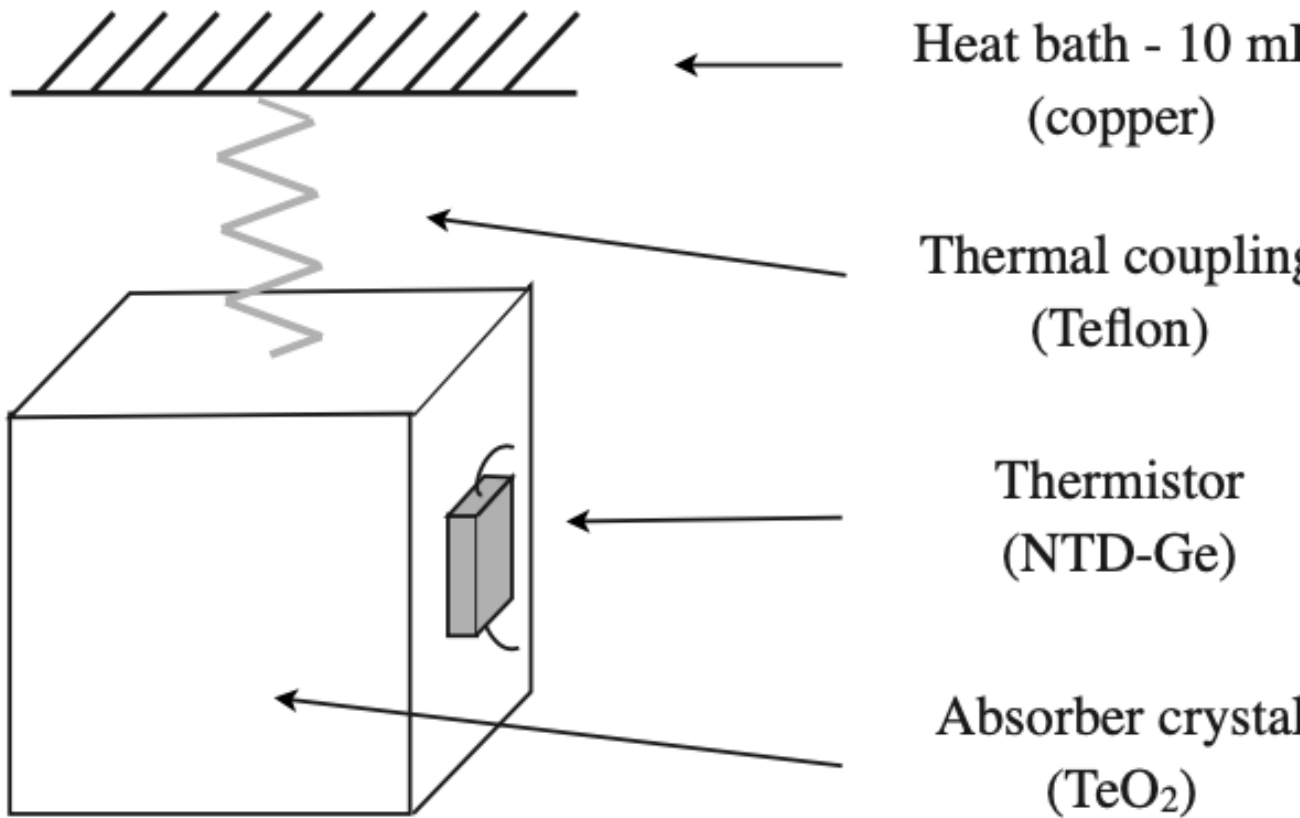
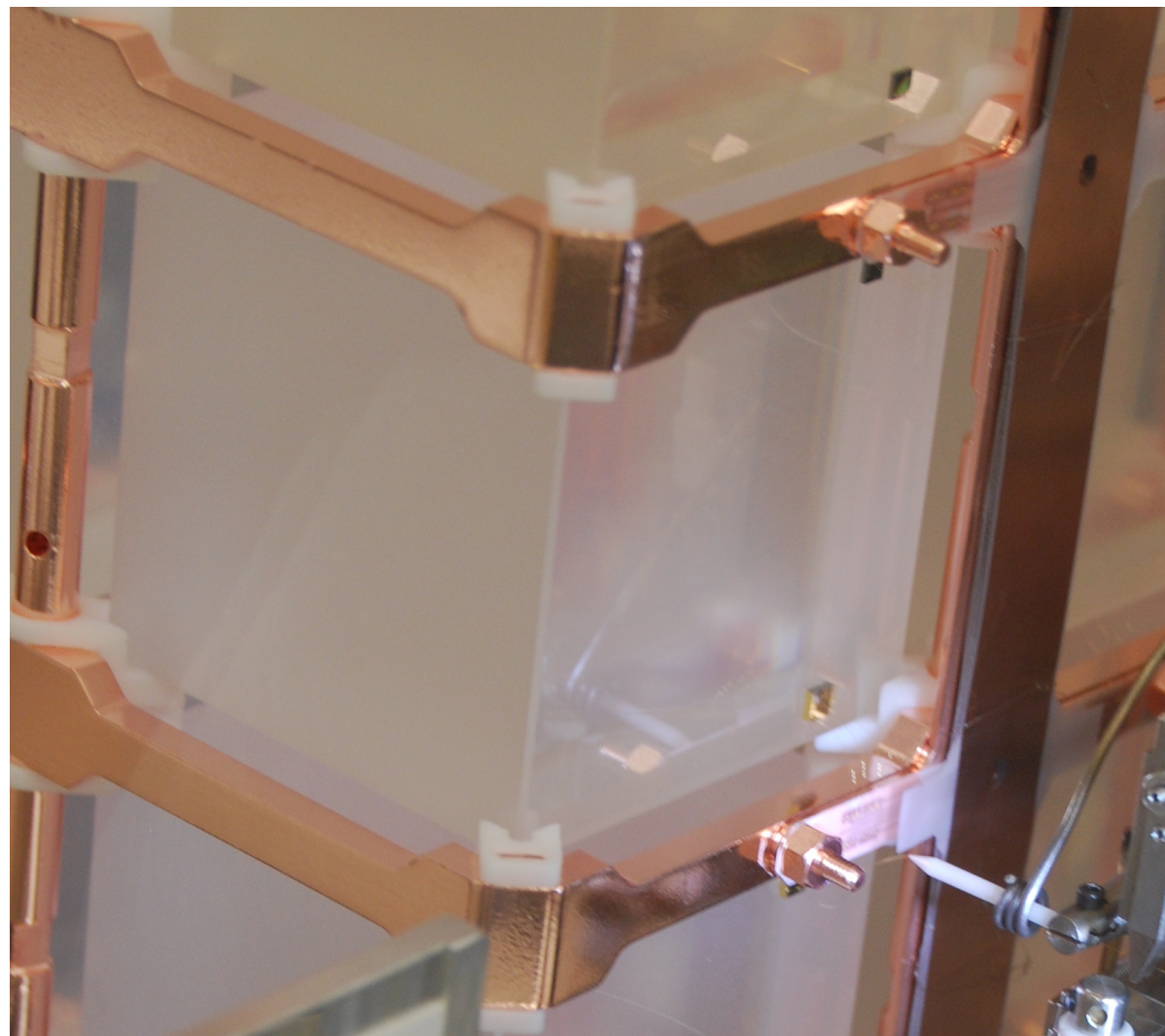
The CUORE experiment

- Cryogenic Underground Observatory for Rare Events
- Hosted underground in the Hall A of the INFN Laboratori Nazionali del Gran Sasso
- 3600 m.w.e. rock overburden
- Main physics goal $0\nu\beta\beta$
- High efficiency (source = detector)
- Ton scale bolometer array
- ~ 10 mK operating temperature

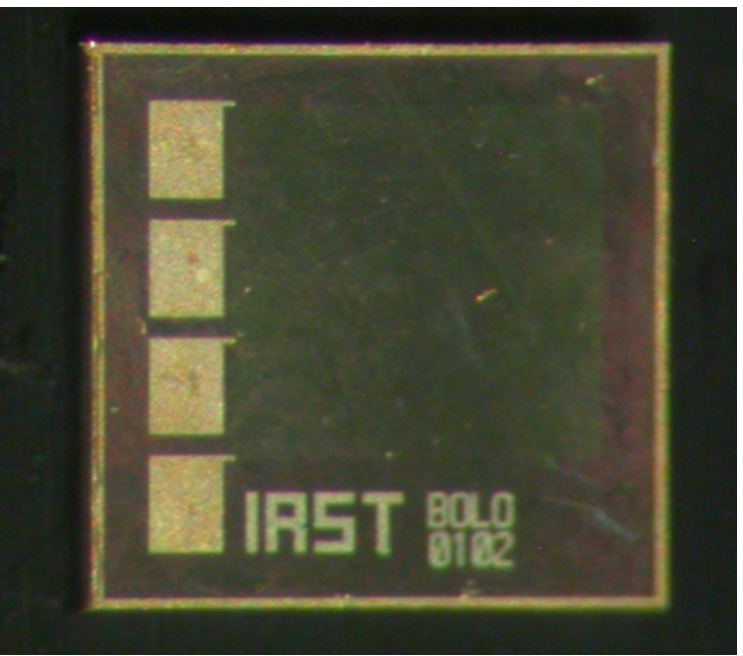
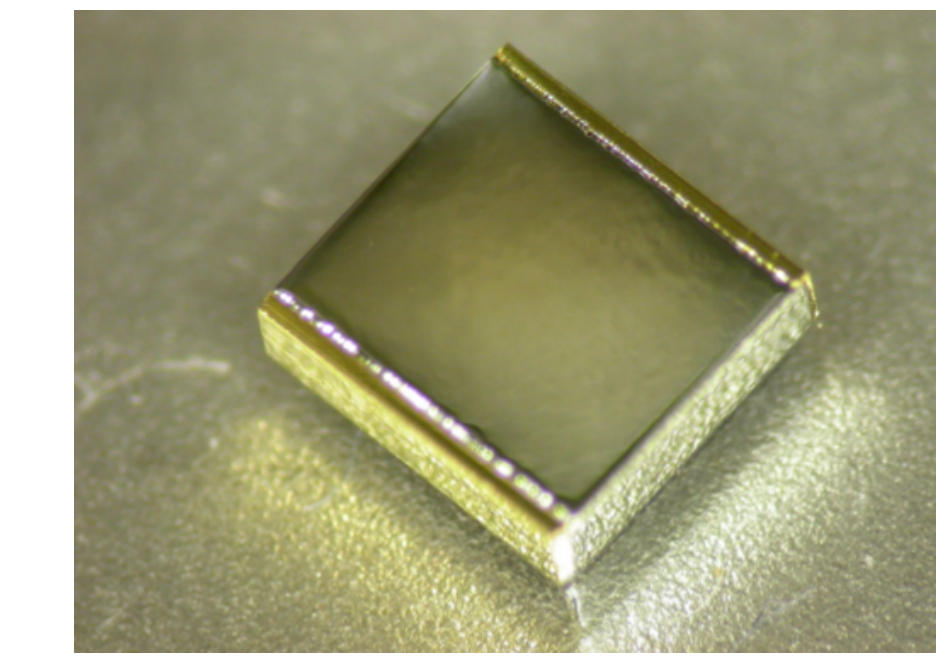


The CUORE experiment

Operating principles



[M. Vignati, Journal of Applied Physics 108, 084903-1]



[C. Alduino et al., JINST 11 P07009 (2016)]

Crystals instrumented with

- NTD Ge thermistor
- Si heater

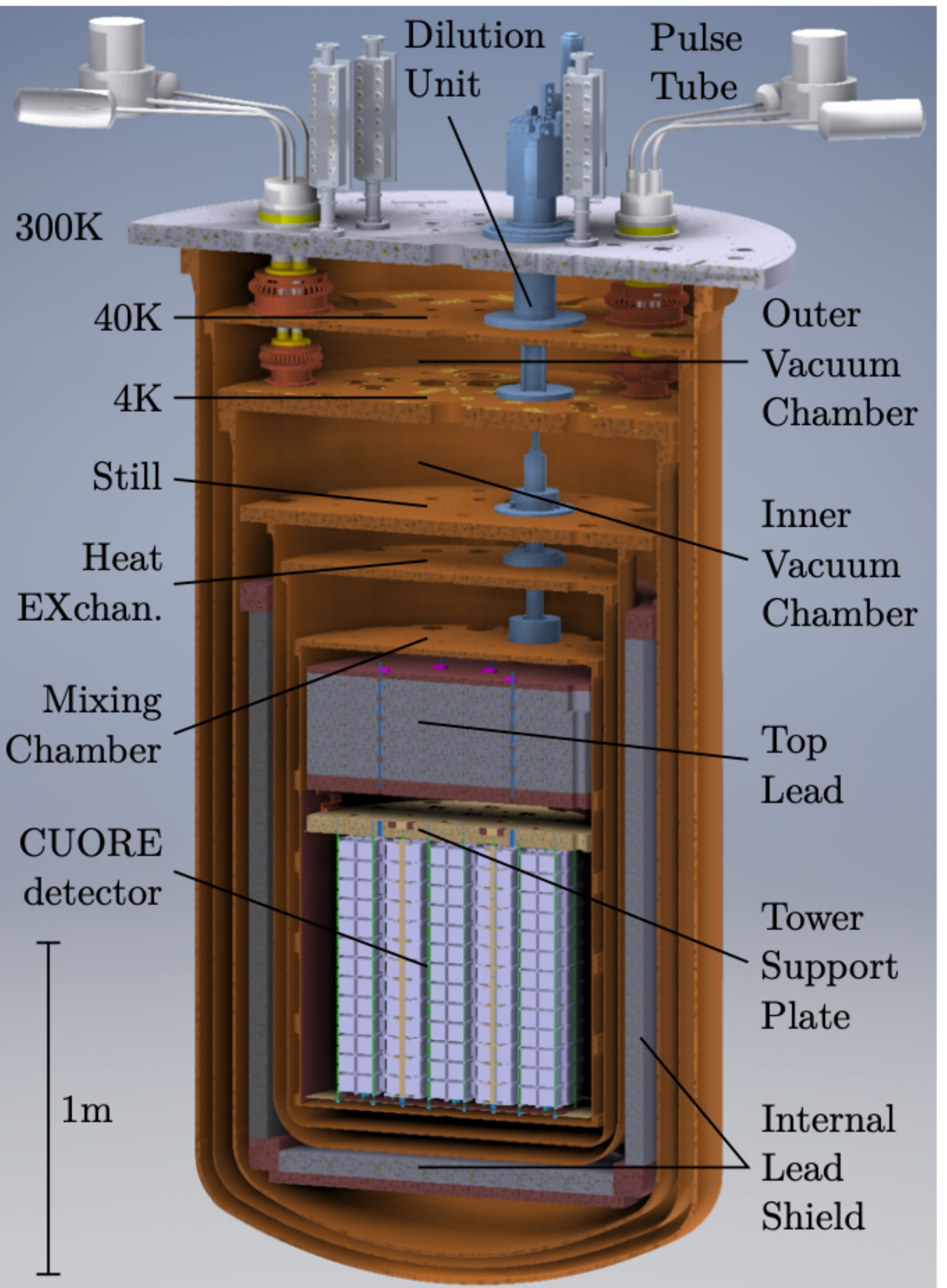
Weak thermal link to heat bath

Particle interactions in the crystals heat them up

Constant NTD current bias produces voltage pulses from temperature variations

The CUORE experiment

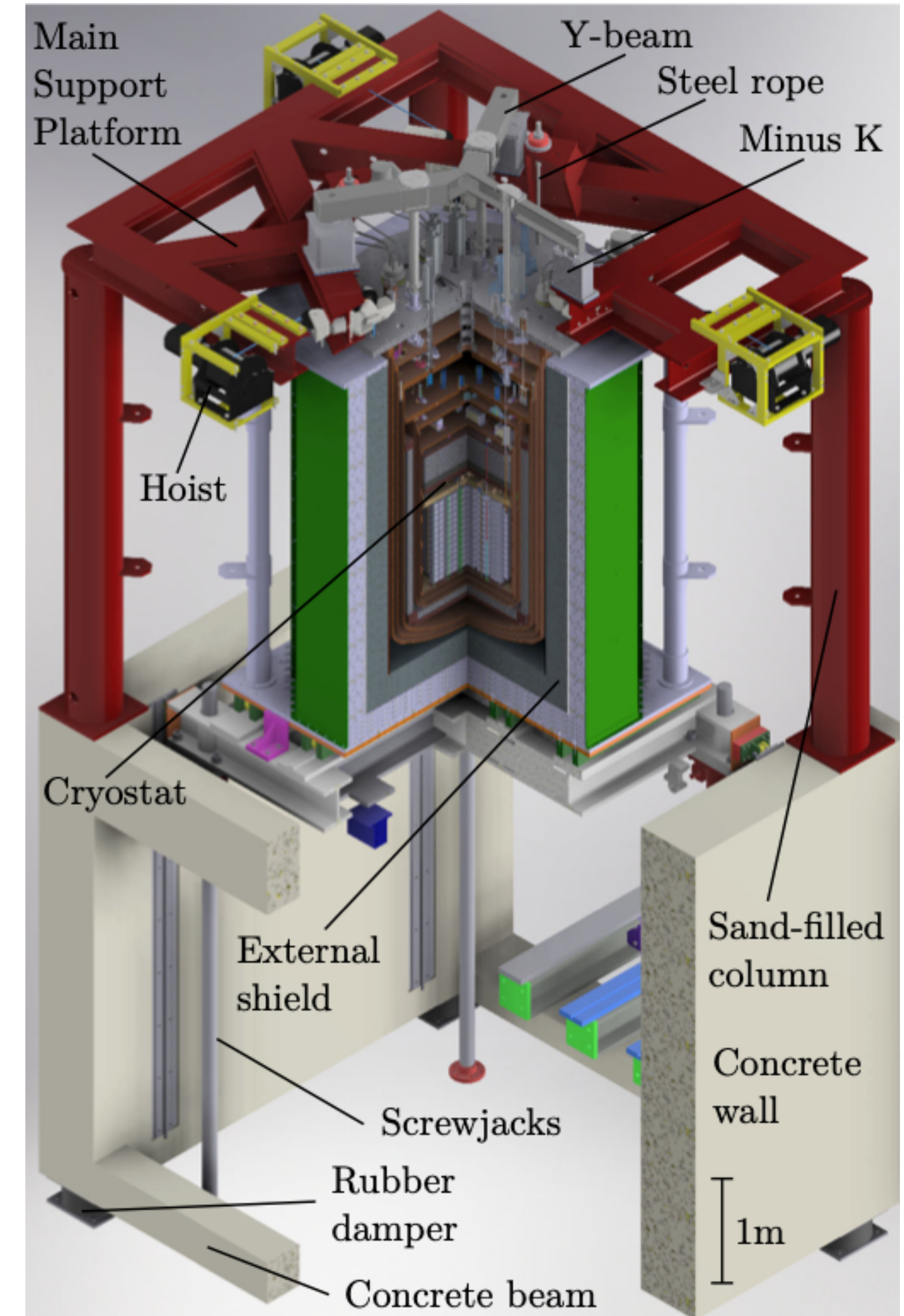
- 988 $5 \times 5 \times 5 \text{ cm}^3$ crystals arranged in 19 towers of 52 channels each
- Total active mass 742 kg
- High natural isotopic abundance ($\sim 206 \text{ kg } ^{130}\text{Te}$)
- Multi-stage cryogen-free $^3\text{He}/^4\text{He}$ dilution refrigerator
- Pre-cooling supplied by Pulse Tube cryocoolers
- $\sim 10 \text{ mK}$ operating temperature
- Good energy resolution $\sim 0.2\%$ FWHM/E



[C. Alduino et al., Cryogenics 102, 9 (2019)]

The CUORE experiment

- Low background goal of $0.01 \text{ cts}/(\text{keV kg yr})$ at $Q_{\beta\beta}$
 - 18 cm polyethylene + 2 cm borated material
 - 30 cm lead
 - Inner ^{210}Pb depleted Roman lead shielding
- Thorough campaign of material assay
- Strict construction, transportation, assembly protocols
- Designed to reduce vibrations

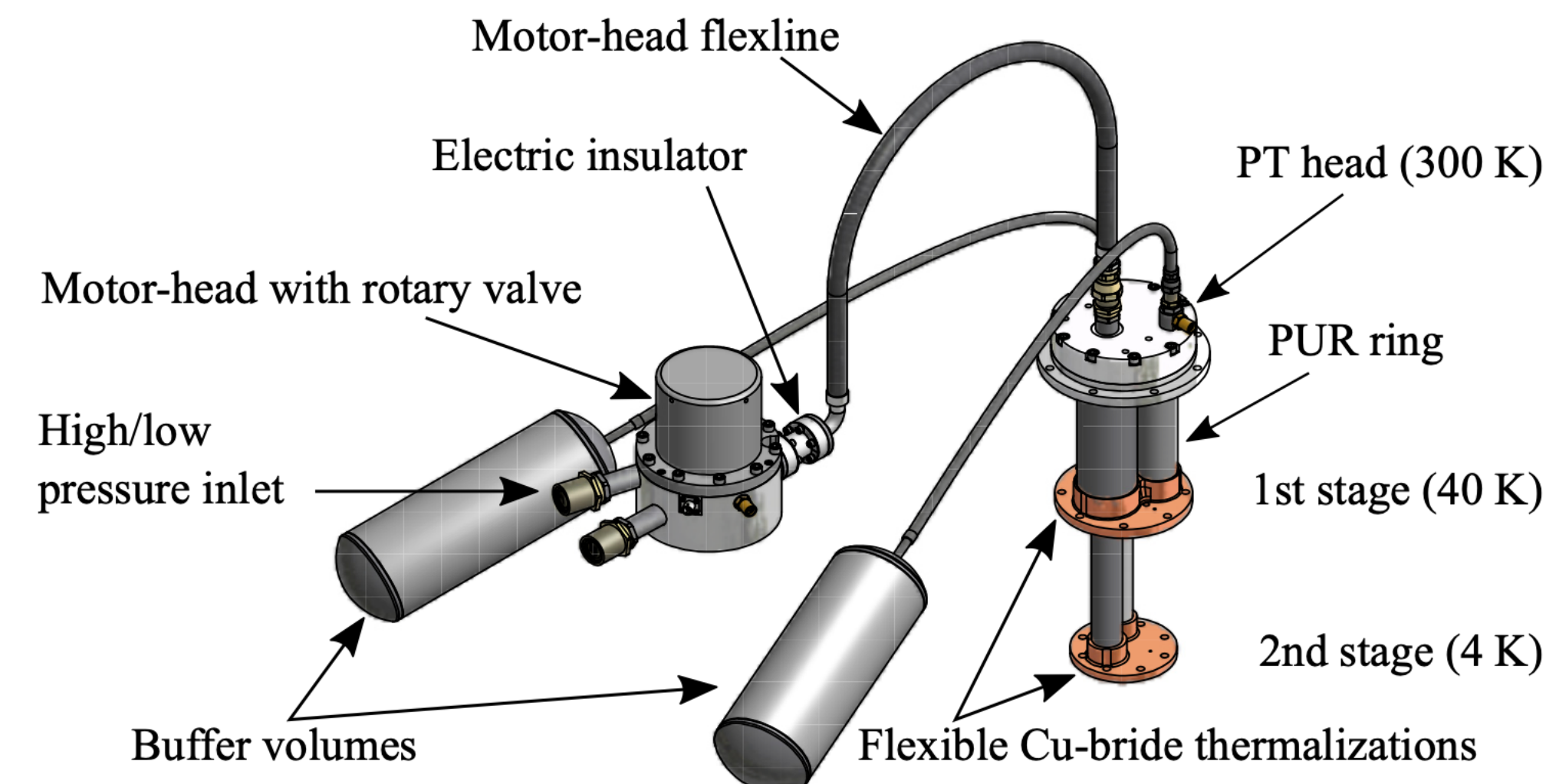
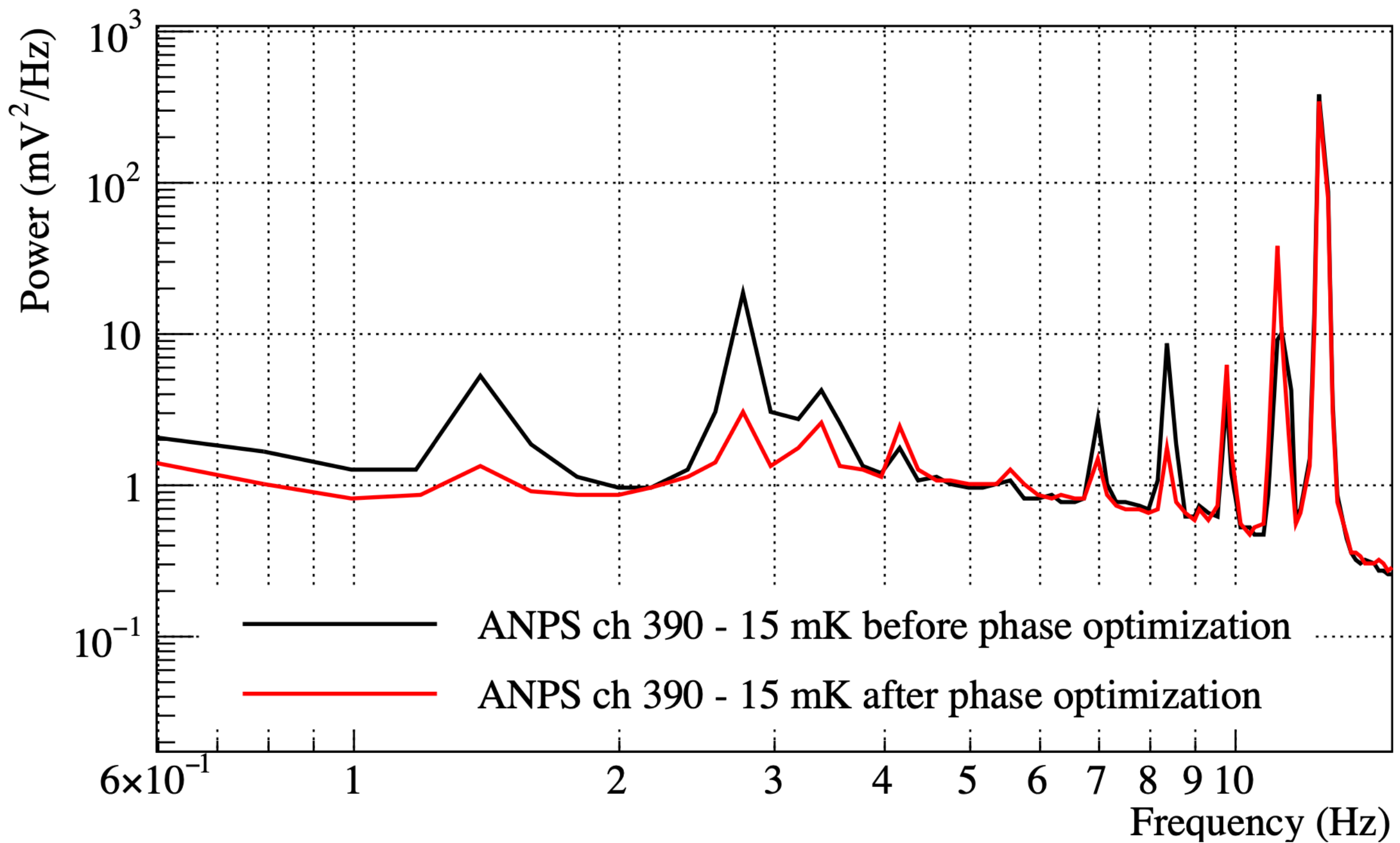


[C. Alduino et al., *Cryogenics* 102, 9 (2019)]

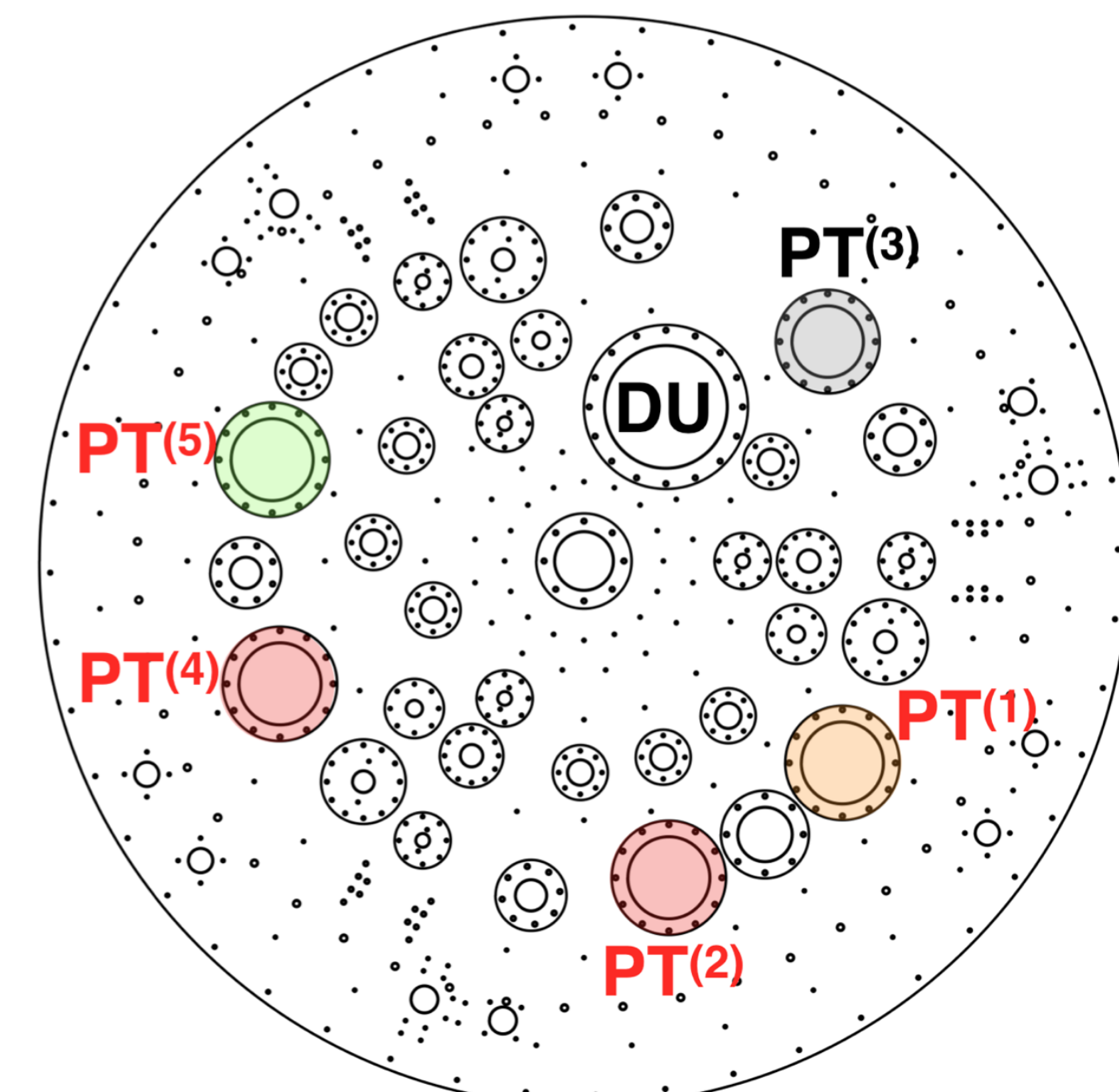
The CUORE experiment

Pulse Tubes noise reduction

Tuning the relative phase of the PT rotary valves allows 1.4 Hz (and higher harmonics) coherent noise suppression

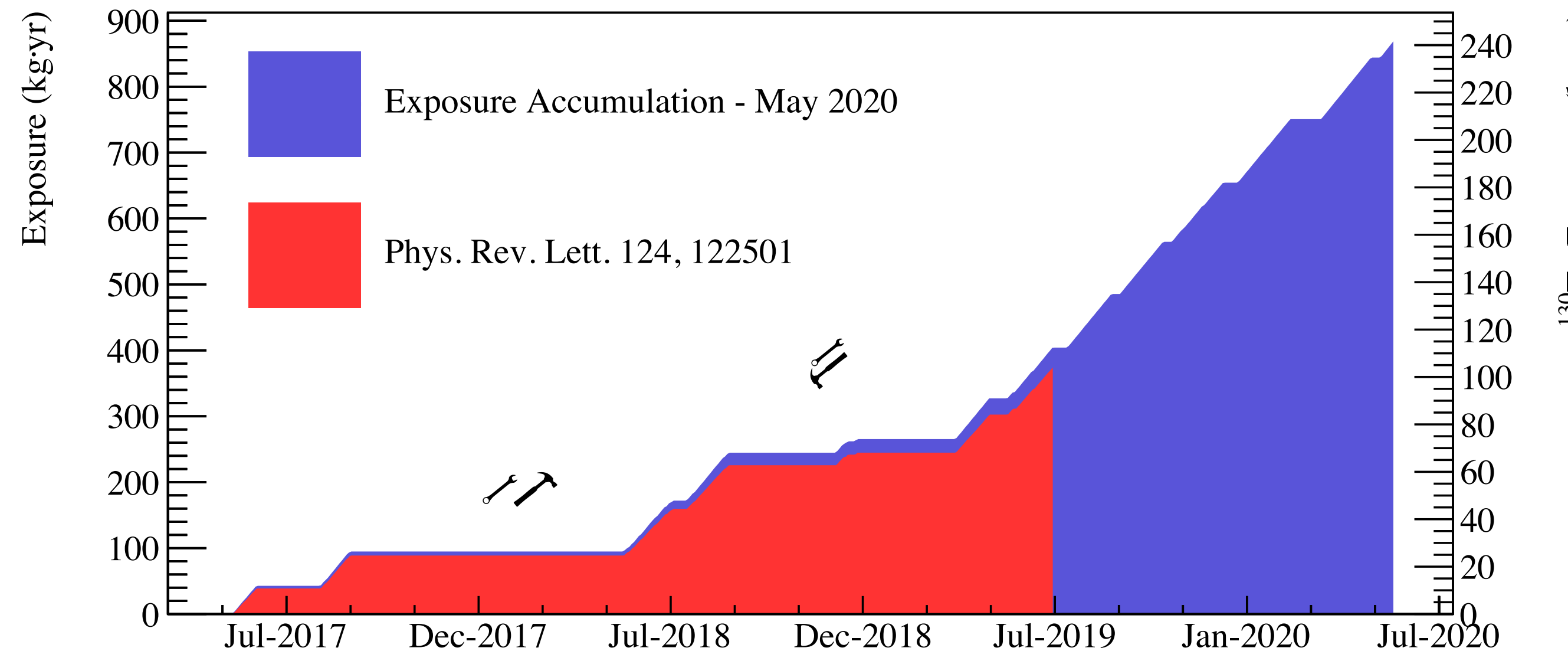


[A. D'Addabbo, Cryogenics 93, 56-65 (2018)]

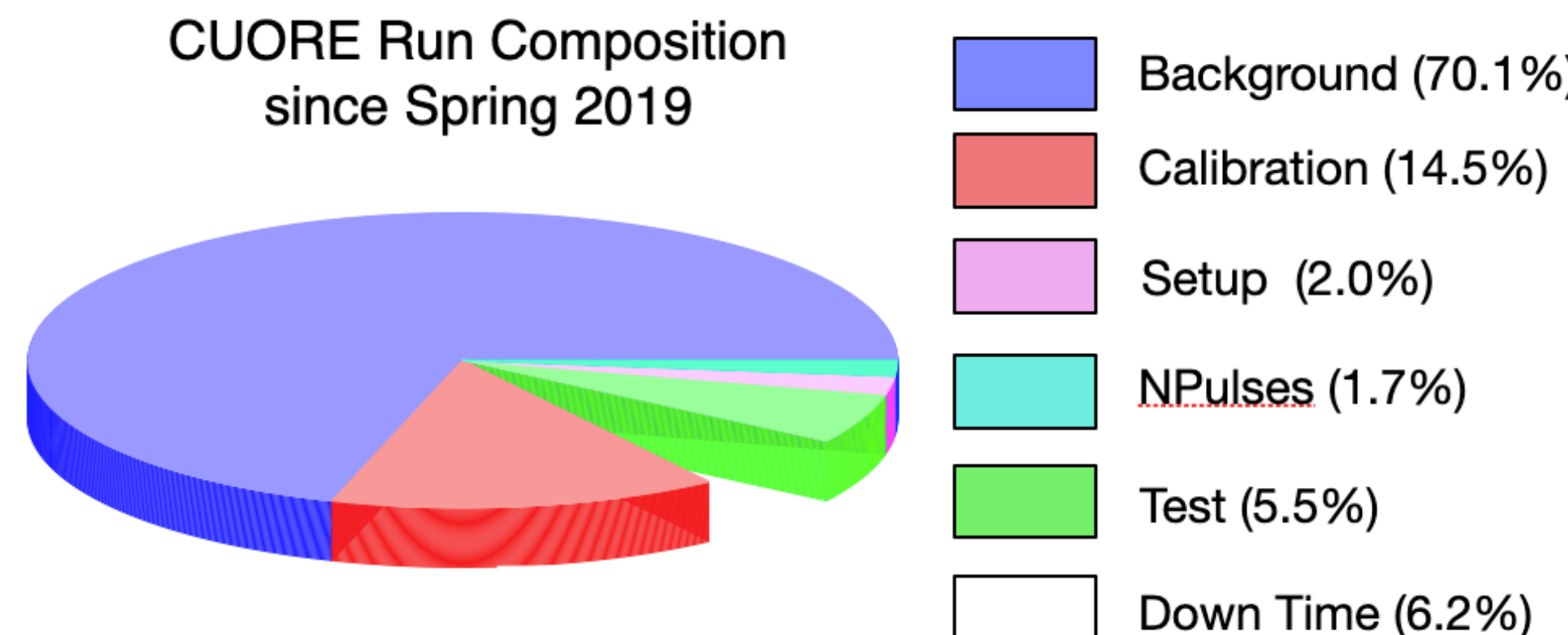


The CUORE experiment

Detector operation



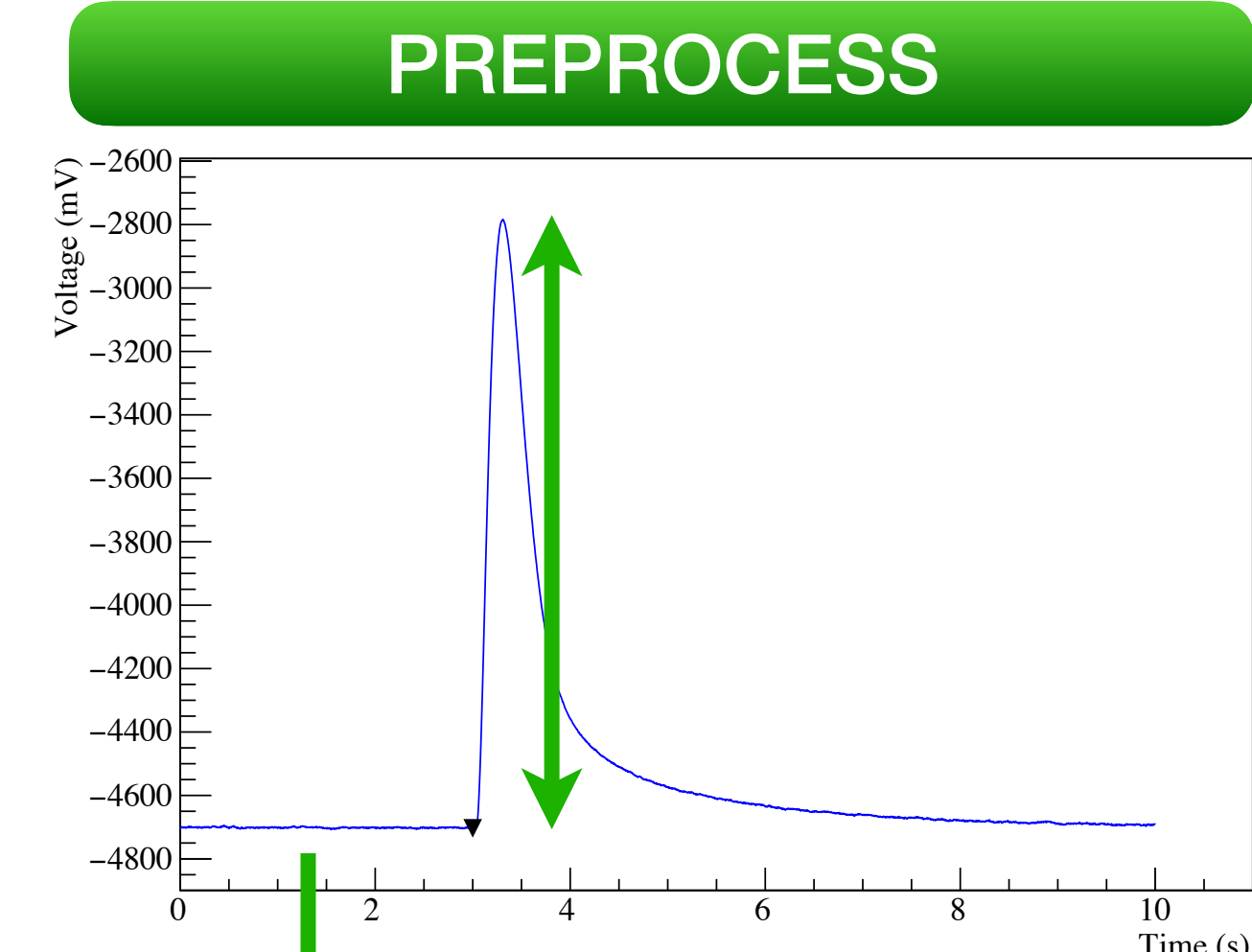
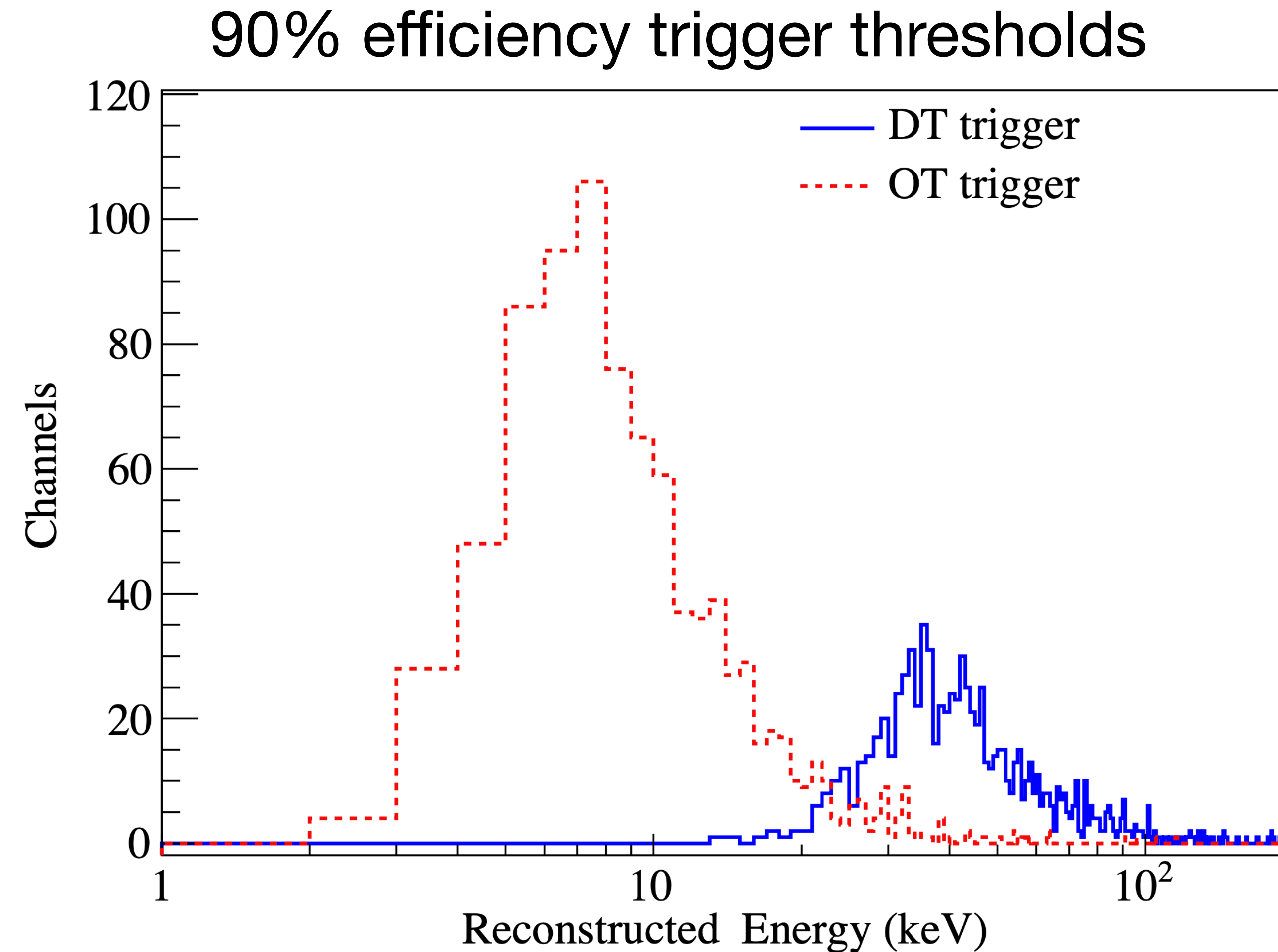
[D. Q. Adams et al., Phys. Rev. Lett. 124, 122501 (2020)]



- Data taking started in Spring 2017
- CUORE “data set”: ~1 month of background data taking with a few days of calibration at the start and end
- Unblinded accumulated exposure $372.5 \text{ kg} \cdot \text{yr}$
- Cryogenic facility for ton-scale bolometer arrays

The CUORE experiment

Data processing



Baseline basic parameters

- value (temperature)
- slope (pile-up)
- RMS (noise)

Waveform basic parameters

- Amplitude (max - min)
- Number of pulses (pile-up)

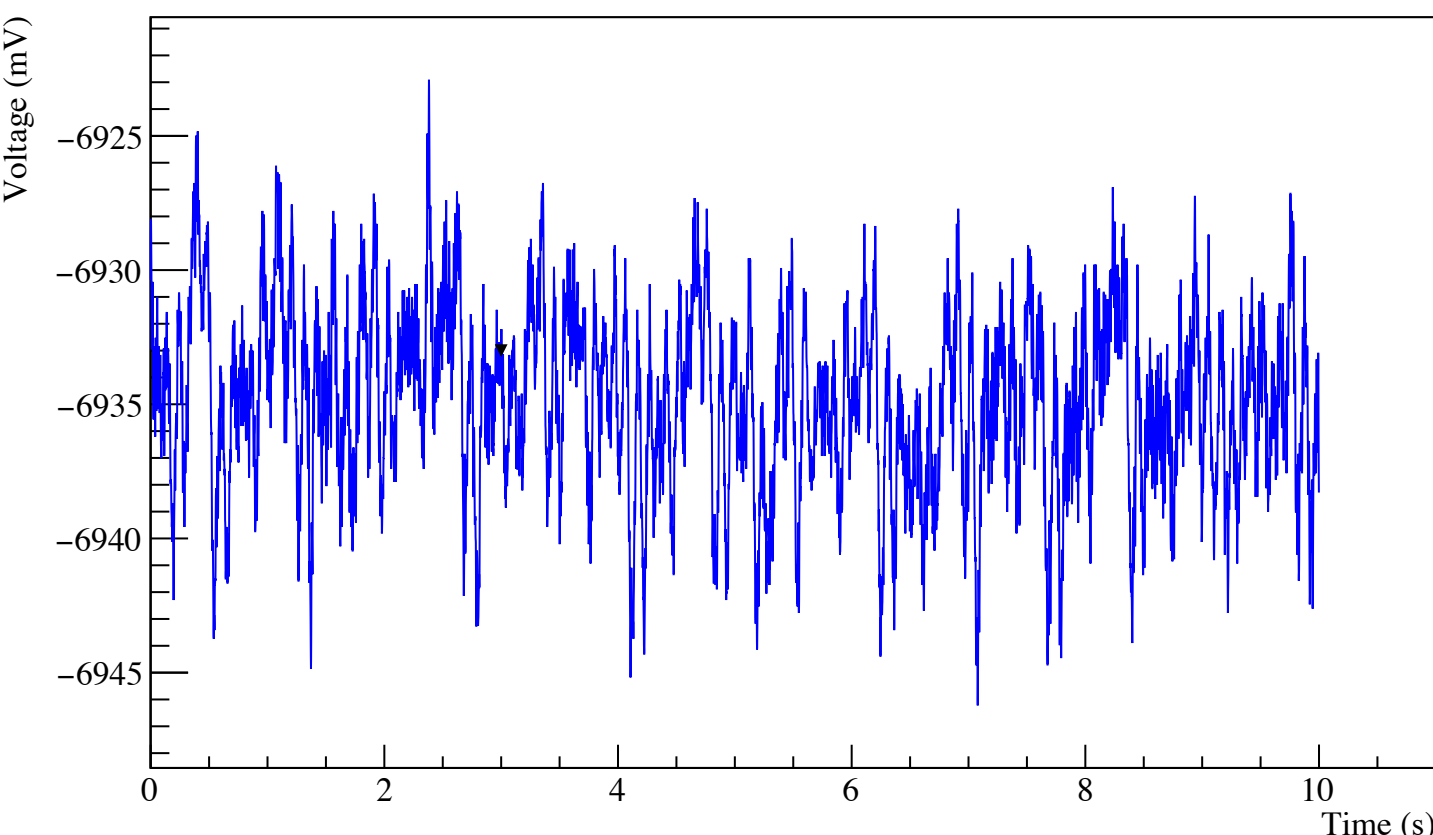
The CUORE experiment

Data processing

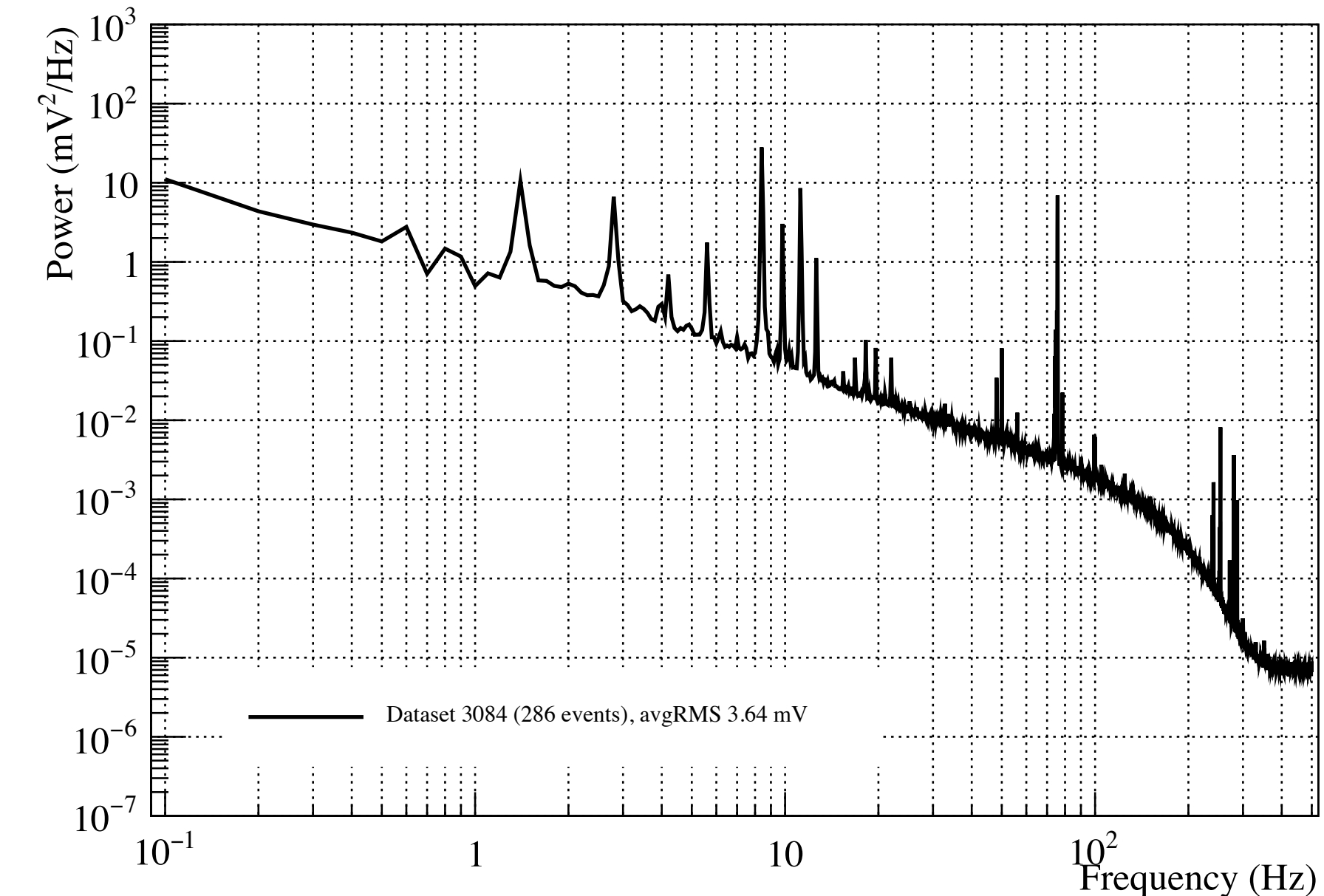
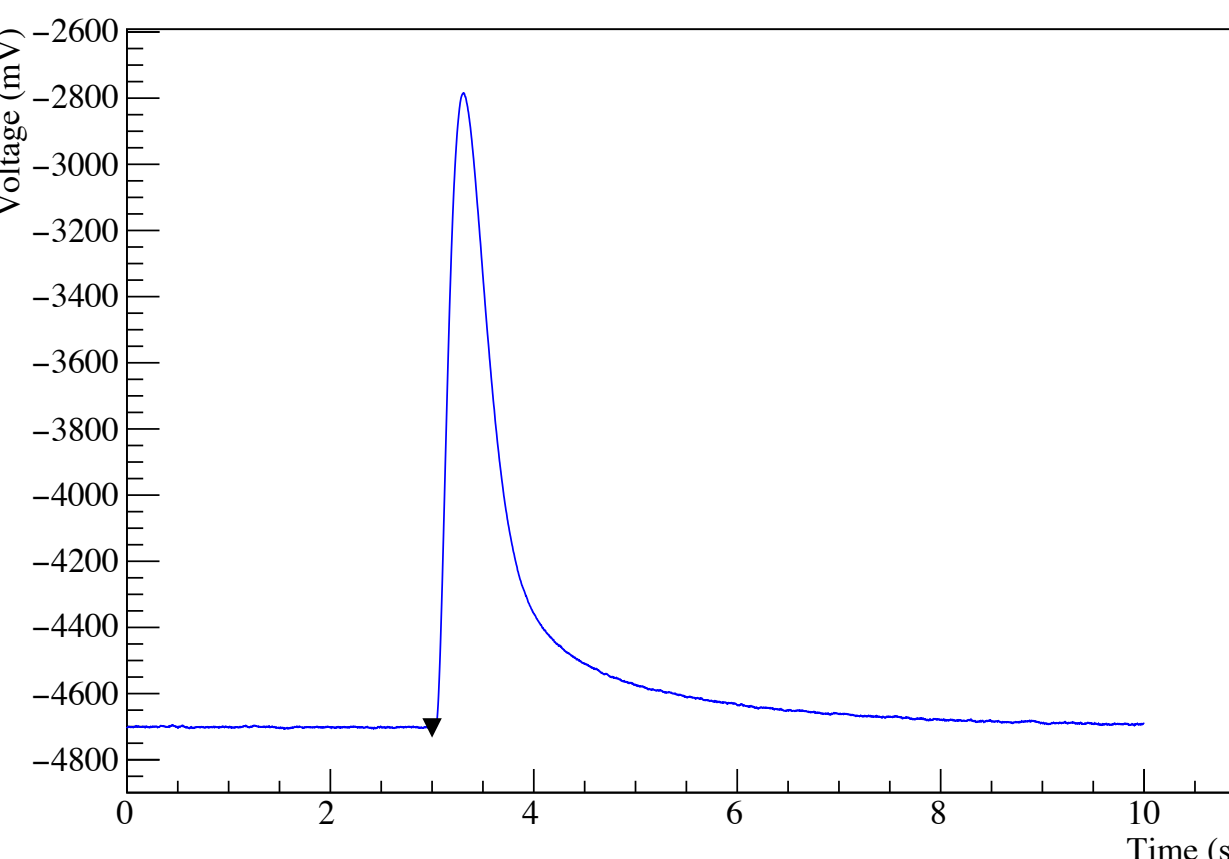
- A sample of clean noise waveforms is used to extract each channel's average noise
- A sample of clean particle pulses is used to compute the average response of each detector

PREPROCESS

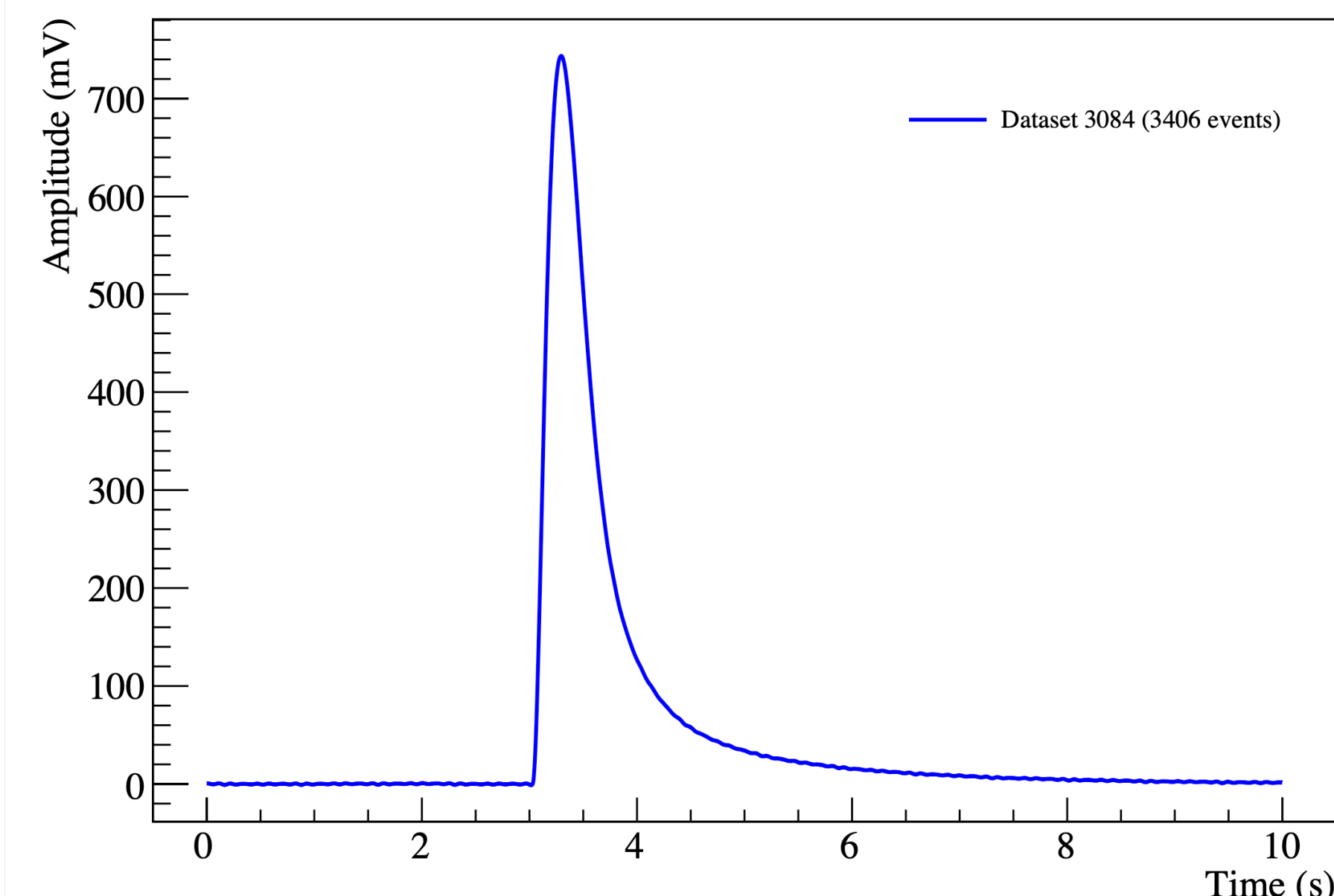
AVERAGE NOISE



AVERAGE PULSE



Average Pulse: ch. 542 - ds 3084



The CUORE experiment

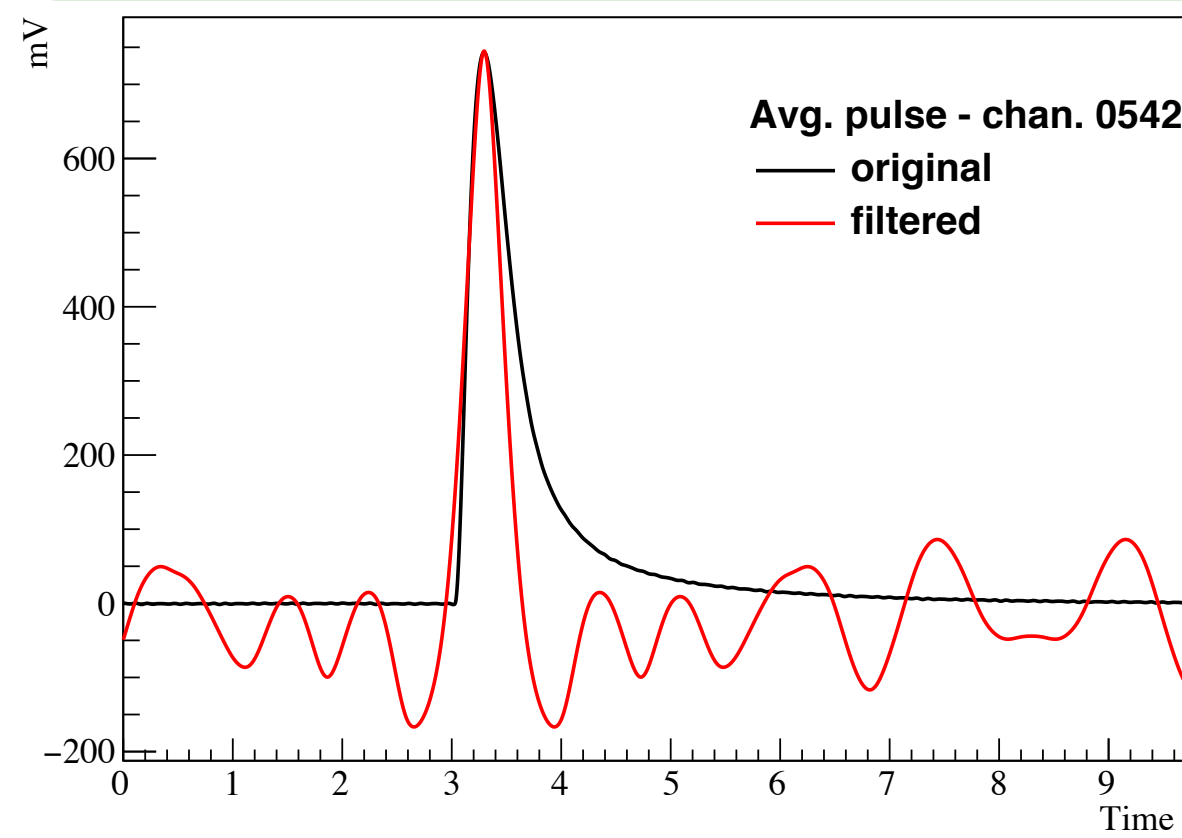
Data processing

PREPROCESS

AVERAGE PULSE

AVERAGE NOISE

AMPLITUDE



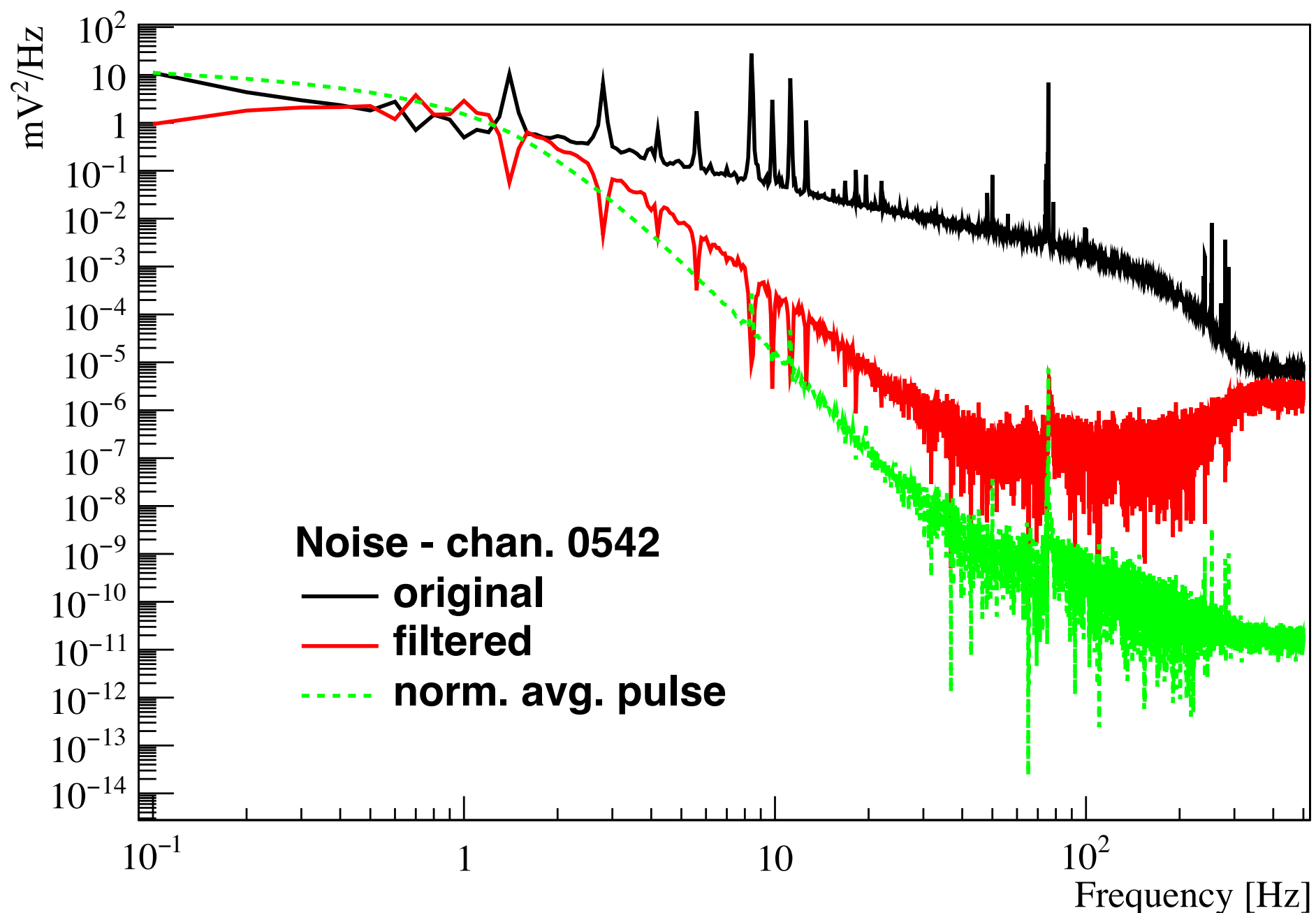
STABILIZATION

CALIBRATION

BLINDING

COINCIDENCES

PULSE SHAPE ANALYSIS



- Stationary noise assumption
- Energy independent pulse shape
- Amplitude extracted with matched filter

The CUORE experiment

Data processing

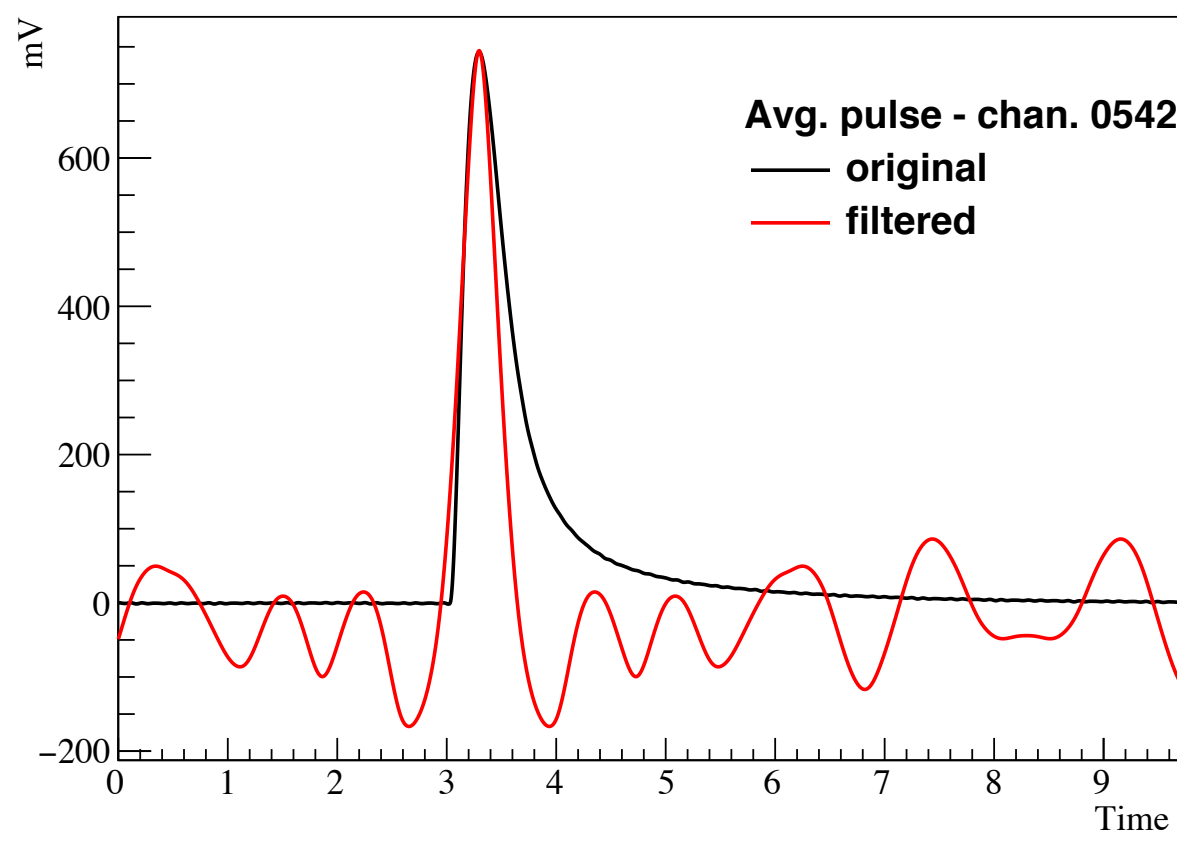
PREPROCESS

AVERAGE PULSE

AVERAGE NOISE

AMPLITUDE

STABILIZATION



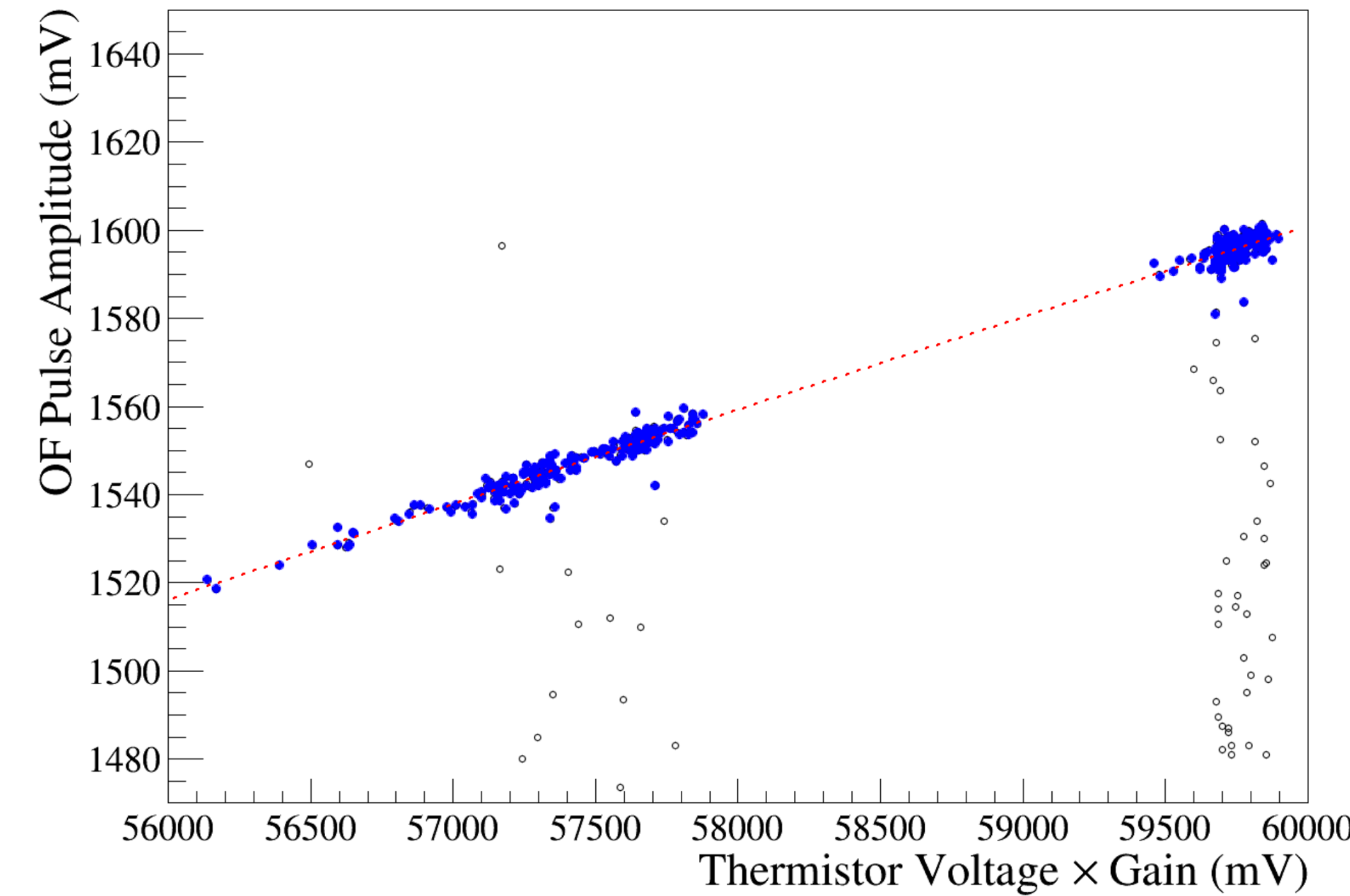
CALIBRATION

BLINDING

COINCIDENCES

PULSE SHAPE ANALYSIS

[C. Alduino *et al.*, Phys. Rev. C 93, 045503 (2016)]

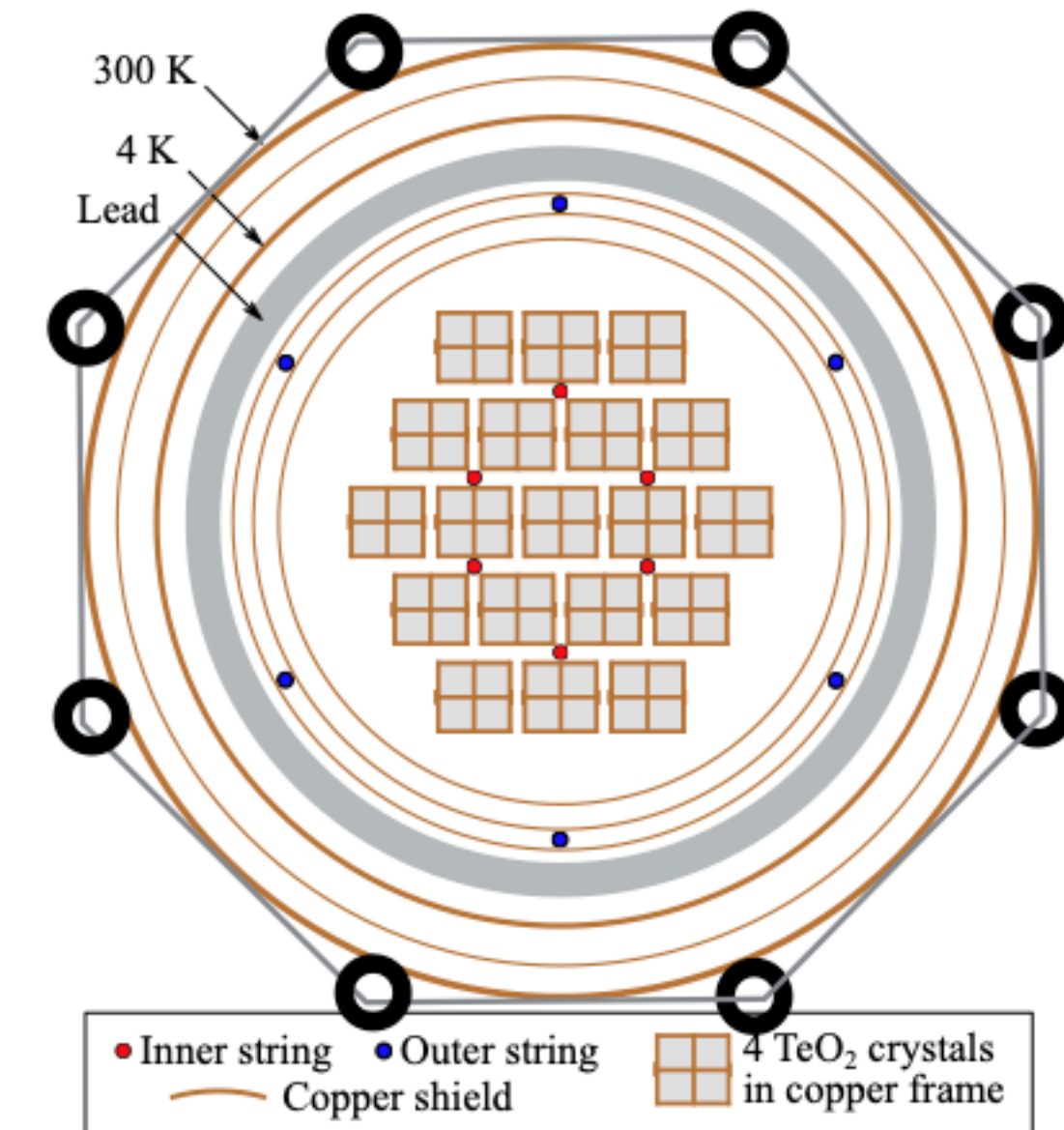
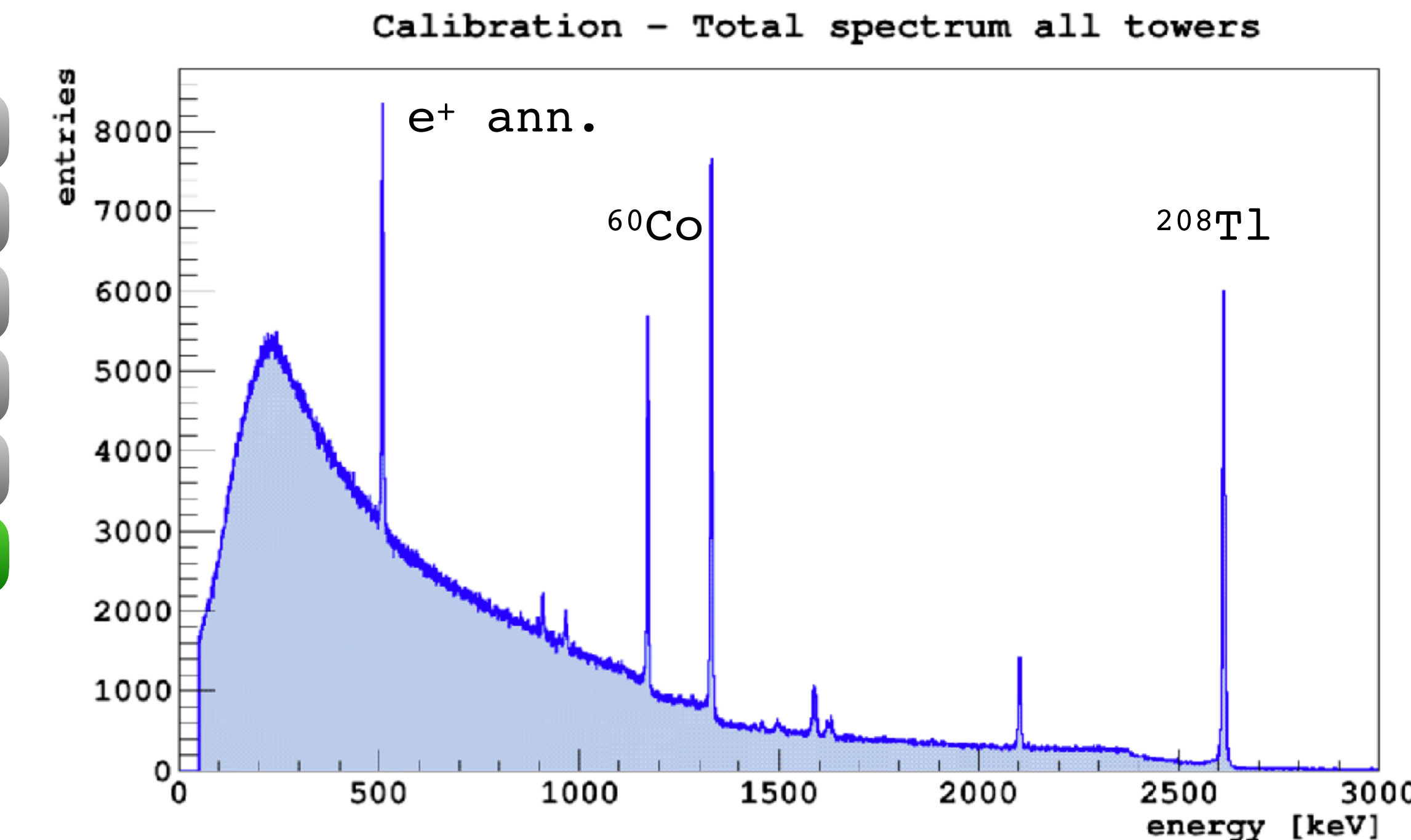
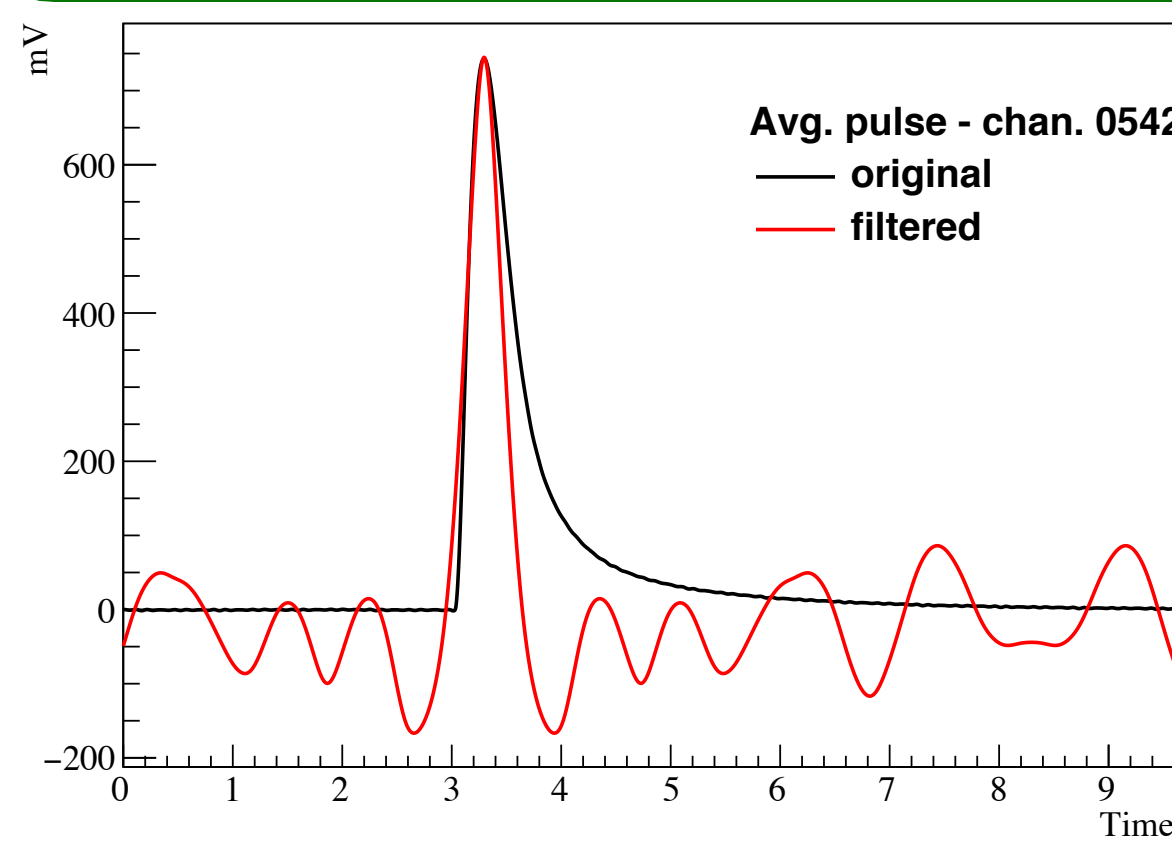


- Fixed amounts of energy periodically injected via heater pulses
- High-statistics 2615 keV line from calibration data
- Temperature fluctuations produce small variations in the heat capacity of the CUORE bolometers (thermal gain)
- A linear correction is applied

The CUORE experiment

Data processing

- PREPROCESS
- AVERAGE PULSE
- AVERAGE NOISE
- AMPLITUDE
- STABILIZATION
- CALIBRATION**



- 8 room temperature calibration strings
- ^{232}Th + ^{60}Co sources
- 2nd order polynomial calibration function

The CUORE experiment

Data processing

PREPROCESS

AVERAGE PULSE

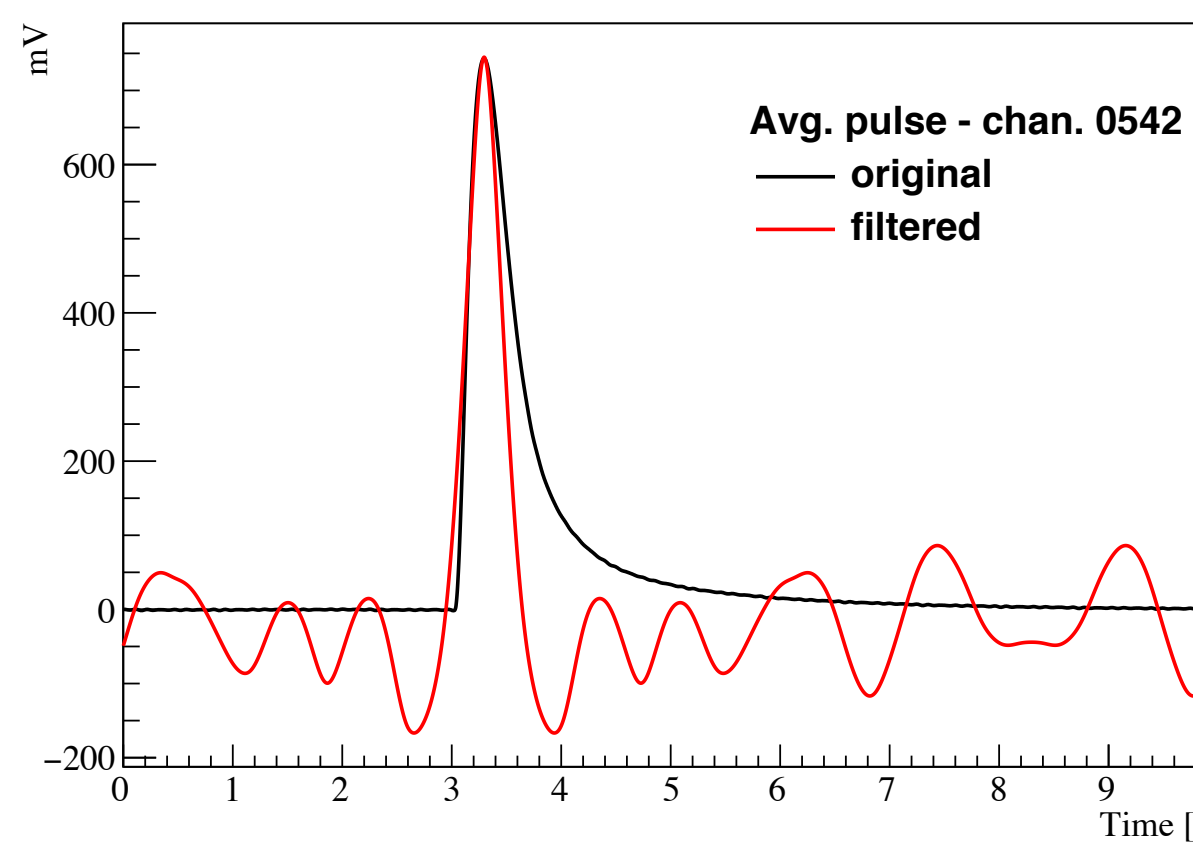
AVERAGE NOISE

AMPLITUDE

STABILIZATION

CALIBRATION

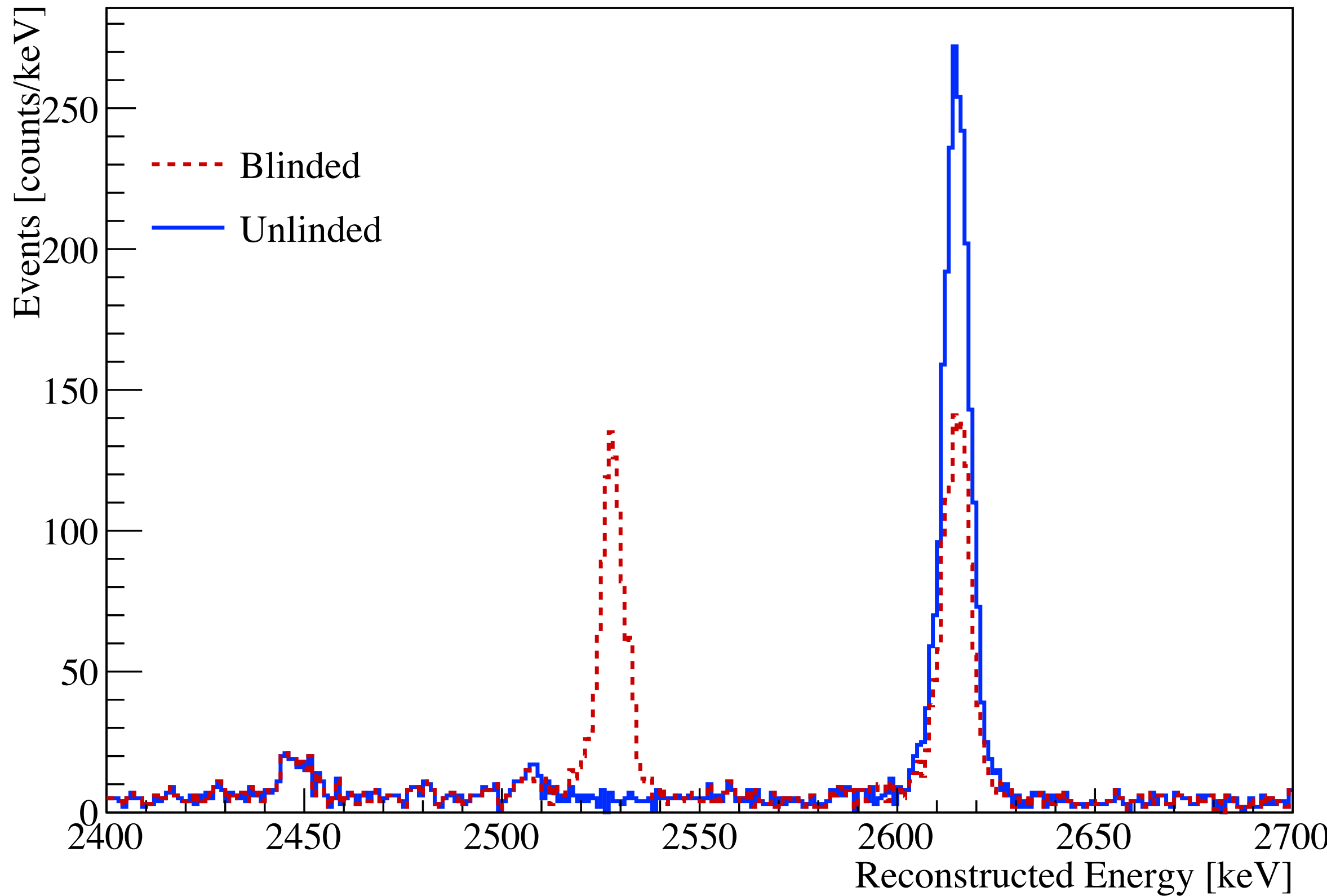
BLINDING



COINCIDENCES

PULSE SHAPE ANALYSIS

Summed Spectrum



Given the seed, a random fraction of events is shifted
from the 2615 keV ^{208}Tl peak to $Q_{\beta\beta}$

The CUORE experiment

Data processing

PREPROCESS

AVERAGE PULSE

AVERAGE NOISE

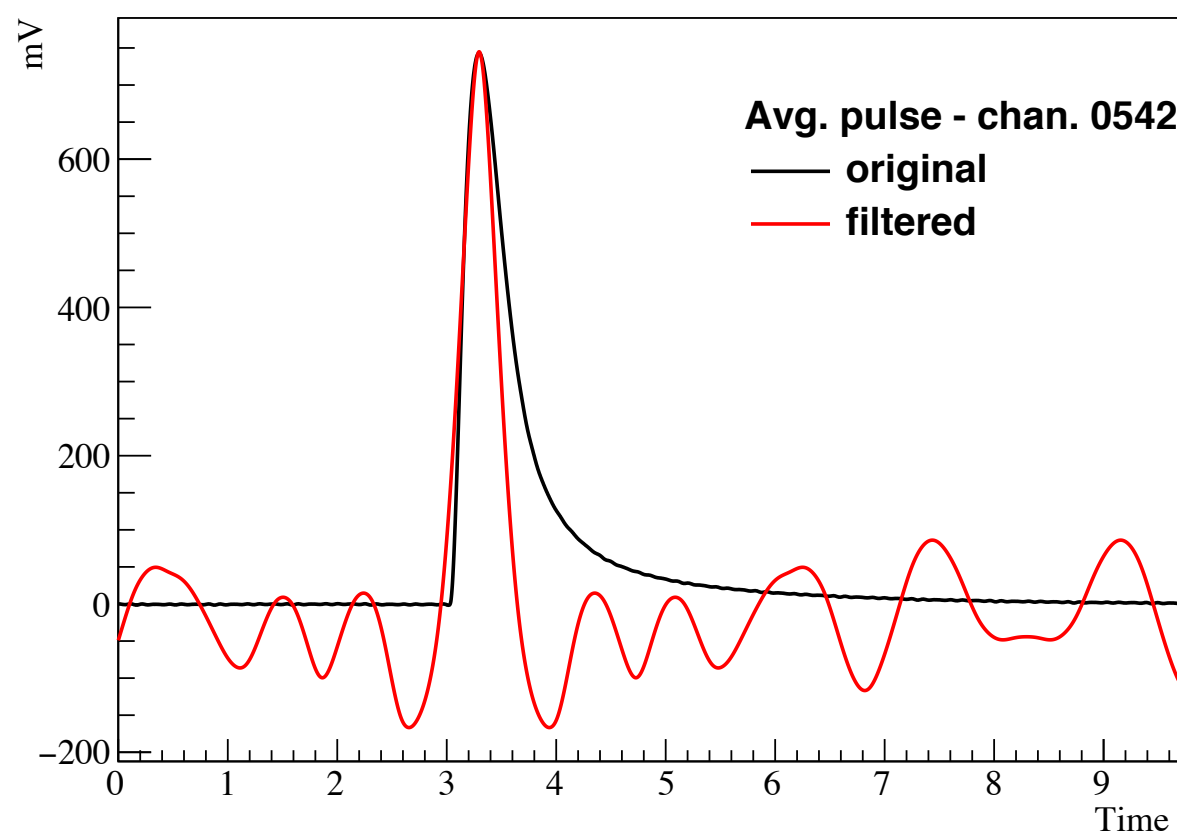
AMPLITUDE

STABILIZATION

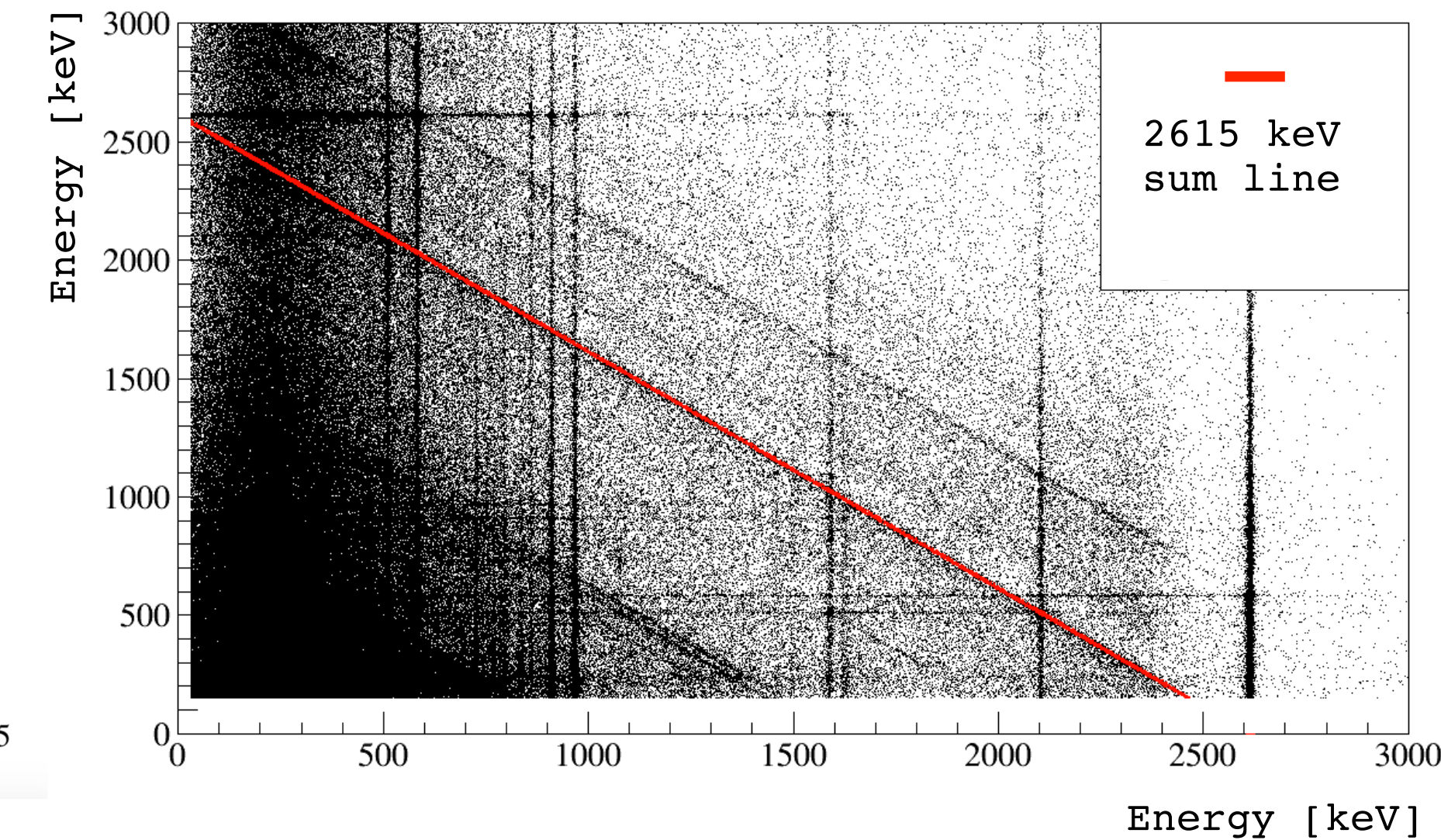
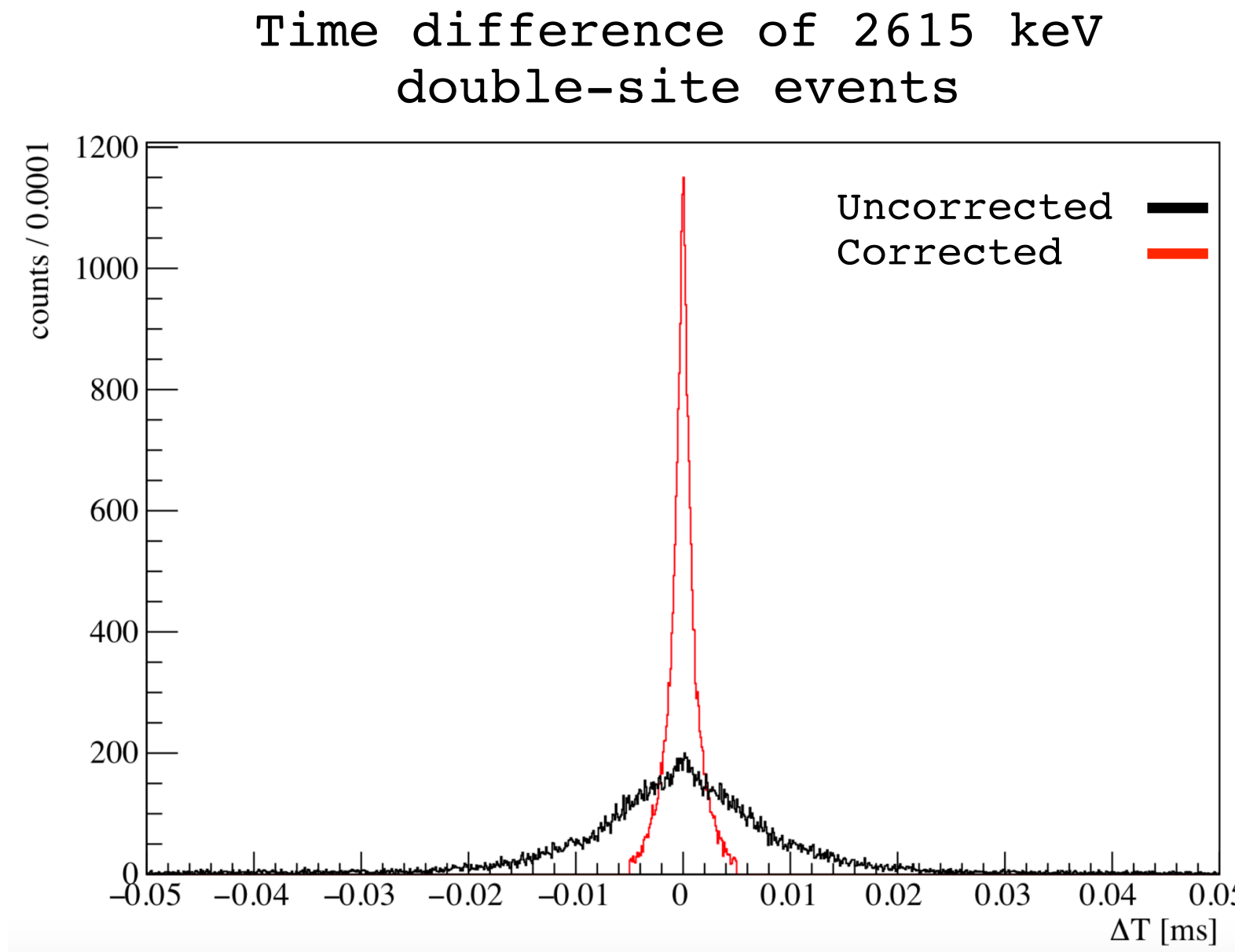
CALIBRATION

BLINDING

COINCIDENCES



PULSE SHAPE ANALYSIS



The event time reconstruction is affected by differences in the pulse rise time among different channels.

A by-channel correction allows to select coincident events in a time window as narrow as ± 5 ms

The CUORE experiment

Data processing

PREPROCESS

AVERAGE PULSE

AVERAGE NOISE

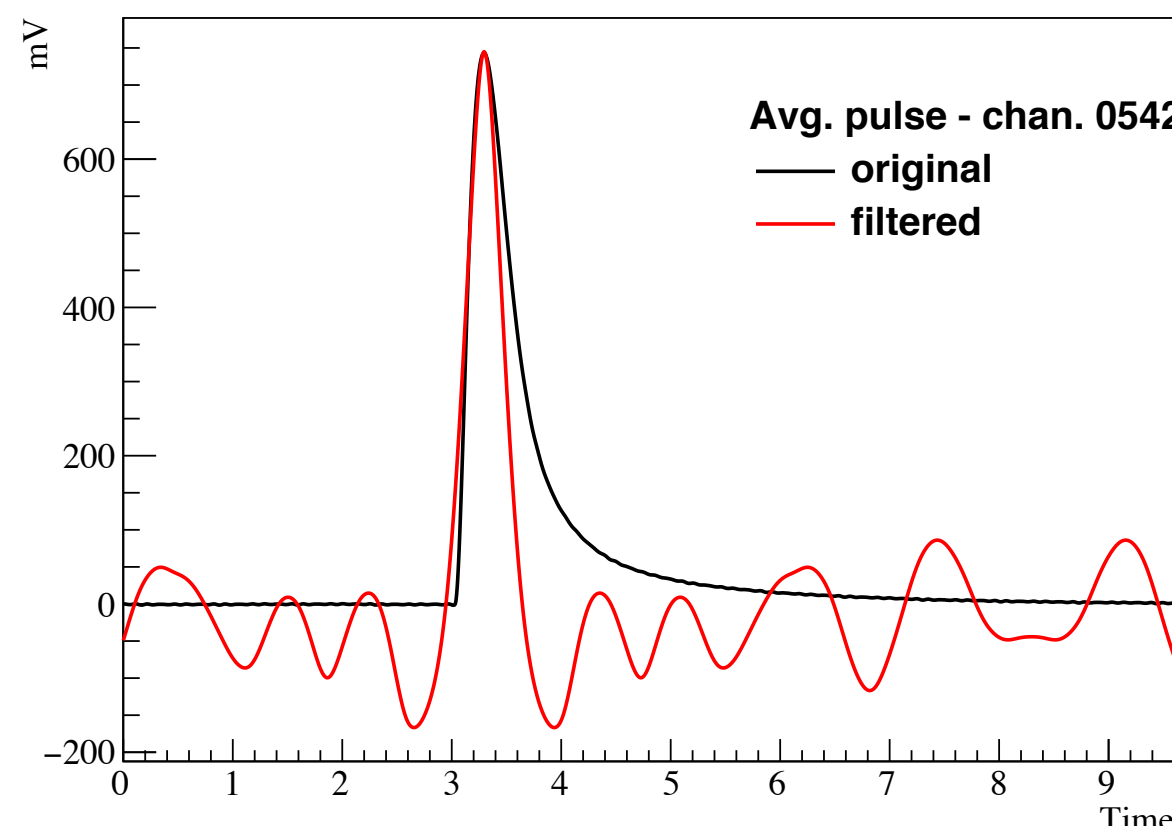
AMPLITUDE

STABILIZATION

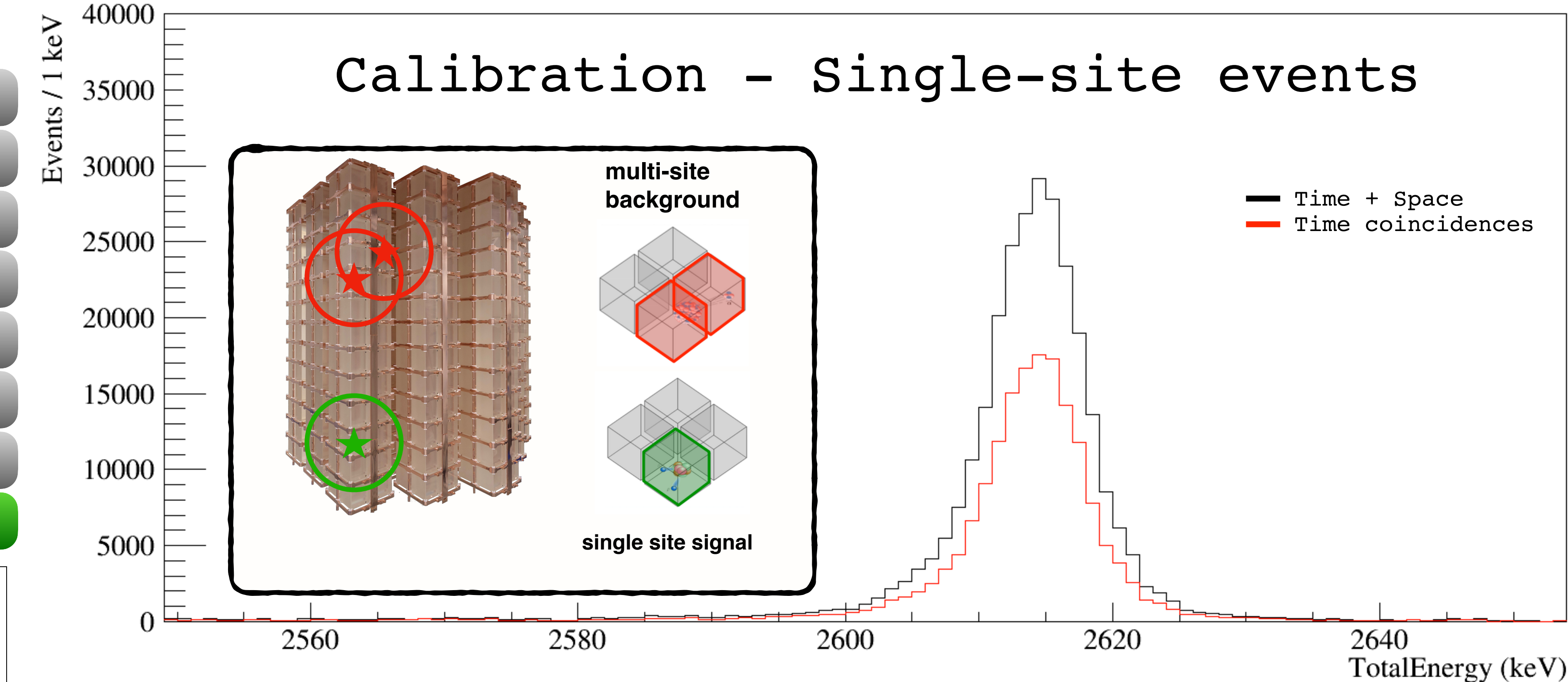
CALIBRATION

BLINDING

COINCIDENCES



PULSE SHAPE ANALYSIS



A space-based definition of coincident events improves signal purity in coincident multiplets

Accidental coincidences strongly suppressed

The CUORE experiment

Data processing

PREPROCESS

AVERAGE PULSE

AVERAGE NOISE

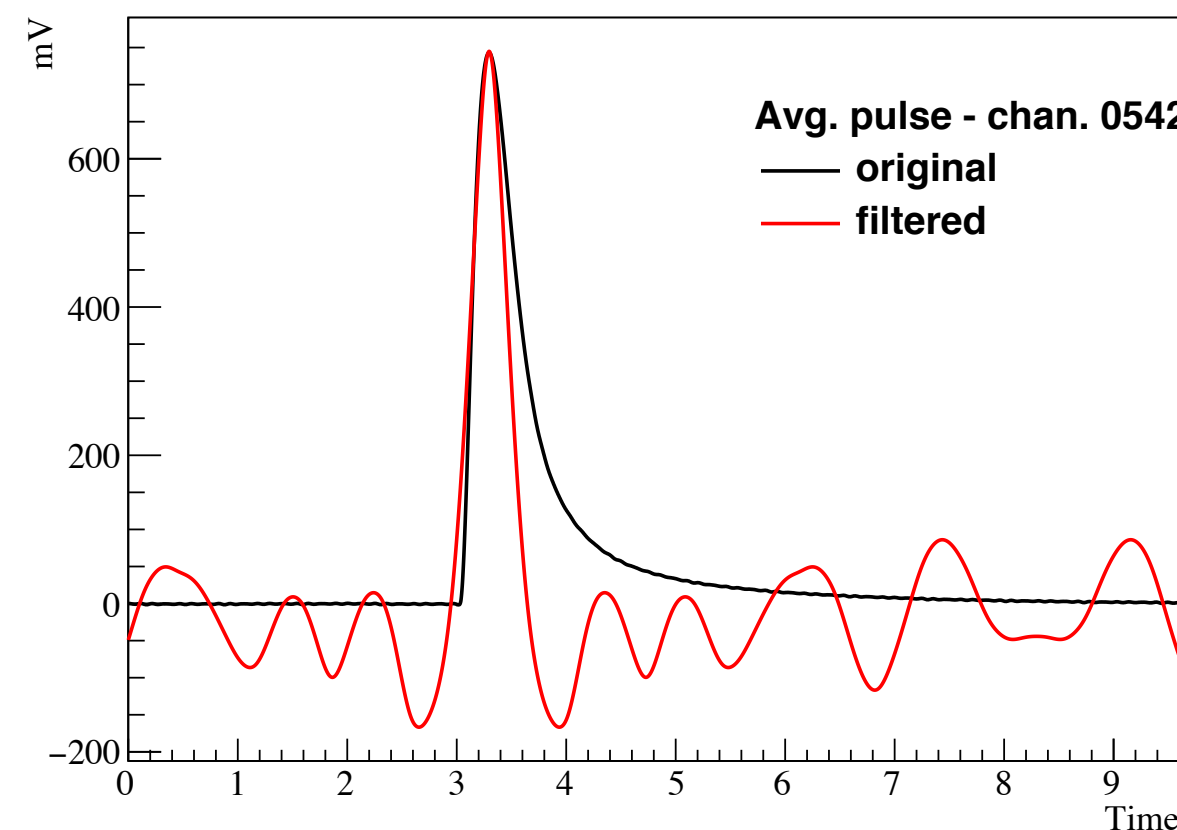
AMPLITUDE

STABILIZATION

CALIBRATION

BLINDING

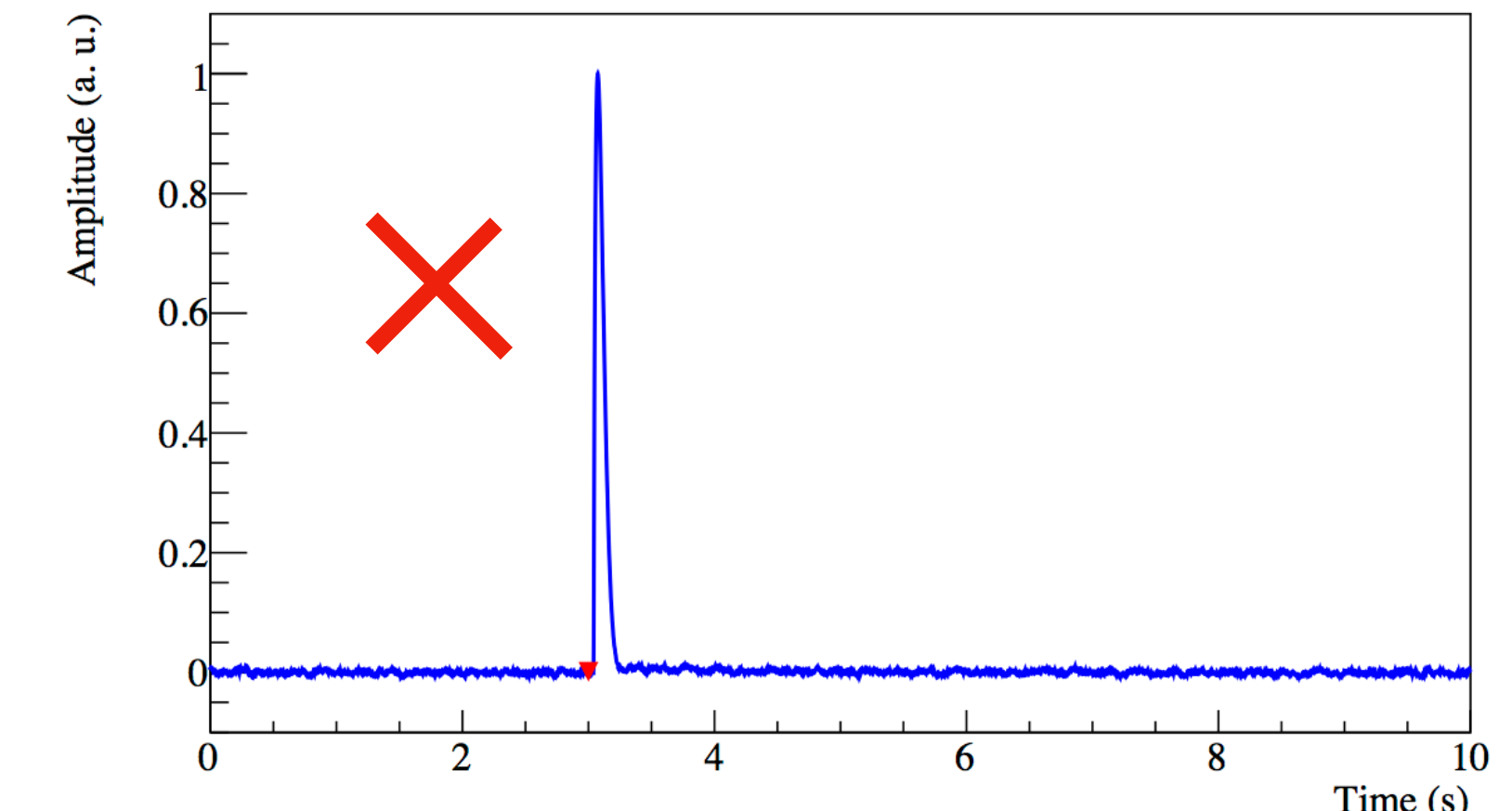
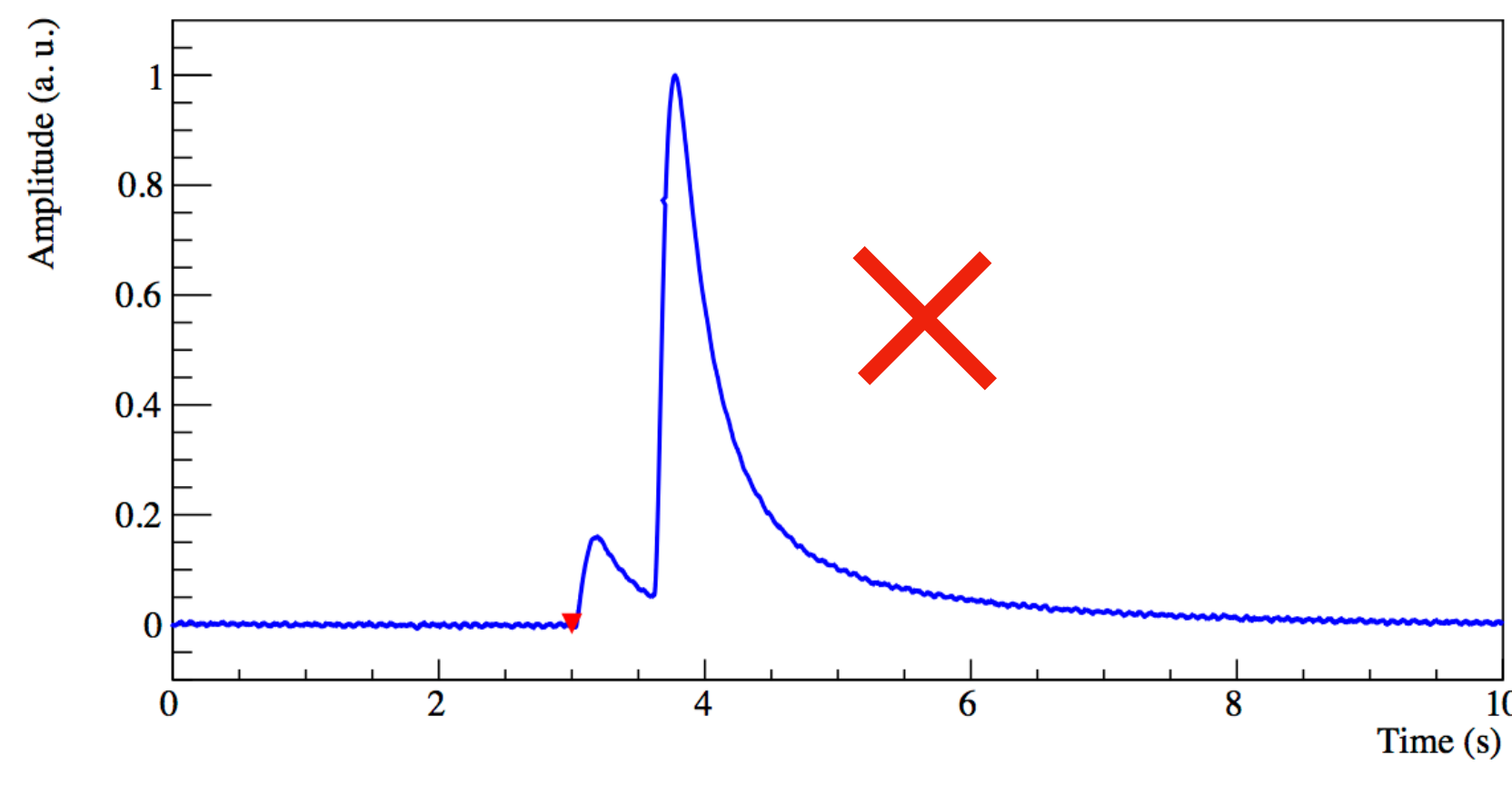
COINCIDENCES

PULSE SHAPE ANALYSIS

6 pulse shape parameters are computed for each event (e.g. rise time) and a 6-dim distance from a control sample is evaluated (Mahalanobis distance)

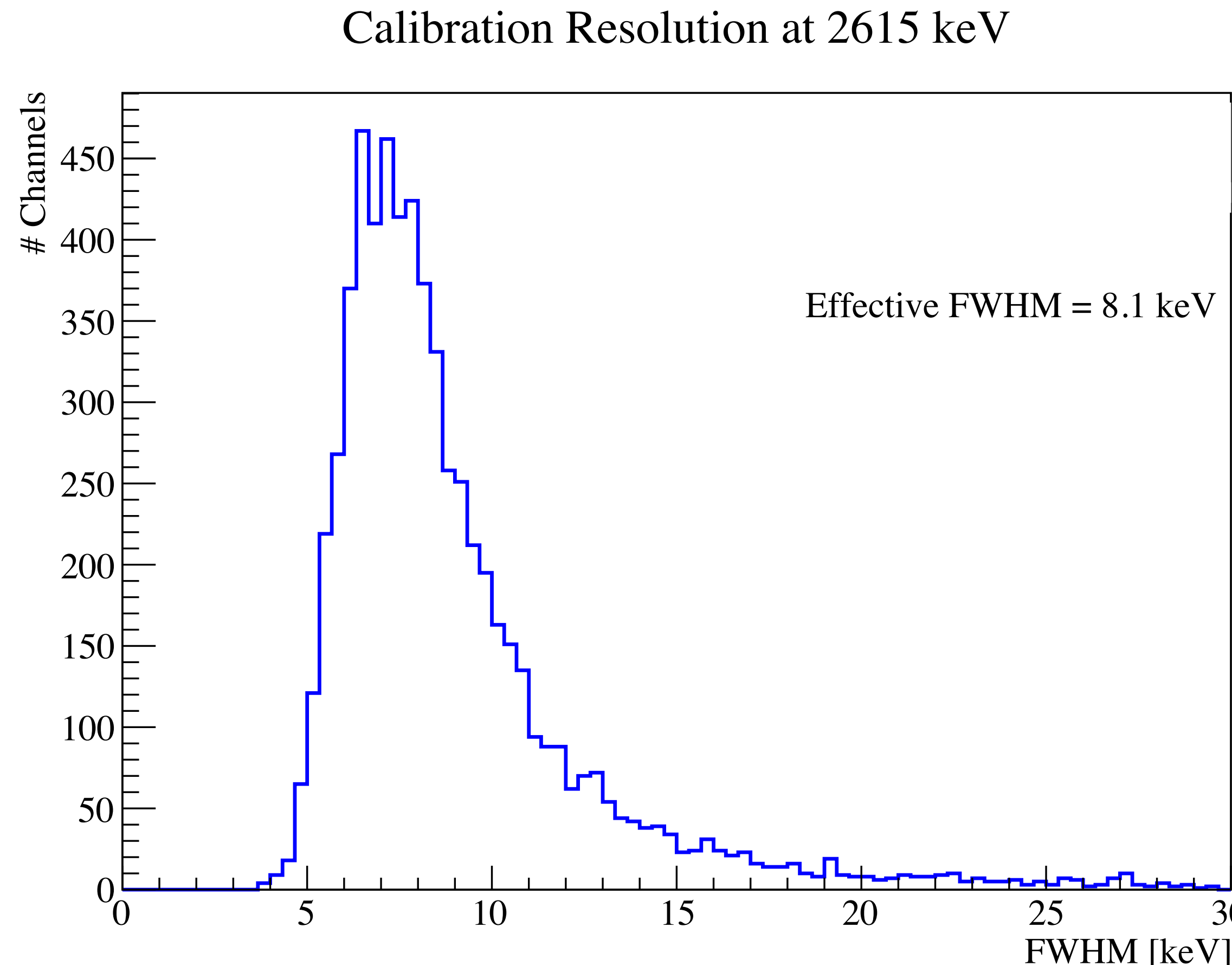
Discards pile-up events

Discards NTD particle interactions



The CUORE experiment

Resolution

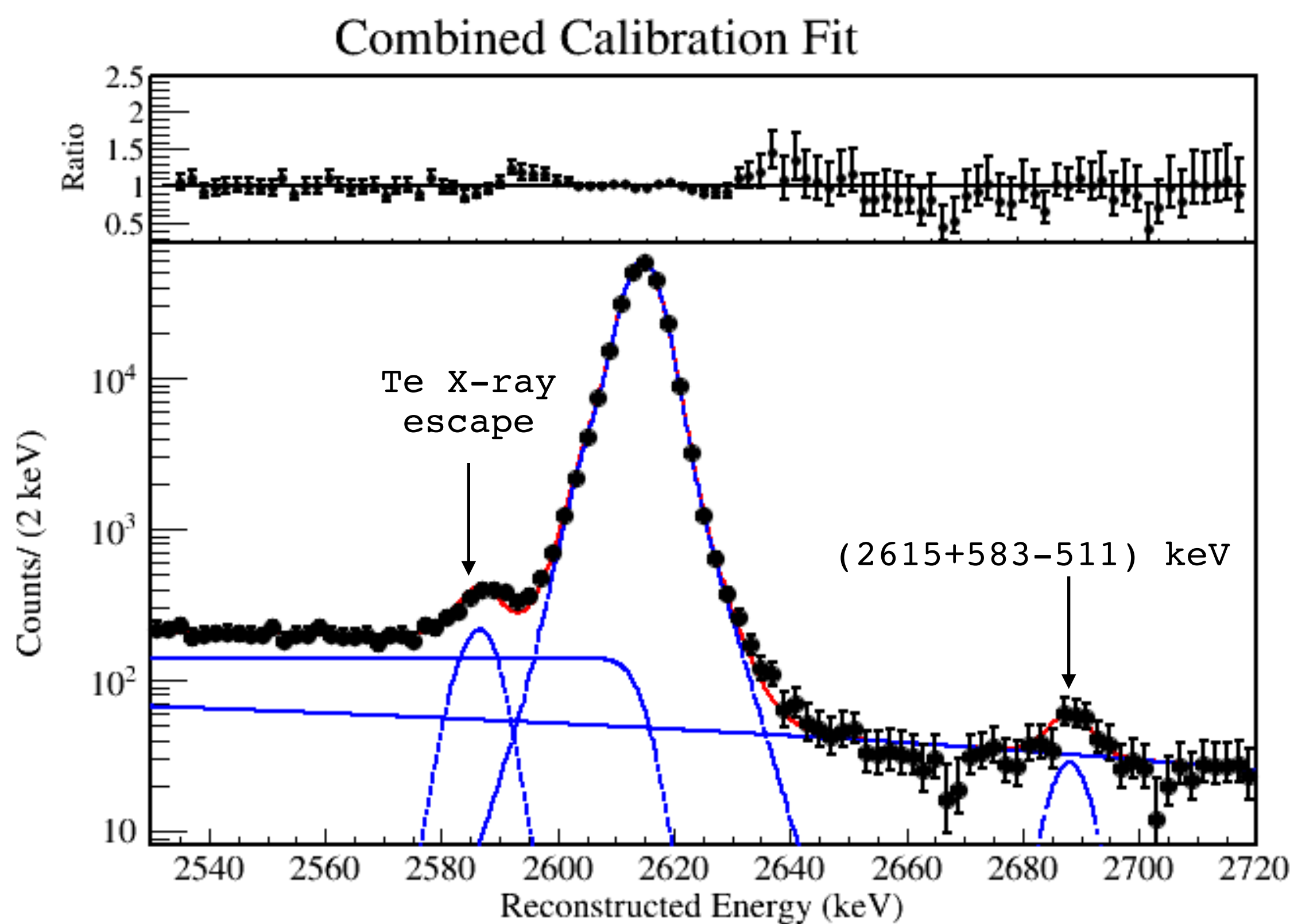


- Full Width Half Maximum (FWHM) resolution computed for each channel-dataset pair
- Exposure weighted harmonic mean effective resolution

$$\frac{1}{\Delta E} = \frac{\sum_{ch,ds} M \Delta t_{ch,ds} / \Delta E_{ch,ds}}{\sum_{ch,ds} M \Delta t_{ch,ds}}$$

The CUORE experiment

Detector response model

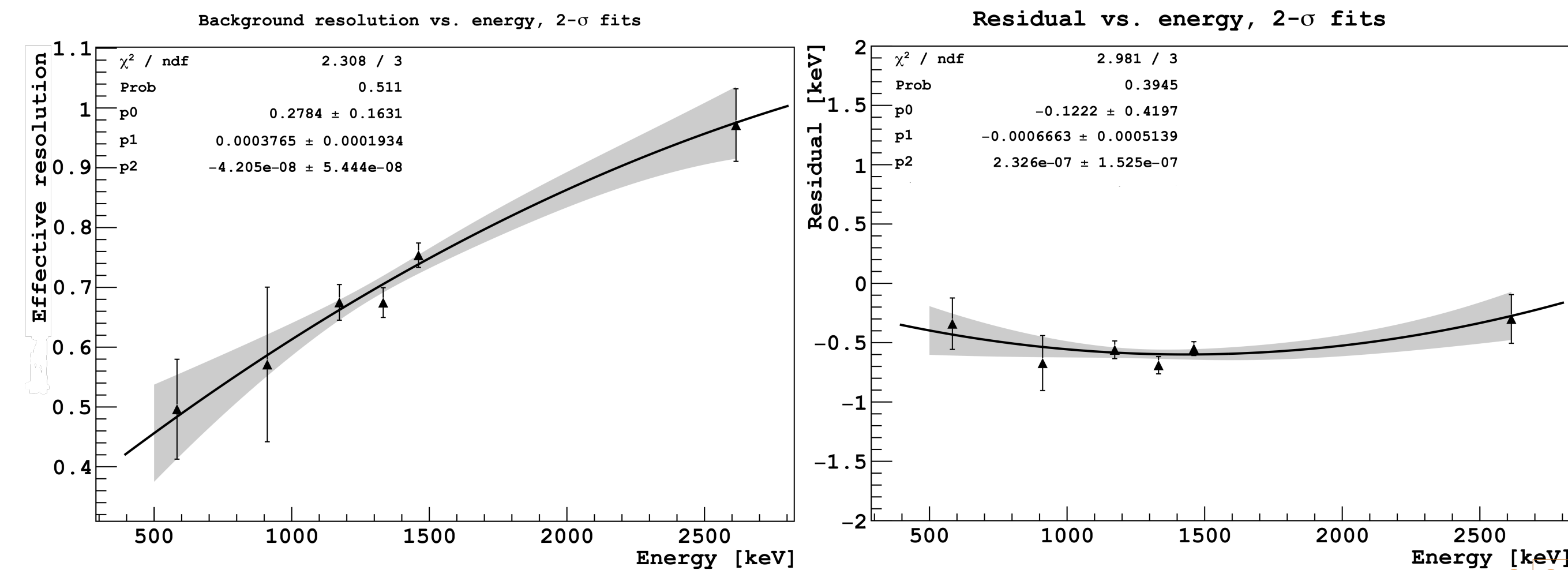
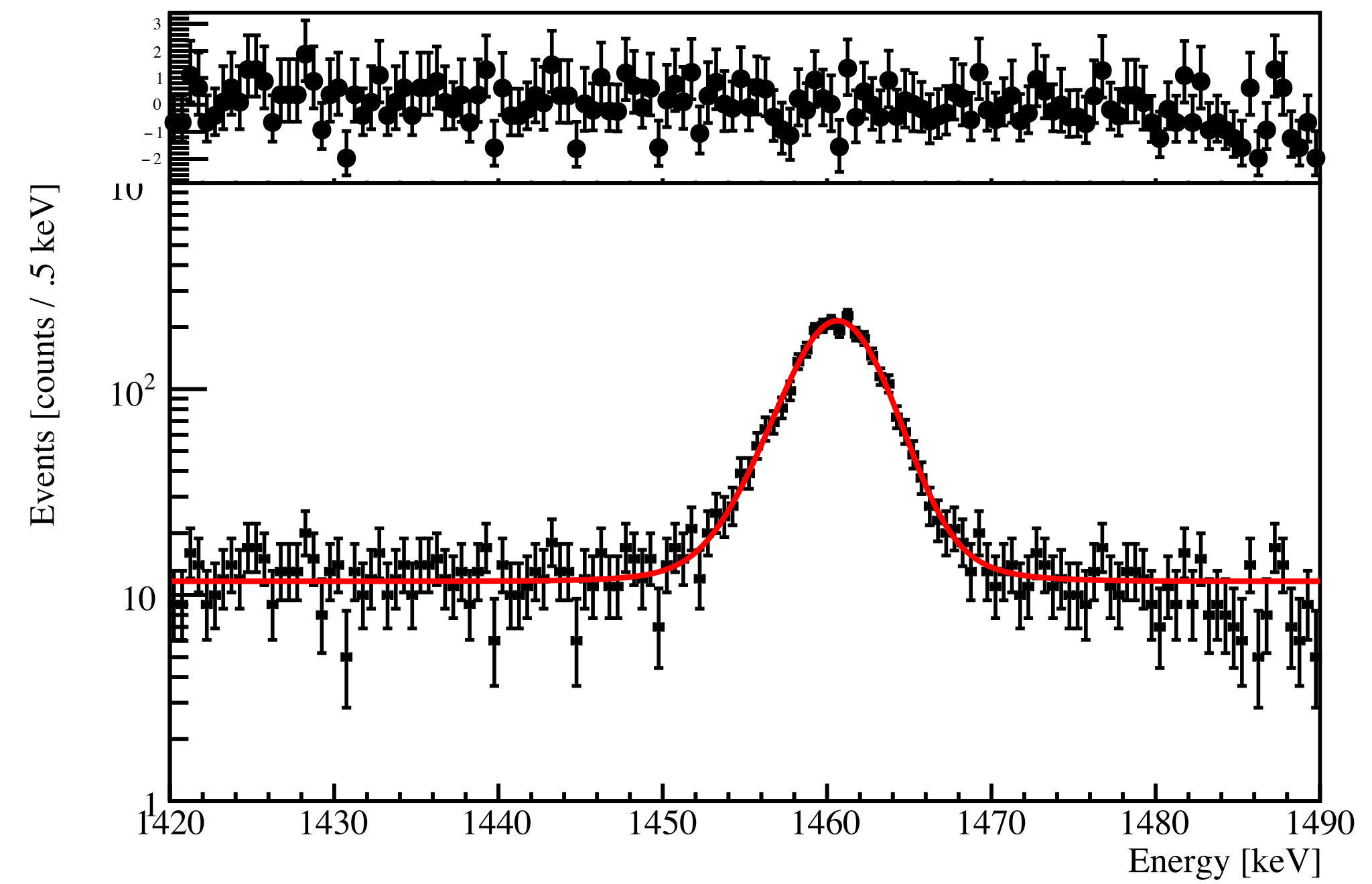


- Fit ^{208}TI line at 2614.5 keV in calibration spectra to precisely evaluate the lineshape on a channel-dataset basis
- Main peak parameterized with a 3-Gaussian superposition
- Fit run simultaneously on each tower to constrain backgrounds and side-structures

The CUORE experiment

Detector response model

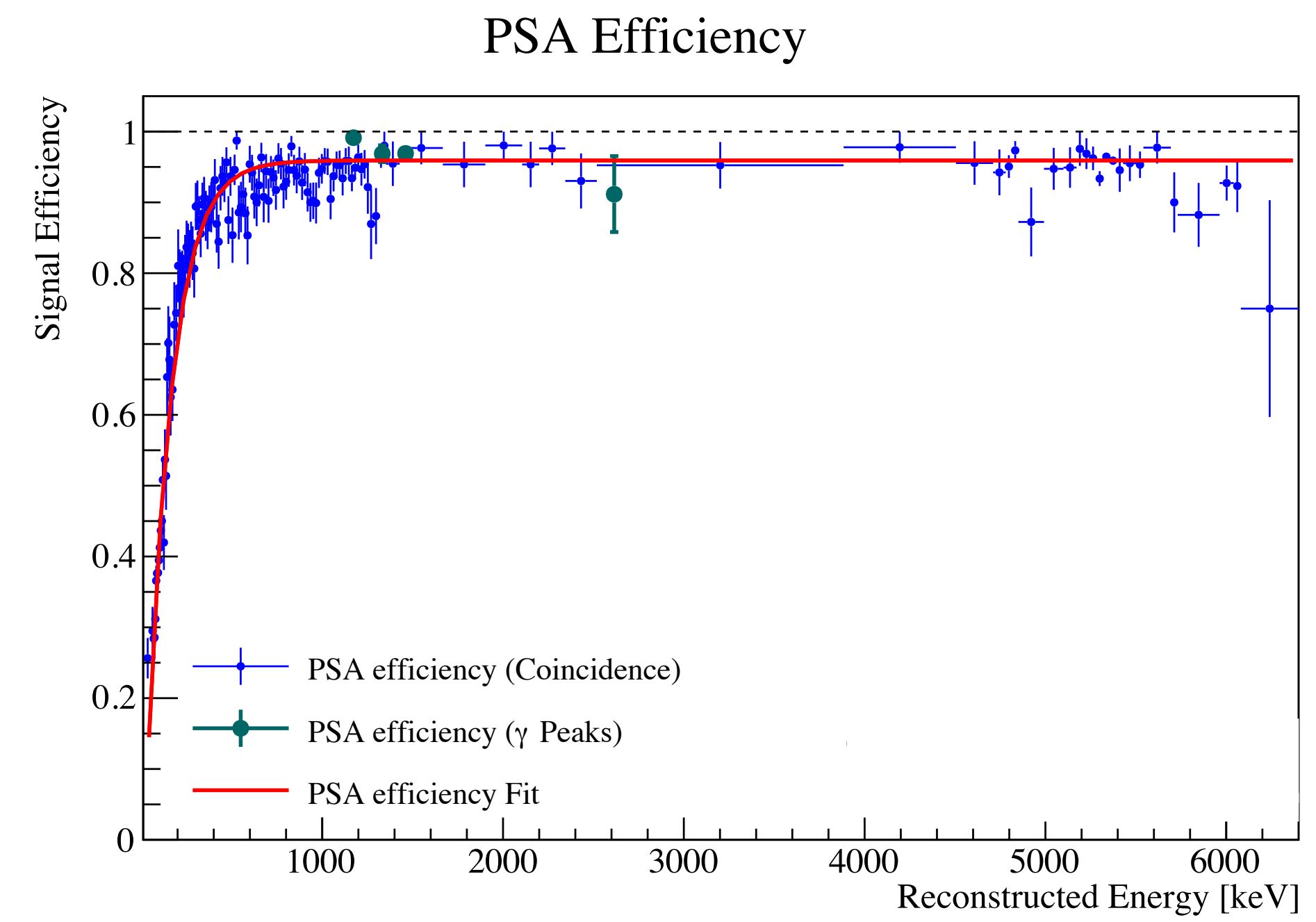
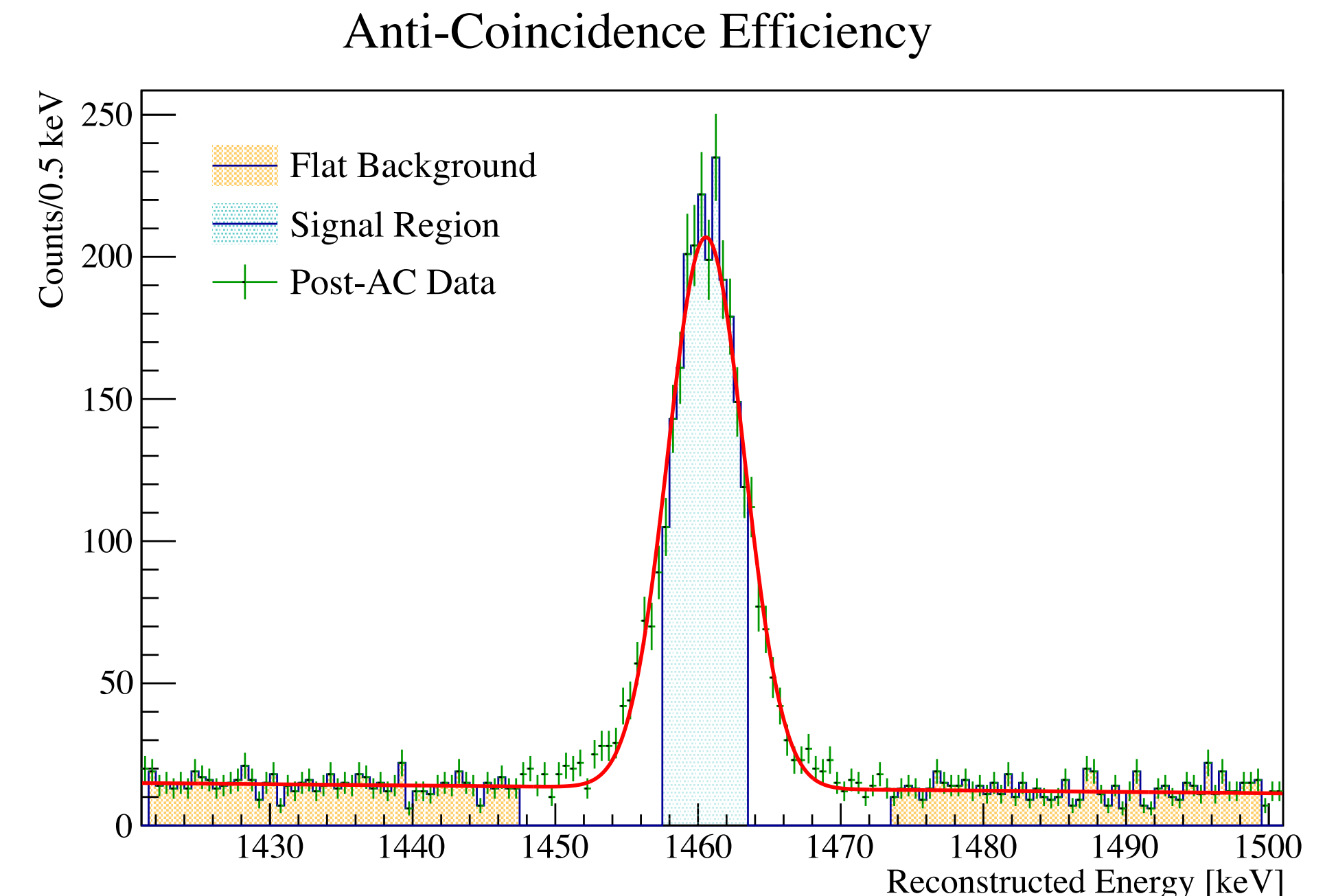
- Extract FWHM from peak fit to physics data
- Fit with 2nd order polynomial and extrapolation to any energy (e.g. Q_{ββ})
- Compute peak position residual from literature values
- Fit with 2nd order polynomial as a function of energy
- Resolution and energy scale uncertainty (systematics)



The CUORE experiment

Detector response model

- Reconstruction efficiency includes
 - ▶ Trigger
 - ▶ Event reconstruction
 - ▶ Pile-up rejection
- Anti-coincidence efficiency quantifies the probability of correctly identifying single-site events
- Pulse Shape Analysis (PSA) Efficiency: fraction of events selected in a 6-dimensional pulse-shape parameter space



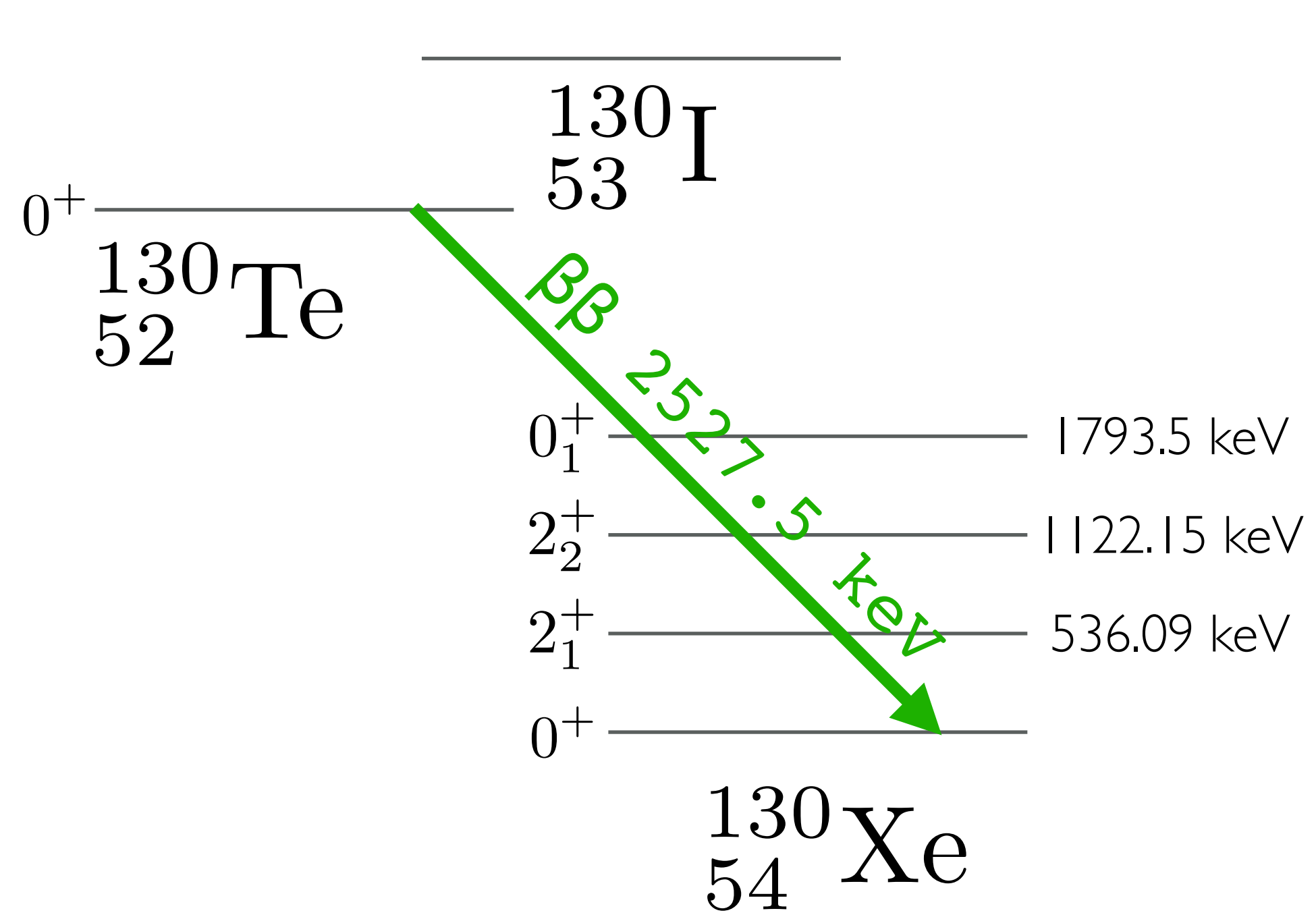


0 $\nu\beta\beta$ Search Ground State Analysis

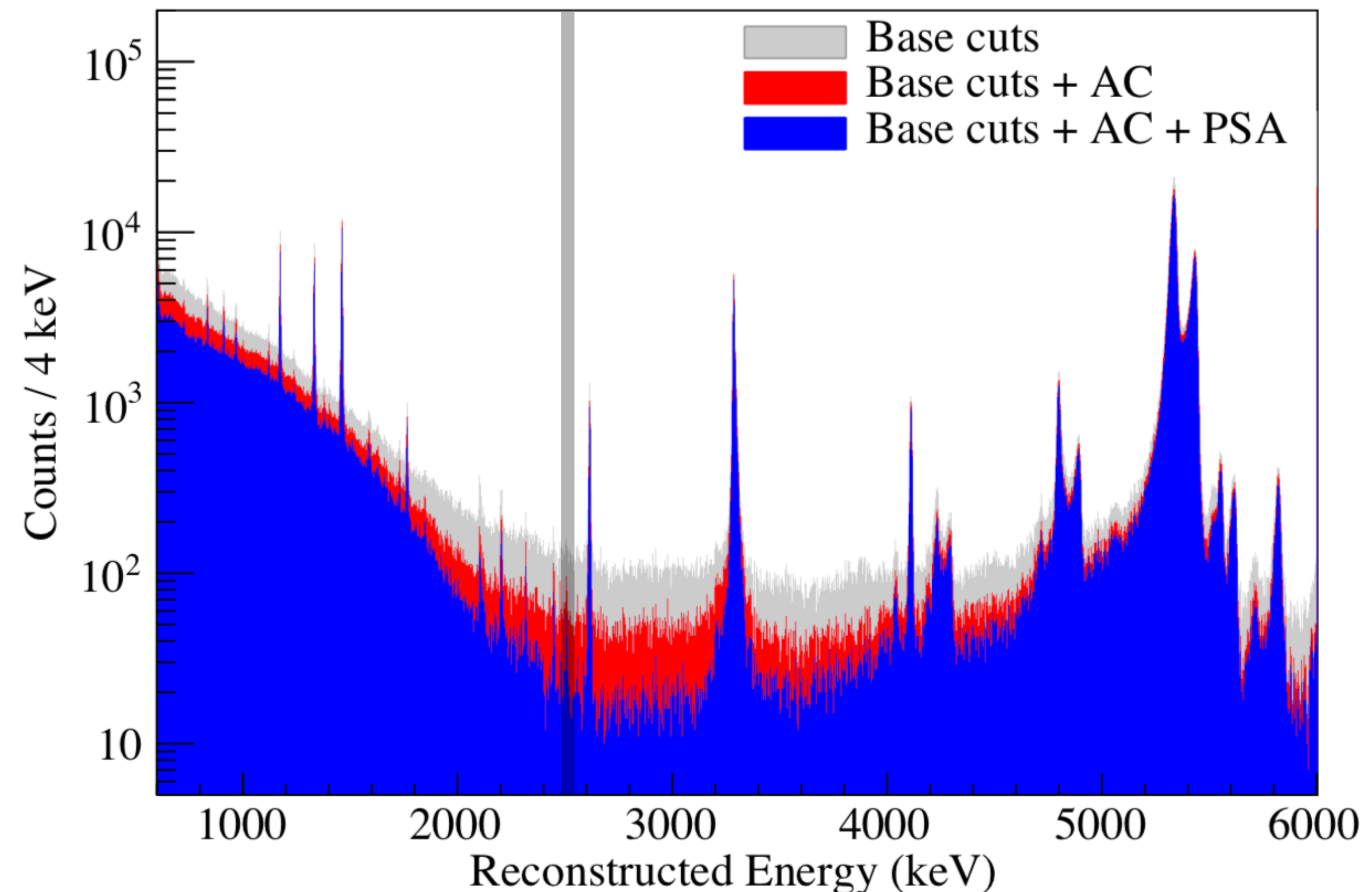


Ground state analysis

[C. Alduino et al., Phys. Rev. Lett. 124, 12 122501 (2020)]



[B. Singh, Nuclear Data Sheets 93, 33 (2001)]

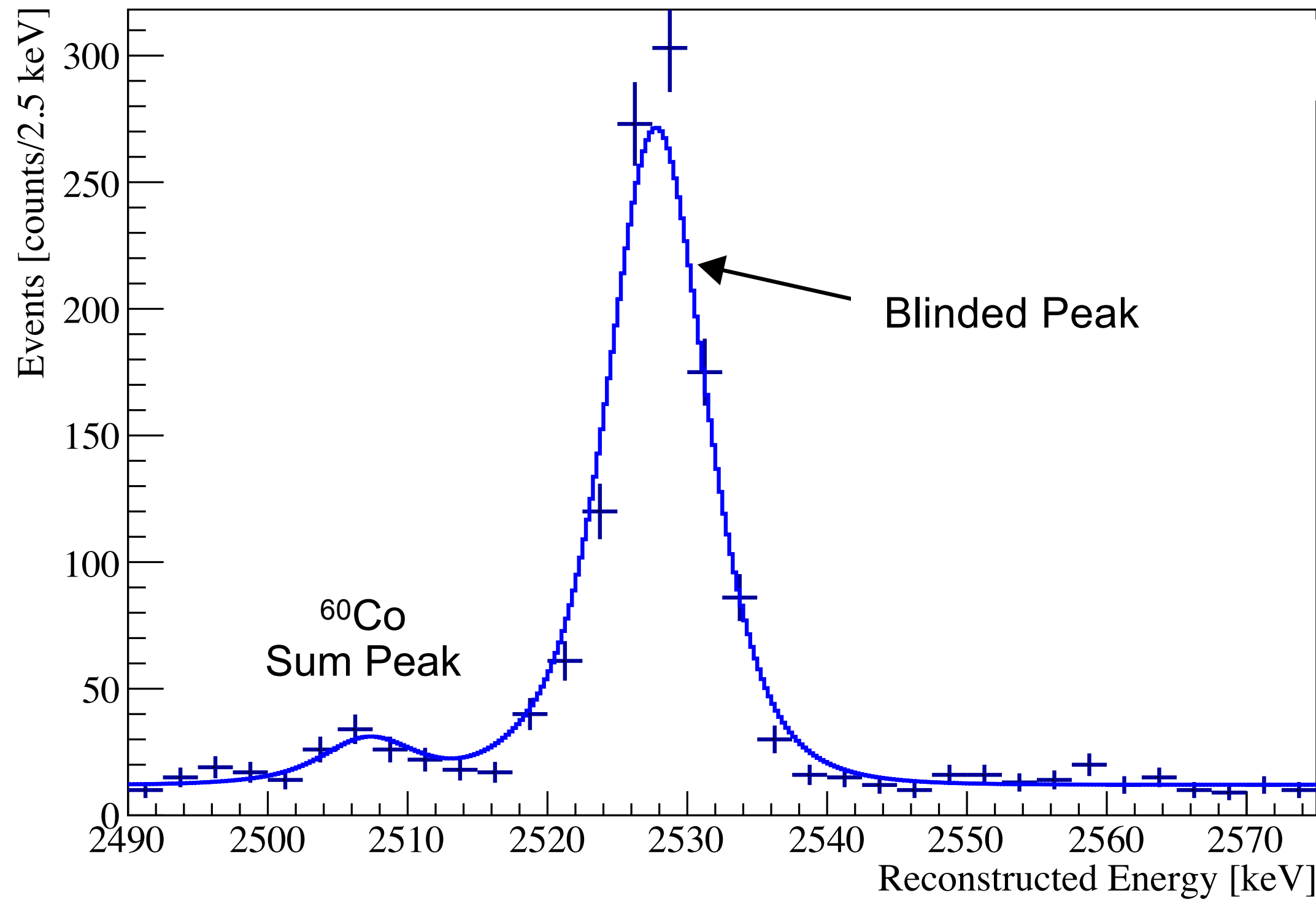


Signal events mostly single-site $\epsilon = 88.3(5) \%$

Ground state analysis

$$P(\vec{\theta} | \vec{E}, H_{S+B}) = \frac{\mathcal{L}(\vec{E} | \vec{\theta}, H_{S+B}) \cdot \pi(\vec{\theta} | H_{S+B})}{\int_{\Omega} \mathcal{L} \pi d\vec{\theta}}$$

$$\mathcal{L}(\vec{E} | \vec{\theta}, H_{S+B}) = \prod_{dataset\ channel} \prod_{channel} \left[\frac{e^{-\lambda} \lambda^n}{n!} \prod_{event\ i} \left(\frac{S}{\lambda} pdf_{0\nu\beta\beta}(E_i | \vec{\theta}) + \frac{C}{\lambda} pdf_{^{60}\text{Co}}(E_i | \vec{\theta}) + \frac{b}{\lambda} \frac{1}{\Delta E} \right) \right]$$

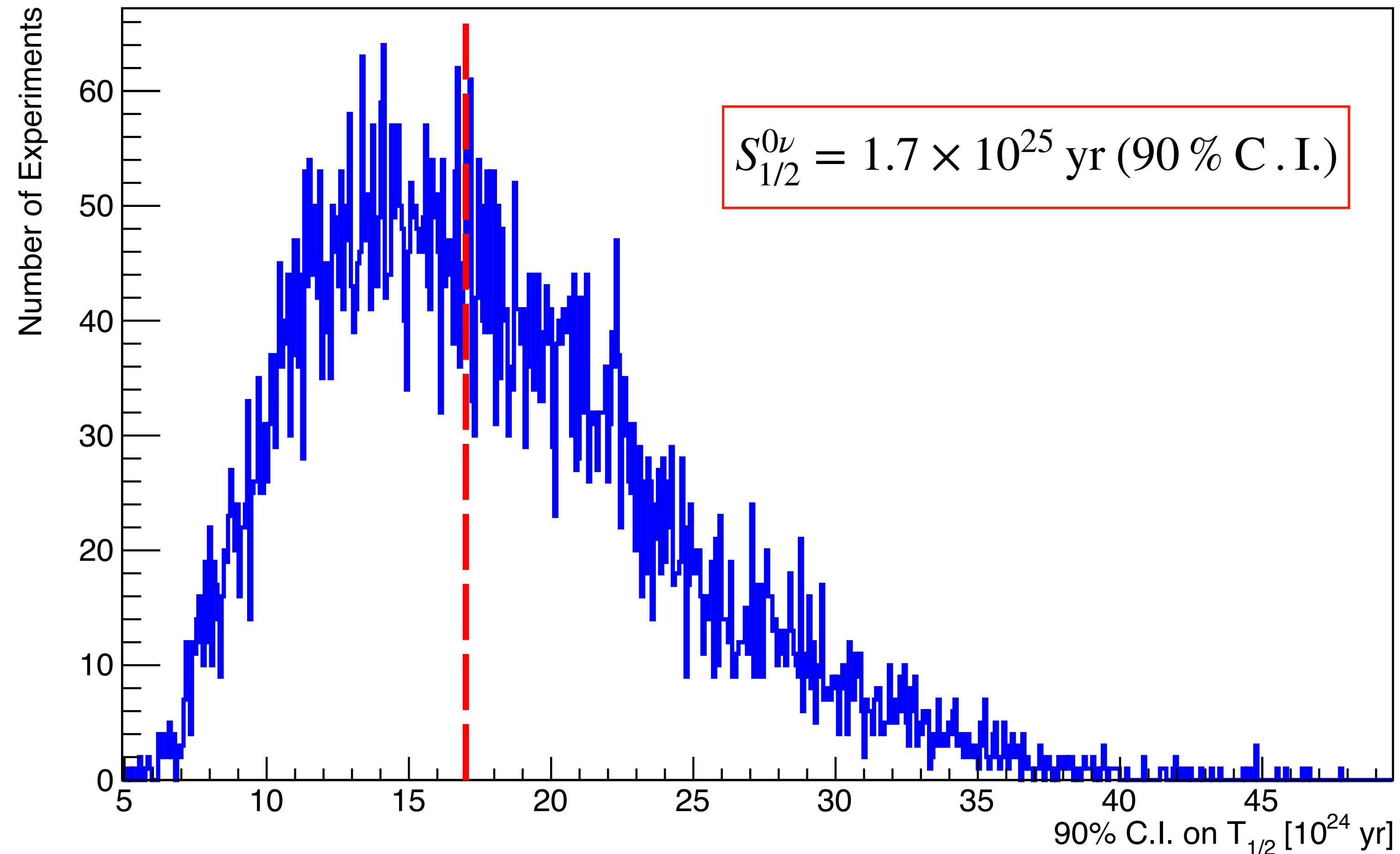


Region Of Interest (ROI)
[2490, 2575] keV

[C. Alduino et al., Phys. Rev. Lett. 124, 12 122501 (2020)]

Ground state analysis

Projected Sensitivity

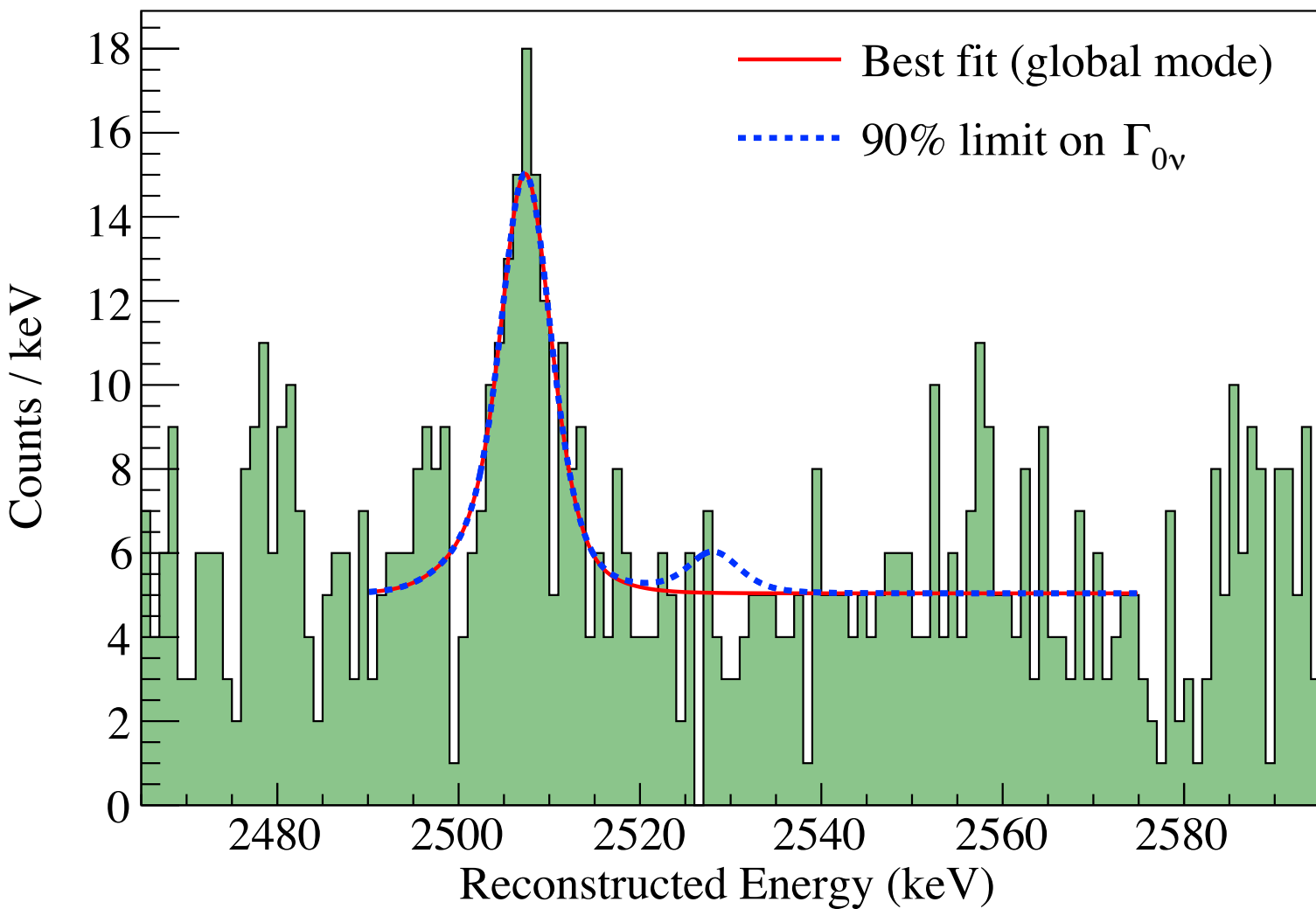
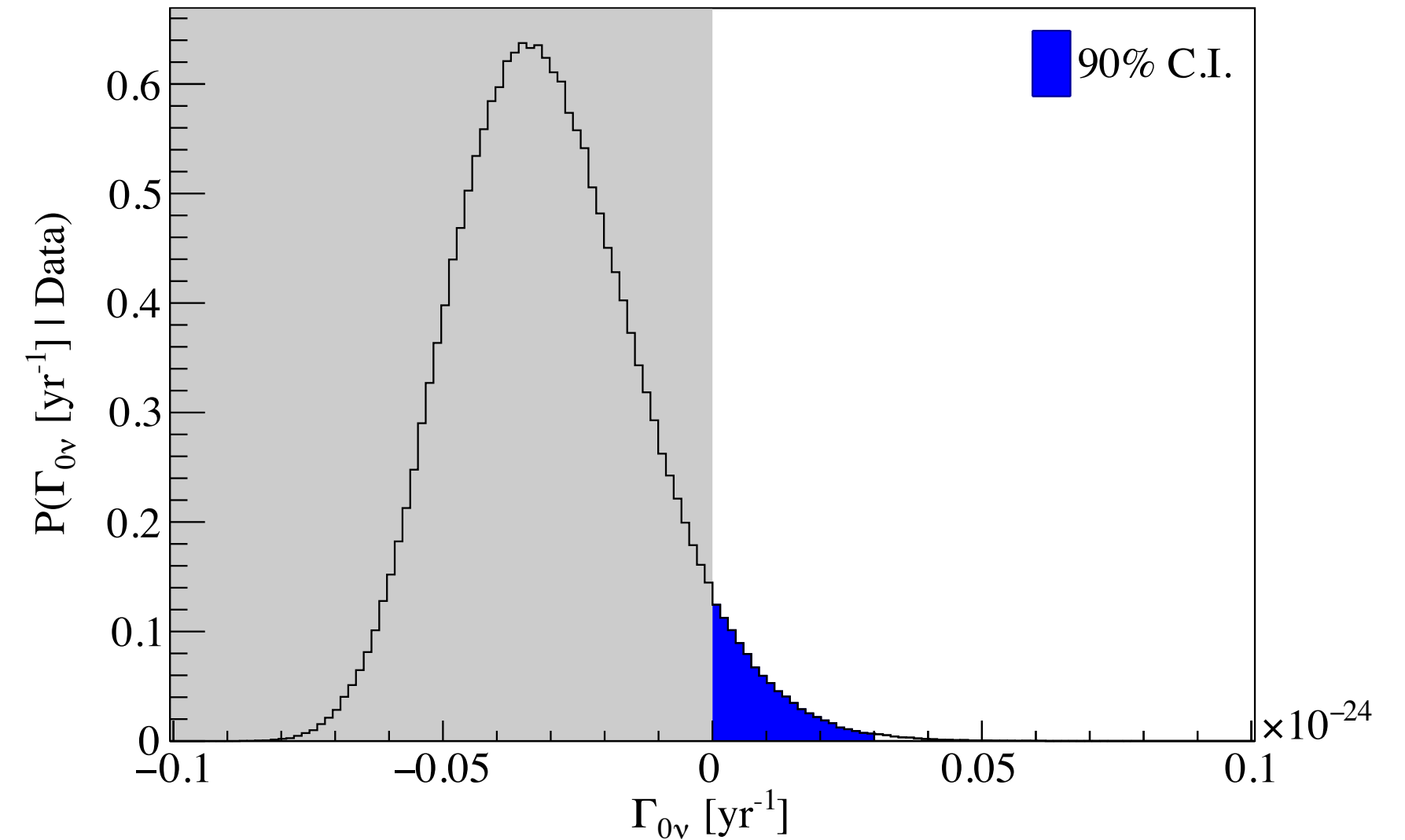


10⁴ Toy Monte Carlo pseudo-experiments are generated and fit to extract the median sensitivity

[C. Alduino et al., Phys. Rev. Lett. 124, 12 122501 (2020)]

Ground state analysis

CUORE ROI Spectrum

Posterior for $\Gamma_{0\nu}$ 

[C. Alduino et al., Phys. Rev. Lett. 124, 12 122501 (2020)]

- Total exposure TeO_2 : $372.5 \text{ kg} \cdot \text{yr}$
- Likelihood model: flat continuum (BI), posited peak for $0\nu\beta\beta$ (rate), peak for ^{60}Co (rate + position)
- Unbinned fit on physical range (rates non-negative), uniform prior on the rate parameter $\Gamma_{0\nu}$
- Systematics: repeat fits with nuisance parameters, allow negative rates (<0.4% impact on limit)

- No evidence for $0\nu\beta\beta$ decay

$$T_{1/2}^{0\nu} > 3.2 \times 10^{25} \text{ yr (90\% C.I.)}$$

- Interpretation in context of light Majorana neutrino exchange

$$m_{\beta\beta} < 75 - 350 \text{ meV}$$

Detector Performance Parameters

Background Index

$$(1.38 \pm 0.07) \times 10^{-2} \text{ cnts}/(\text{keV} \cdot \text{kg} \cdot \text{yr})$$

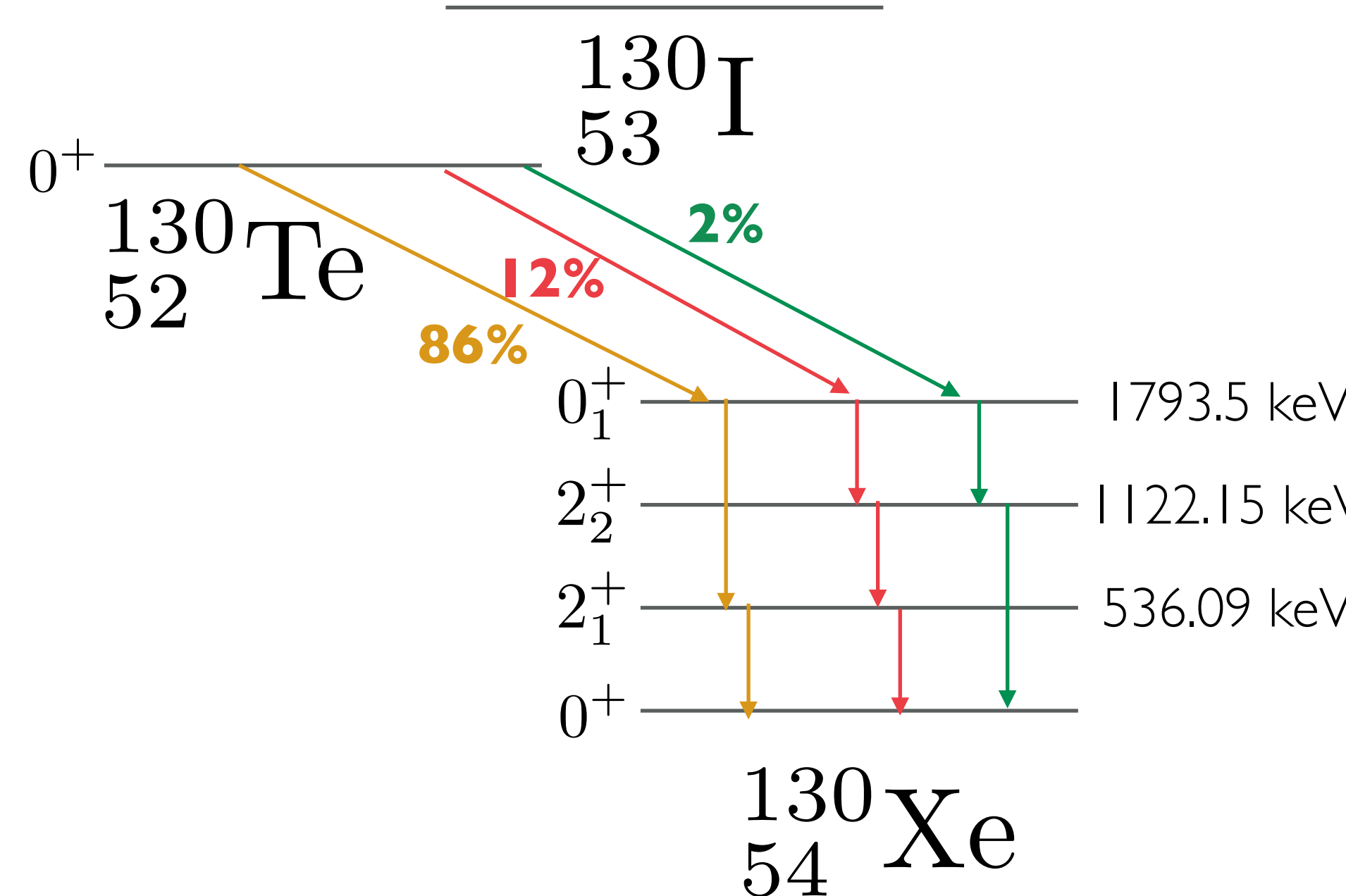
Characteristic FWHM ΔE at $Q_{\beta\beta}$

$$7.0 \pm 0.3 \text{ keV}$$

$\beta\beta$ Search Excited State Analyses



Excited states analysis



[B. Singh, Nuclear Data Sheets 93, 33 (2001)]

There are 3 possible de-excitation patterns:

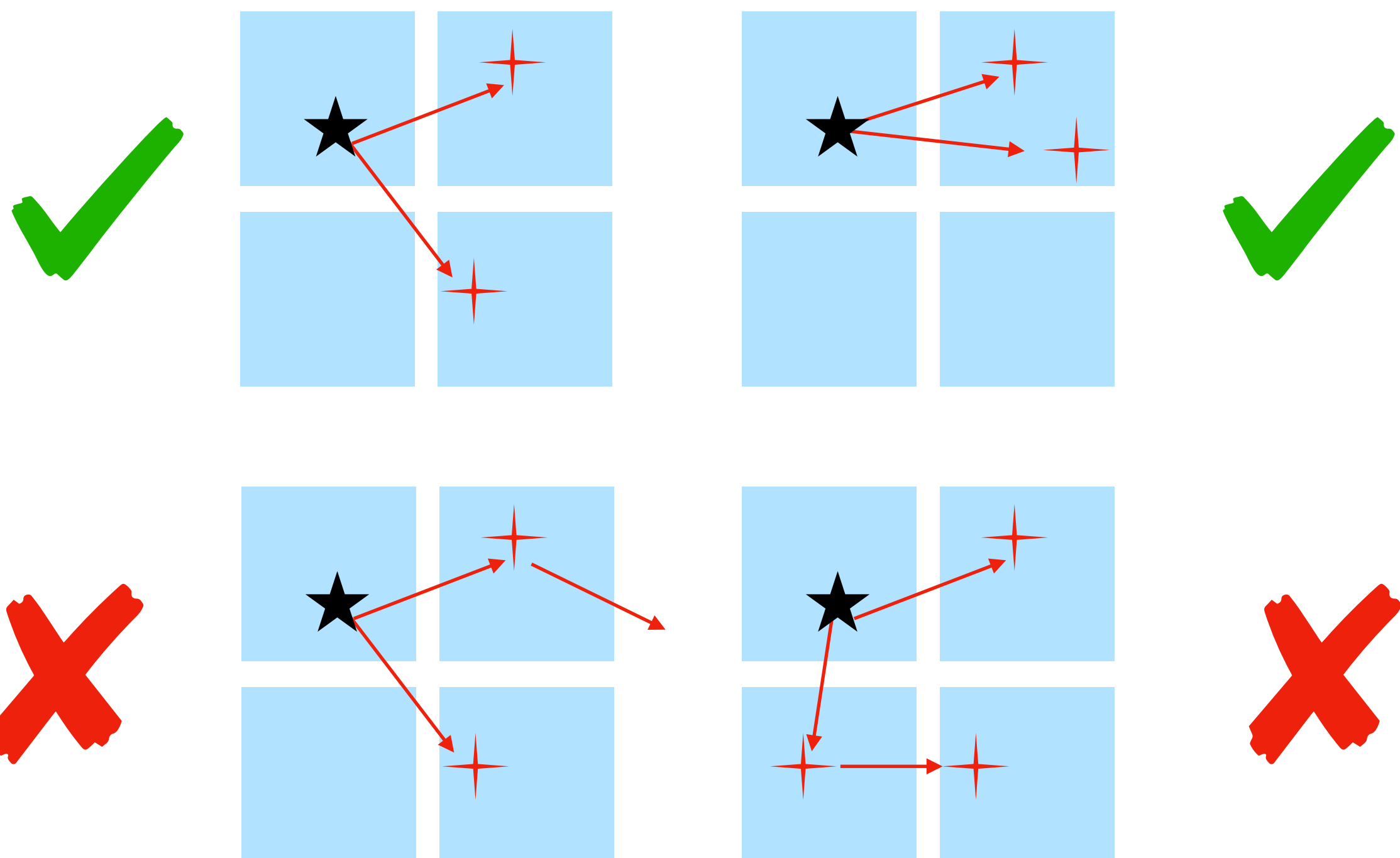
- A. (86%) $\beta\beta_{0-734} + \gamma_{1257} + \gamma_{536}$
- B. (12%) $\beta\beta_{0-734} + \gamma_{671} + \gamma_{586} + \gamma_{536}$
- C. (2%) $\beta\beta_{0-734} + \gamma_{1122} + \gamma_{671}$

Excited states analysis

Full containment requirement

- Each final state particle (except neutrinos) must fully release its energy in no more than one crystal
- Not considering partially contained signatures
- Significantly simpler analysis
- Significant efficiency loss due to this choice

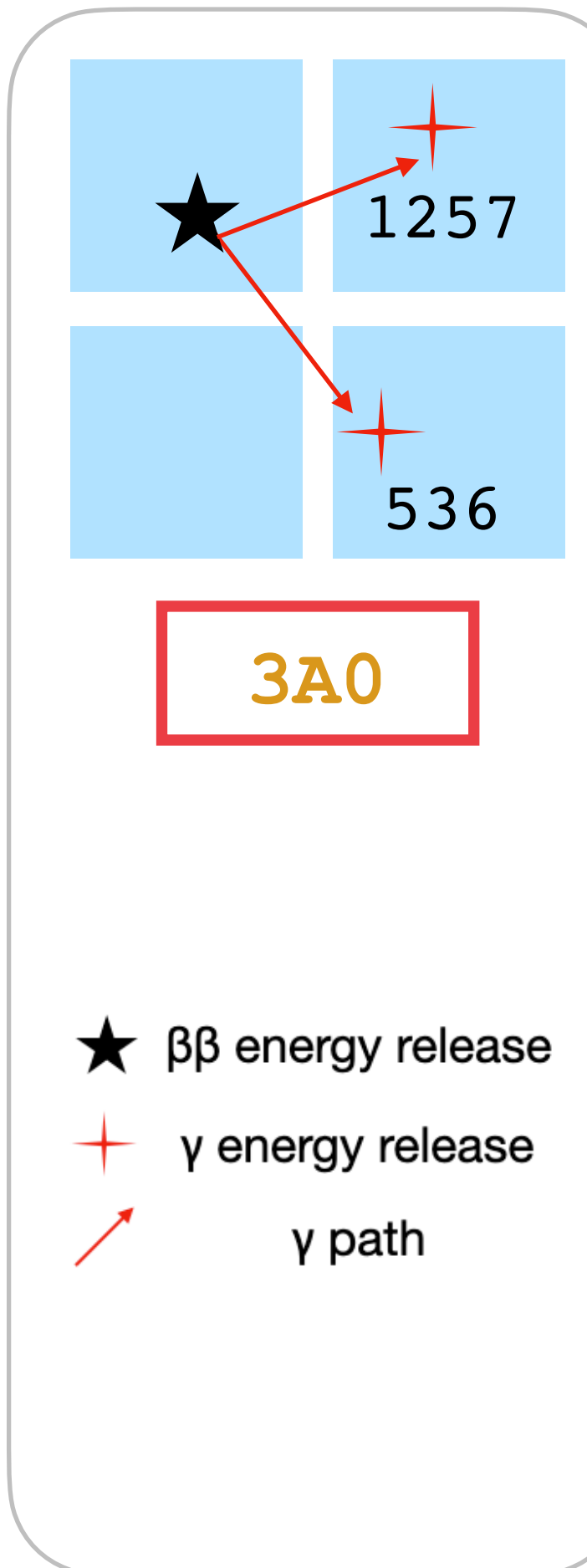
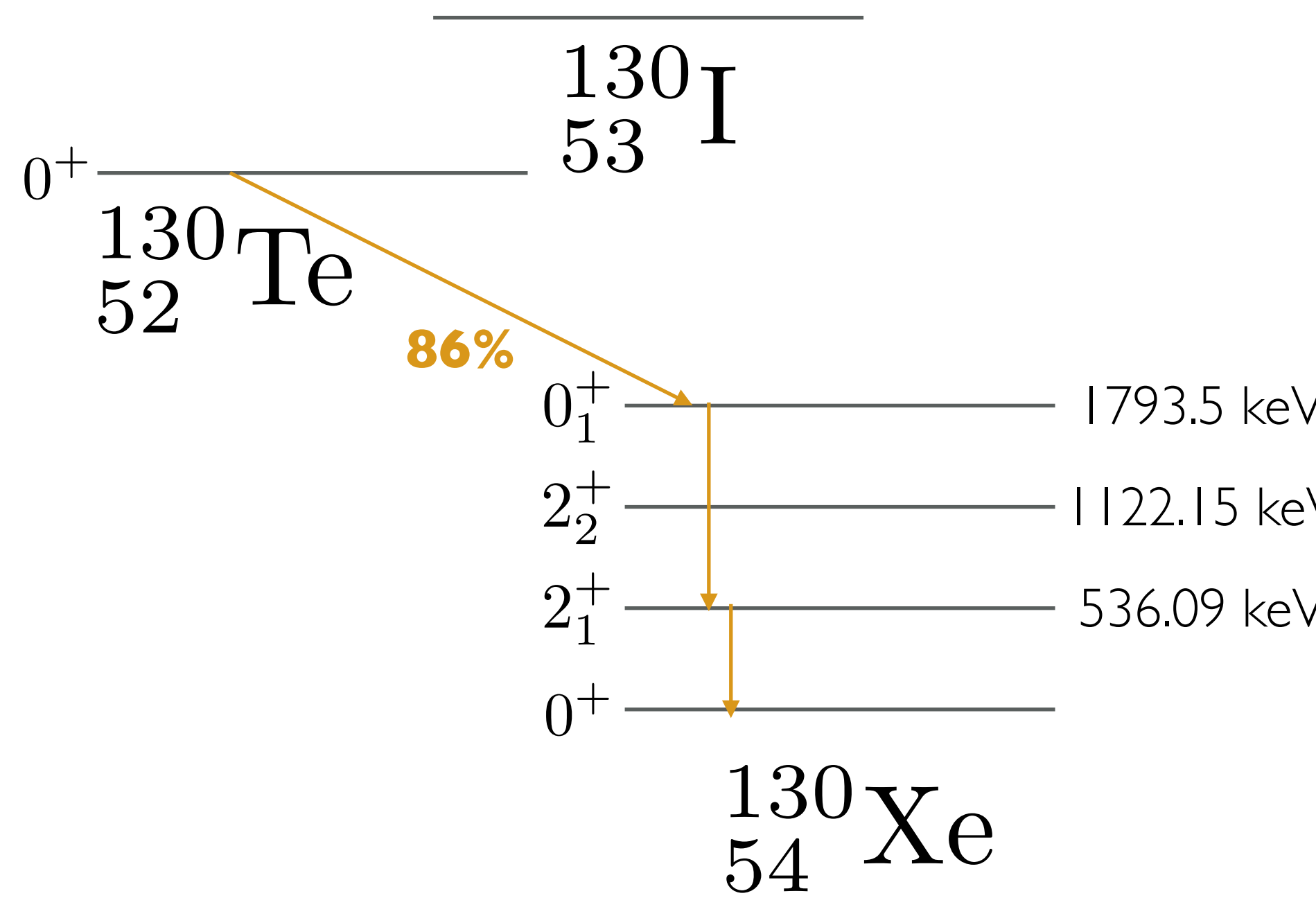
★ $\beta\beta$ energy release
+ γ energy release
→ γ path



Excited states analysis

Labelling signatures

Let us build a **Multiplicity 3** (3 crystals involved) signature coming from de-excitation **pattern A**



Number of involved crystals

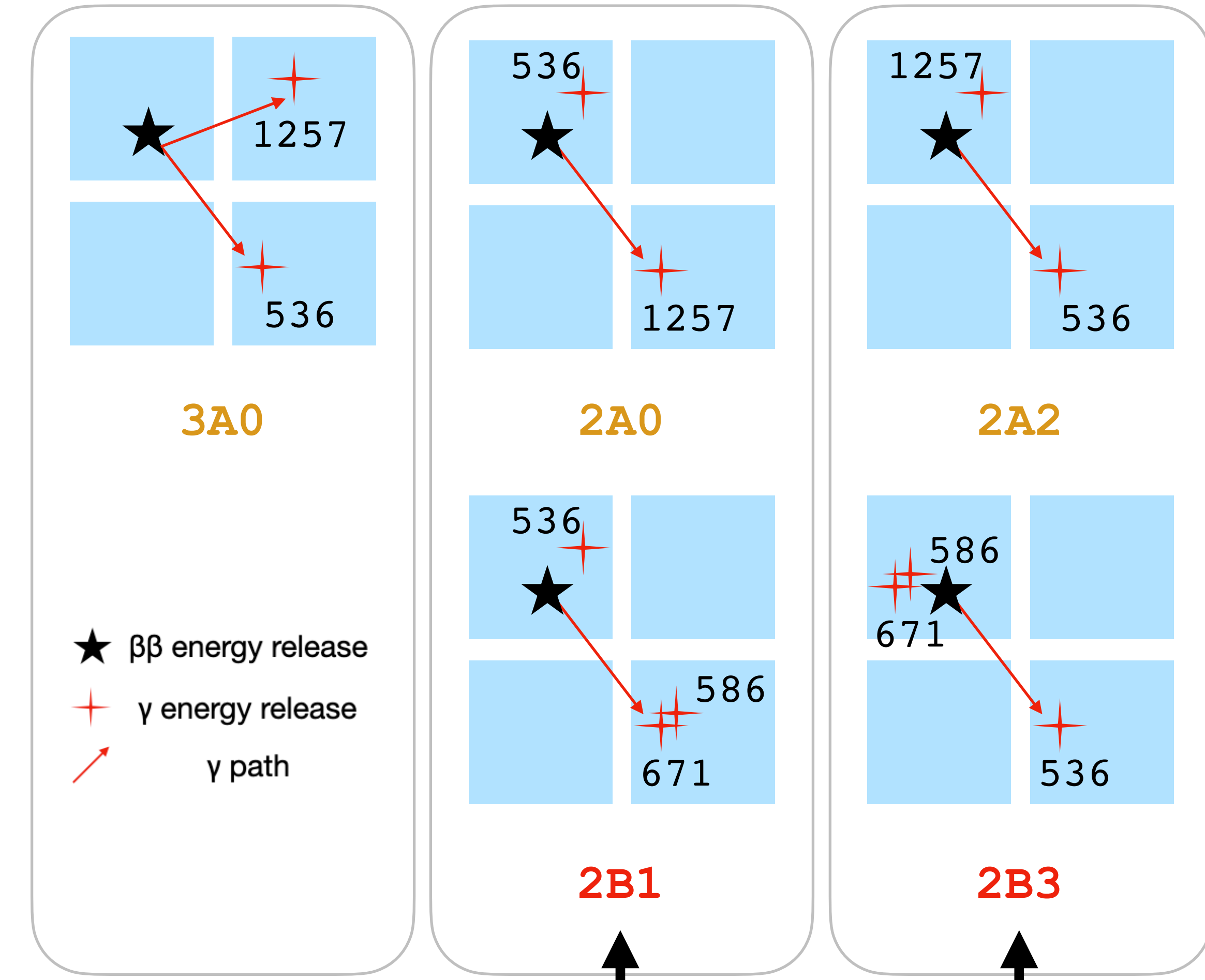
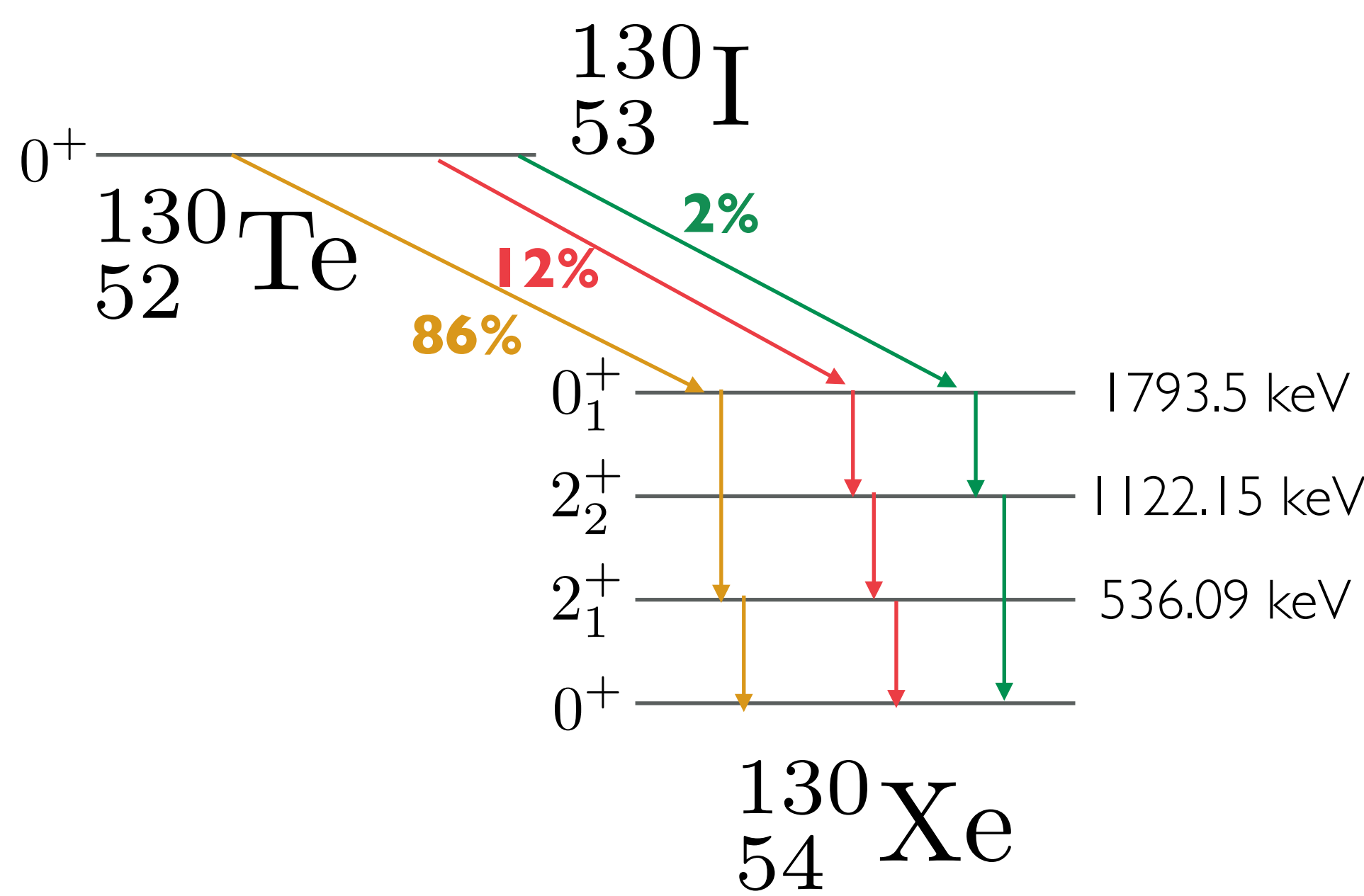
[Multiplicity] [Pattern] [integer index]

^{130}Xe de-excitation gamma pattern

Indexing possible combinations

Excited states analysis

Experimental signatures



Same experimental signature, 2 different de-excitation patterns

Excited states analysis

Ranking experimental signatures

$$S(\epsilon_s, B_s) = \theta(B_s - 1) \frac{\epsilon_s}{\sqrt{B}} + \theta(1 - B_s) \frac{5\epsilon_s}{-\ln(3 \cdot 10^{-7})}$$

background-free background-dominated

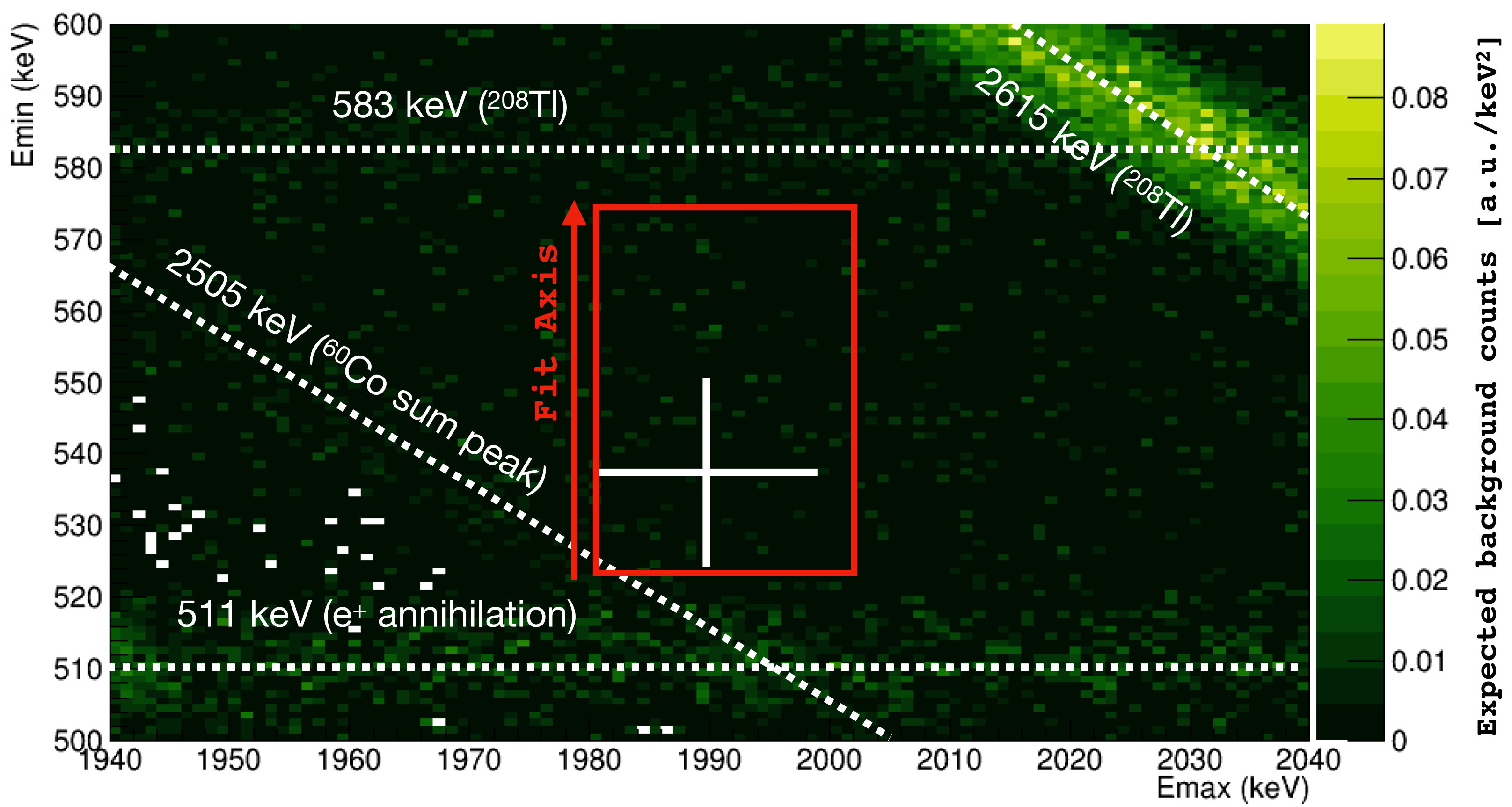
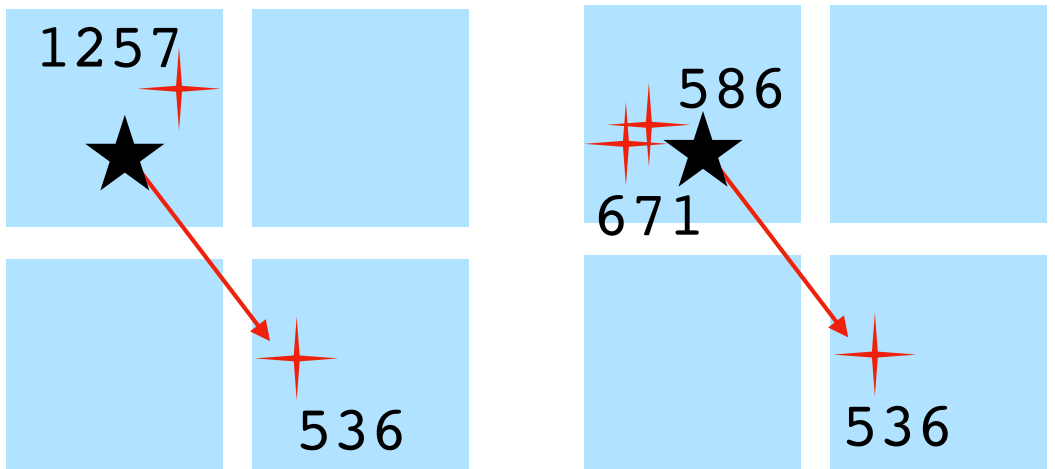
- Many possible signatures
- Most contribute negligibly to the sensitivity
- A threshold of $S > 5\%$ was set
- Three signatures account for 80-90% of the overall sensitivity

$S_{2\nu}(S_{0\nu})$ Signature	Crystal 1 [keV]	Crystal 2 [keV]	Crystal 3 [keV]	Crystal 4 [keV]
39.8% (38.5%) 2A0-2B1	$\beta\beta + \gamma_{(A2)}$ $\beta\beta + \gamma_{(B3)}$ 536 - 1270	$\gamma_{(A1)}$ $\gamma_{(B1)} + \gamma_{(B2)}$ 1257		
	$\gamma_{(A1)} + \gamma_{(A2)}$ $\gamma_{(B1)} + \gamma_{(B2)} + \gamma_{(B3)}$ $\gamma_{(C1)} + \gamma_{(C2)}$ 1793	$\beta\beta$ $\beta\beta$ $\beta\beta$ 0 - 734		
21.6% (24.7%) 2A2-2B3	$\beta\beta + \gamma_{(A1)}$ $\beta\beta + \gamma_{(B1)} + \gamma_{(B2)}$ 1257 - 1991	$\gamma_{(A2)}$ $\gamma_{(B3)}$ 536		
25.5% (20.3%) 3A0	$\gamma_{(A1)}$ 1257	$\beta\beta$ 0 - 734	$\gamma_{(A2)}$ 536	
2.4% (2.8%) 2B0-2C2	$\beta\beta + \gamma_{(B2)} + \gamma_{(B3)}$ $\beta\beta + \gamma_{(C1)}$ 1122 - 1856	$\gamma_{(B1)}$ $\gamma_{(C2)}$ 671		
0.2% (0.1%) 2B4	$\beta\beta + \gamma_{(B2)}$ 586 - 1320	$\gamma_{(B1)} + \gamma_{(B3)}$ 1207		
1.4% (2.0%) 2B5	$\beta\beta + \gamma_{(B1)} + \gamma_{(B3)}$ 1207 - 1941	$\gamma_{(B2)}$ 536		
1.0% (0.9%) 2B6-2C0	$\beta\beta + \gamma_{(B1)}$ $\beta\beta + \gamma_{(C2)}$ 671 - 1405	$\gamma_{(B2)} + \gamma_{(B3)}$ $\gamma_{(C1)}$ 1122		
1.1% (1.1%) 3B0	$\beta\beta + \gamma_{(B3)}$ 536 - 1270	$\gamma_{(B1)}$ 671	$\gamma_{(B2)}$ 586	
0.8% (0.5%) 3B1-3C0	$\gamma_{(B2)} + \gamma_{(B3)}$ $\gamma_{(C1)}$ 1122	$\beta\beta$ $\beta\beta$ 0 - 734	$\gamma_{(B1)}$ $\gamma_{(C2)}$ 671	
0.1% (0.1%) 3B2	$\gamma_{(B1)} + \gamma_{(B2)}$ 1257	$\beta\beta$ 0 - 734	$\gamma_{(B3)}$ 536	
1.3% (1.0%) 3B3	$\beta\beta + \gamma_{(B2)}$ 586 - 1320	$\gamma_{(B1)}$ 671	$\gamma_{(B3)}$ 536	
0.1% (0.1%) 3B4	$\gamma_{(B1)} + \gamma_{(B3)}$ 1207	$\beta\beta$ 0 - 734	$\gamma_{(B2)}$ 536	
1.5% (1.0%) 3B5	$\beta\beta + \gamma_{(B1)}$ 671 - 1405	$\gamma_{(B2)}$ 586	$\gamma_{(B3)}$ 536	
0.8% (0.6%) 4B0	$\beta\beta$ 0 - 734	$\gamma_{(B1)}$ 671	$\gamma_{(B2)}$ 586	$\gamma_{(B3)}$ 536

Excited states analysis

Selection cut definition

- The ROI for each signature is defined in an ordered energy space
- Selection cuts based on Monte Carlo (MC) simulations of the CUORE background
- Analytical description of the background based on simulations



Excited states analysis

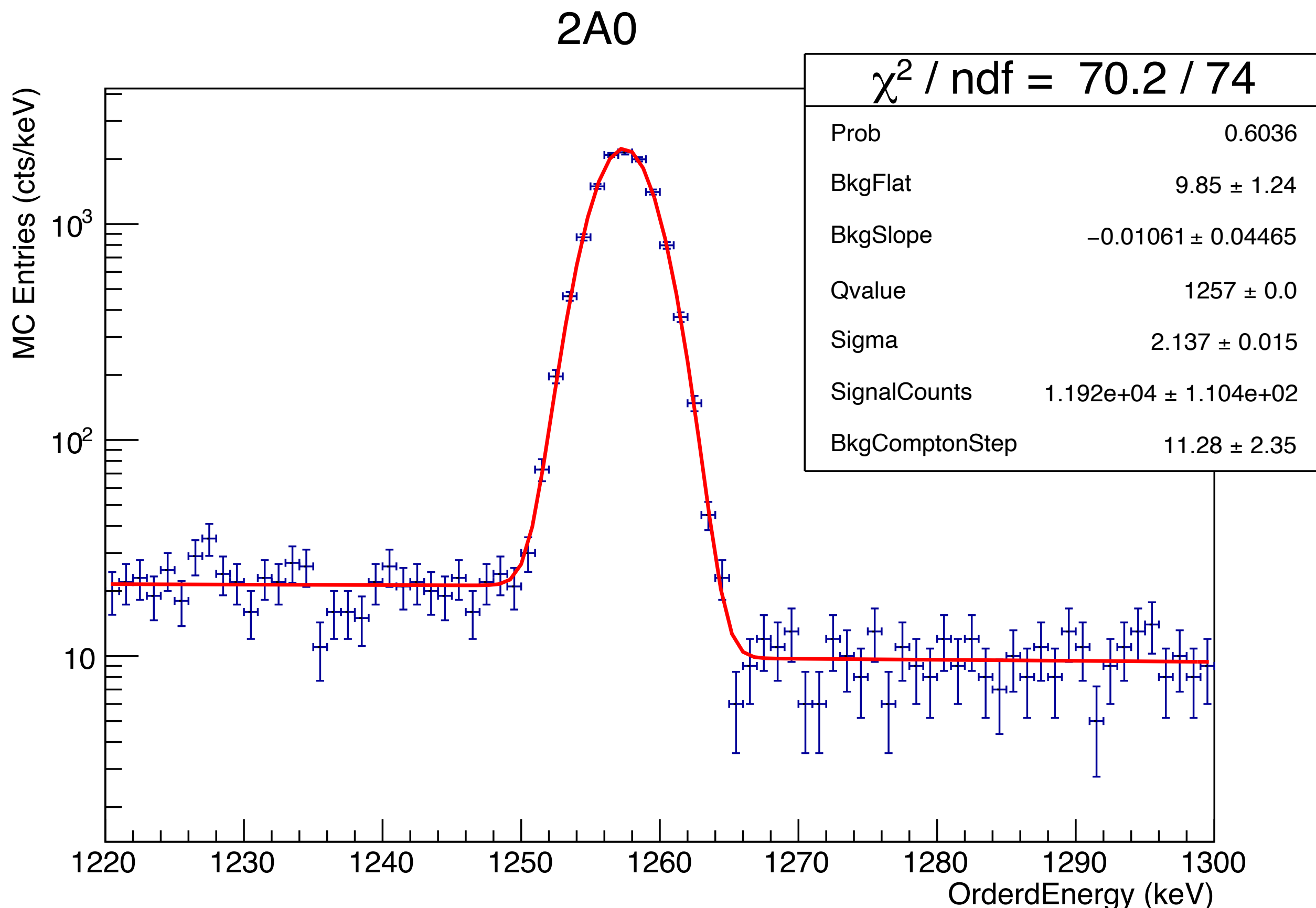
Ranking experimental signatures

0νββ				
Scenario	Multiplicity	Score	Cut	Selection
2A0 - 2B1	2	39%	<u>1247 keV < E_{min} < 1280 keV</u> 1247 keV < E _{max} < 1280 keV	E _{min} = γ(1257) E _{max} = ββ(734) + γ(536)
2A2 - 2B3	2	25%	<u>523 keV < E_{min} < 573 keV</u> 1981 keV < E _{max} < 2001 keV	E _{min} = γ(536) E _{max} = ββ(734) + γ(1257)
3A0	3	20%	526 keV < E _{min} < 546 keV <u>700 keV < E_{med} < 760 keV</u> 1247 keV < E _{max} < 1267 keV	E _{min} = γ(536) E _{med} = ββ(734) E _{max} = γ(1257)
2νββ				
Scenario	Multiplicity	Score	Cut	Selection
2A0 - 2B1	2	40%	620 keV < E _{min} < 1150 keV <u>1220 keV < E_{max} < 1300 keV</u>	E _{min} = ββ(0-734) + γ(536) E _{max} = γ(1257)
2A2 - 2B3	2	22%	<u>523 keV < E_{min} < 573 keV</u> 1360 keV < E _{max} < 1990 keV	E _{min} = γ(536) E _{max} = ββ(0-734) + γ(1257)
3A0	3	26%	400 keV < E _{min} < 523 keV <u>523 keV < E_{med} < 573 keV</u> 1779 keV < E _{med} + E _{max} < 1807 keV	E _{min} = ββ(0-734) E _{med} = γ(536) E _{max} = γ(1257)

- Blind selections
(defined on MC simulations)
in ordered energy space
- Expected background
shape: flat or linear
- No background peaks
expected

Excited states analysis

Containment efficiency



Once the selection cuts are fixed, the efficiency is obtained from a fit to Monte Carlo simulations of signal events

Excited states analysis

Model

$$\log \mathcal{L}_{s,ds}(\vec{E} | \vec{\theta}, H_{S+B}) = -(\lambda_{s,ds}^{(S)} + \lambda_{s,ds}^{(B)}) + \sum_{ev \in (s,ds)} \log \left[\lambda_{s,ds}^{(S)} \frac{M\Delta t_{ch}}{M\Delta t_{ds}} pdf^{(S)}(\vec{E}) + \lambda_{s,ds}^{(B)} \frac{M\Delta t_{ch}}{M\Delta t_{ds}} pdf^{(B)}(\vec{E}) \right]$$

- Bayesian Analysis (BAT)
- Likelihood model: linear background, peak for $\beta\beta/\gamma$
- Unbinned fit on physical range (non-negative rate), uniform prior on Γ
- Systematics addressed repeating fit with additional nuisance parameters

$$\epsilon_s = \left[\sum_p BR_p \cdot \frac{[N_{MC}^{(sel)}]_p^{(s)}}{[N_{MC}^{(tot)}]_p} \right] \epsilon_{cut}^M \epsilon_{acc}$$

leading efficiency term

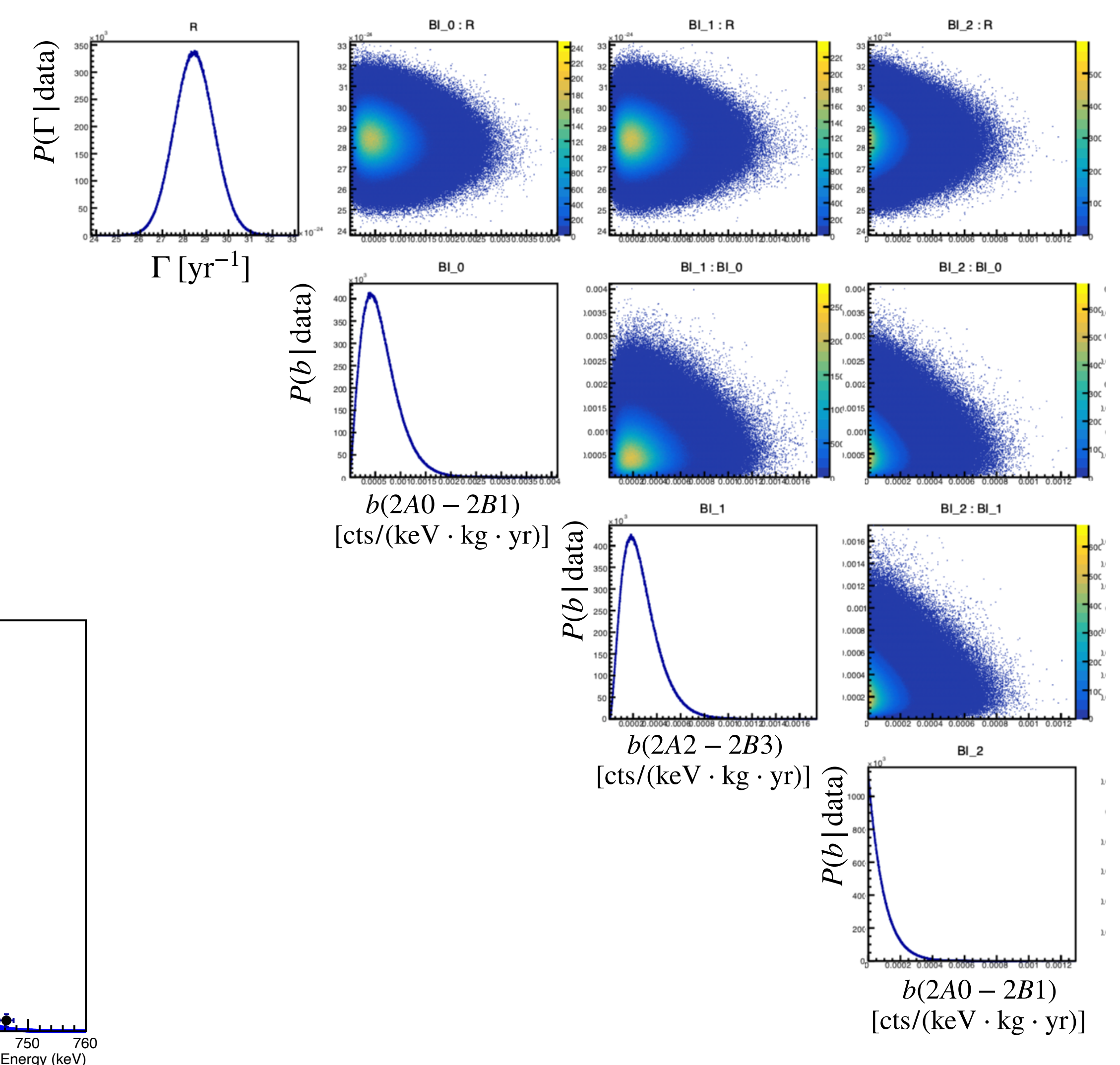
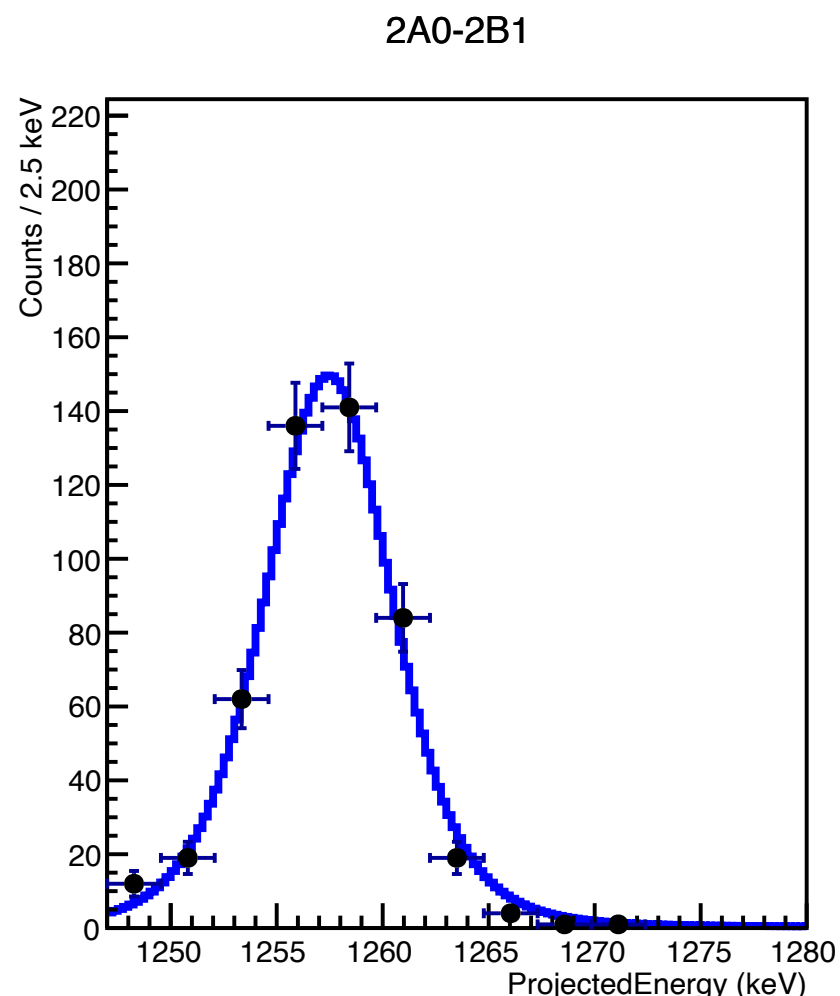
Process	Containment	Cut	Accidentals	Total
$0\nu\beta\beta$	10.0%	88.7%	98.7%	8.7%
$2\nu\beta\beta$	6.8%			5.9%

Effective efficiencies
 containment summed over signatures
 other components exposure averaged

Excited states analysis

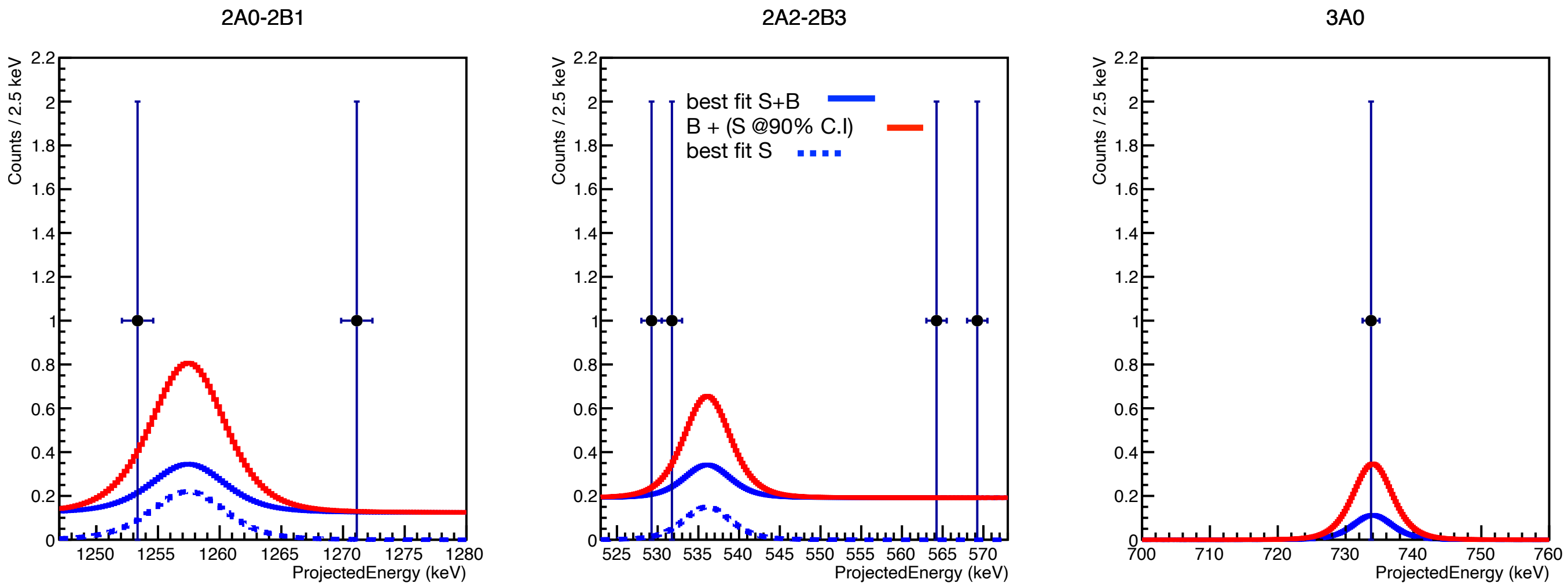
Blinded fit ($0\nu\beta\beta$)

- Monte Carlo signal events injected into physics data
- Background shape validation
- Unbiased background estimation
- Allows a preliminary sensitivity computation

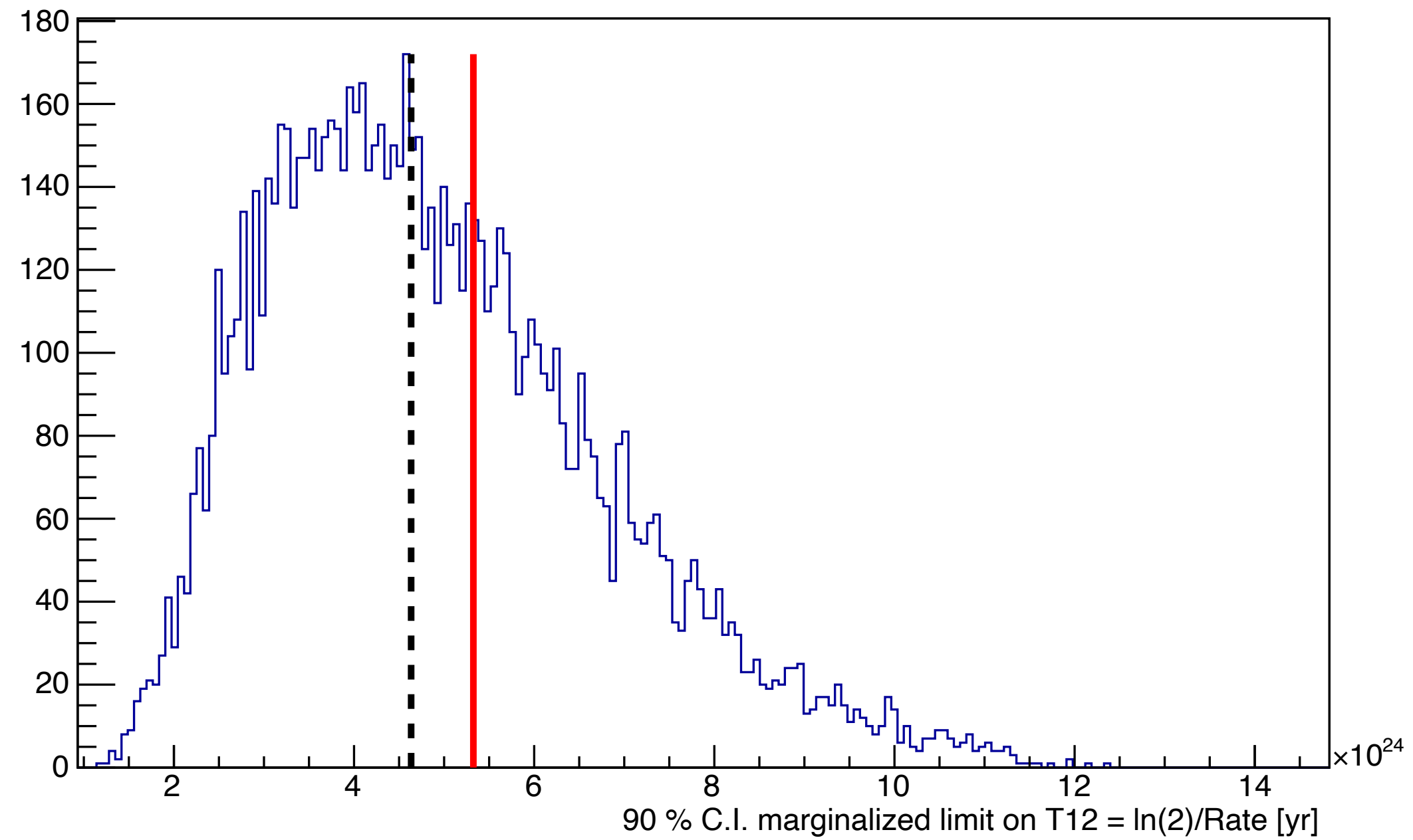


Excited states analysis

$0\nu\beta\beta$ unblinded fit and sensitivity



Expected limit setting sensitivity - Median: 4.63e+24 [yr] MAD: 1.25e+24 [yr]



Marg. Post.	Mean	St. Dev.	Units
Rate	6.37	4.85	10^{-26} 1/yr
b (2A0-2B1)	2.15	1.38	10^{-4} cts/(keV kg yr)
b (2A2-2B3)	2.56	1.20	10^{-4} cts/(keV kg yr)
b (3A0)	5.67	5.42	10^{-5} cts/(keV kg yr)

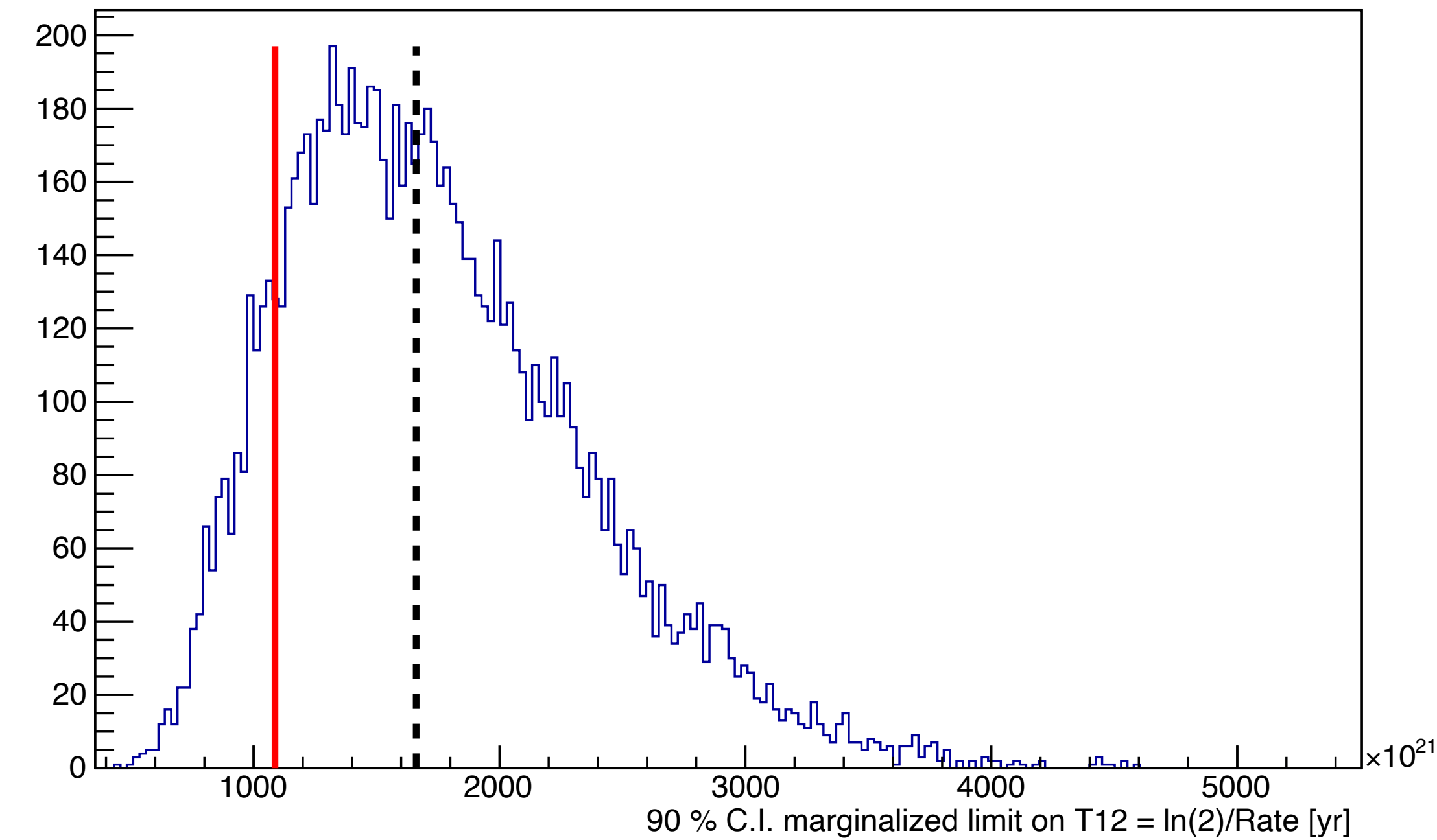
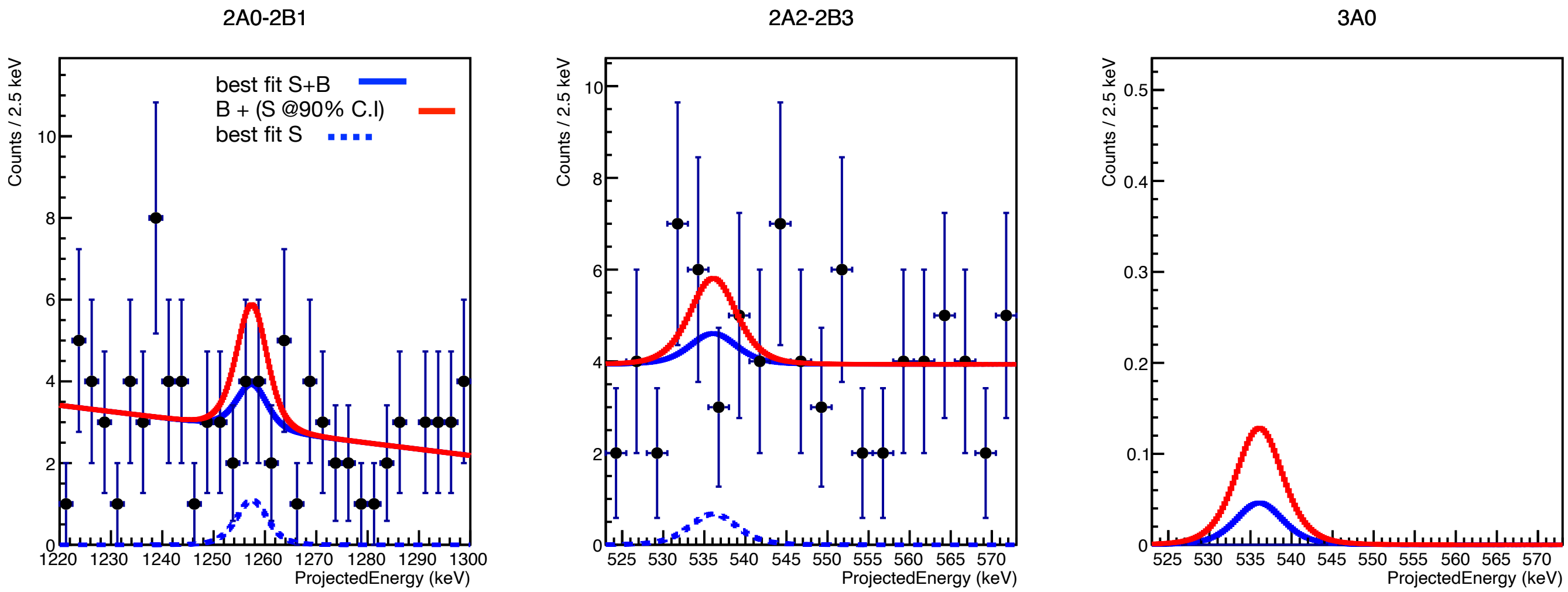
$$T_{1/2}^{0\nu} > 5.4 \times 10^{24} \text{ yr (90 \% C . I.)}$$

systematics not included

Excited states analysis

$2\nu\beta\beta$ unblinded fit and sensitivity

Expected limit setting sensitivity - Median: 1.66e+24 [yr] MAD: 3.99e+23 [yr]



Marg. Post.	Mean	St. Dev.	Units
Rate	3.33	2.18	10^{-25} 1/yr
b (2A0-2B1)	3.01	0.33	10^{-3} cts/(keV kg yr)
b (2A2-2B3)	4.23	0.49	10^{-3} cts/(keV kg yr)
b (3A0)	5.37	5.36	10^{-5} cts/(keV kg yr)
slope (3A0)	-5.17	4.23	10^{-3} 1/keV

$$T_{1/2}^{2\nu} > 1.1 \times 10^{24} \text{ yr (90 \% C . I.)}$$

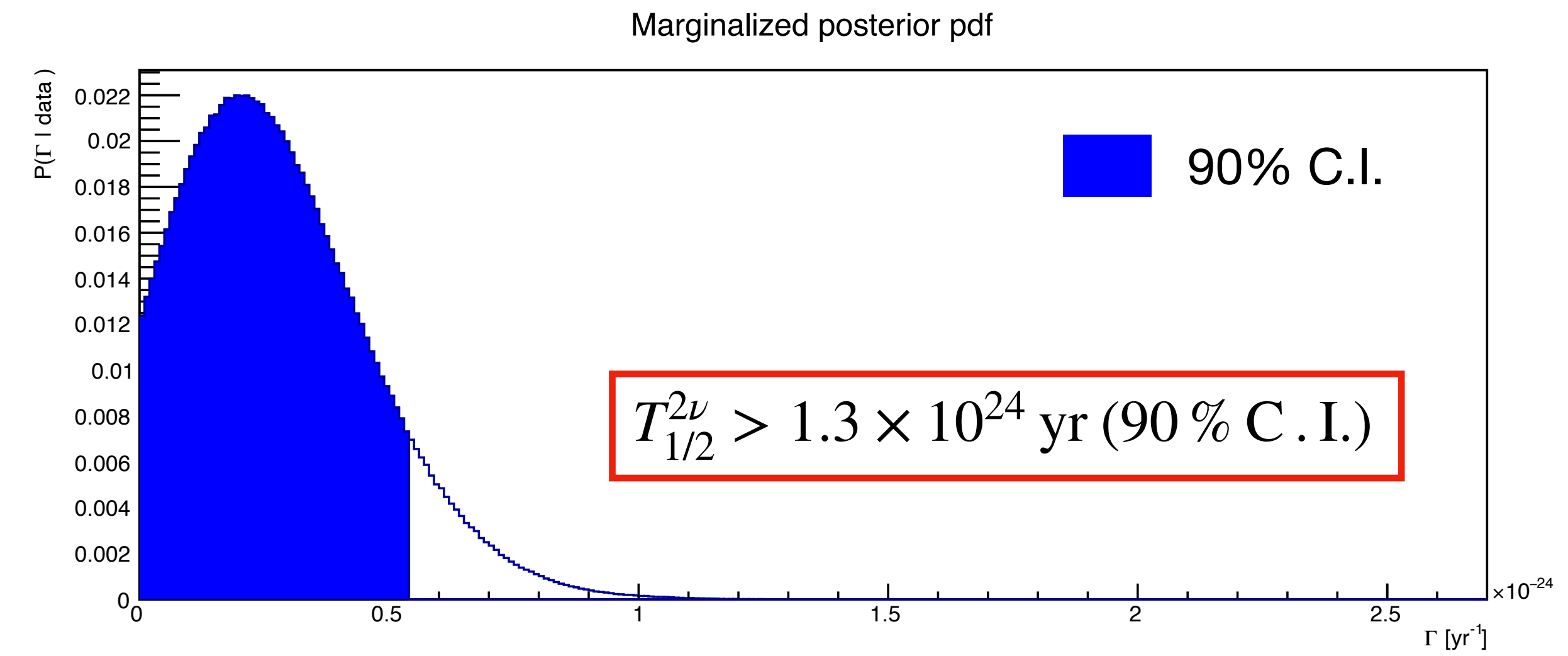
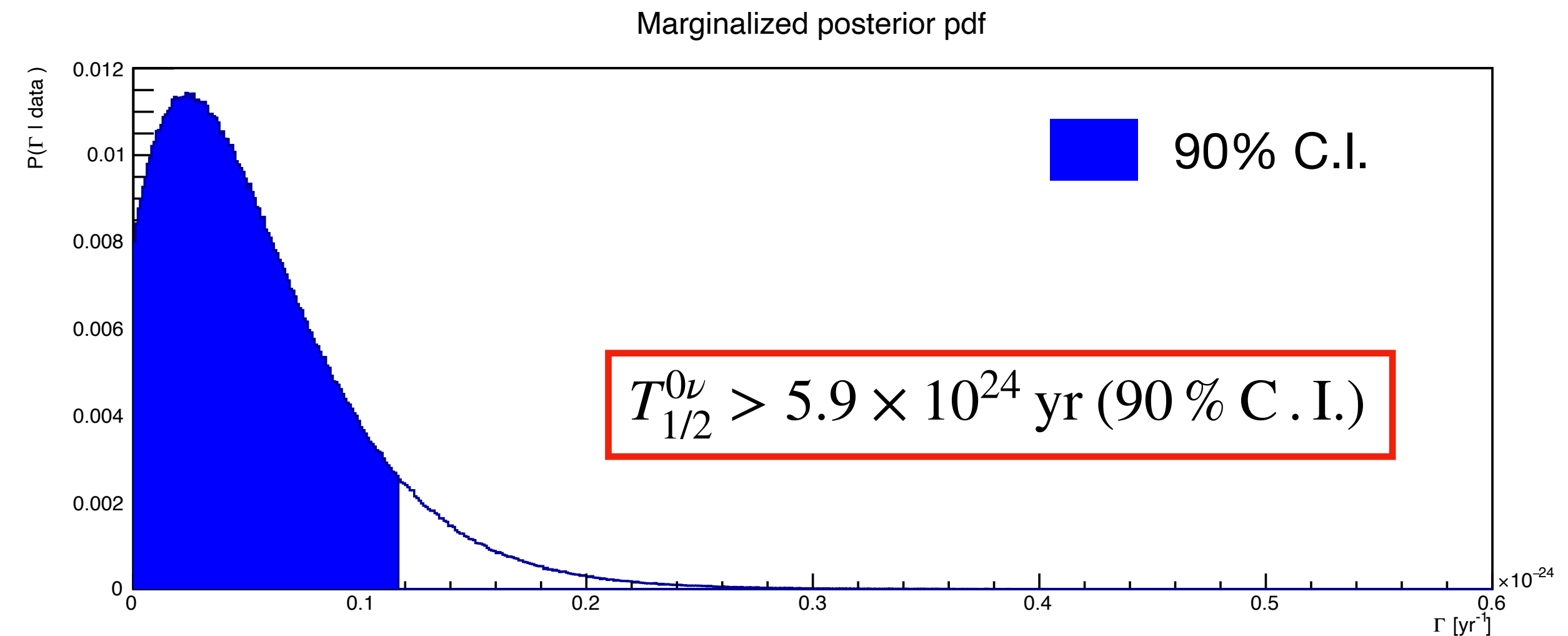
systematics not included

Excited states analysis

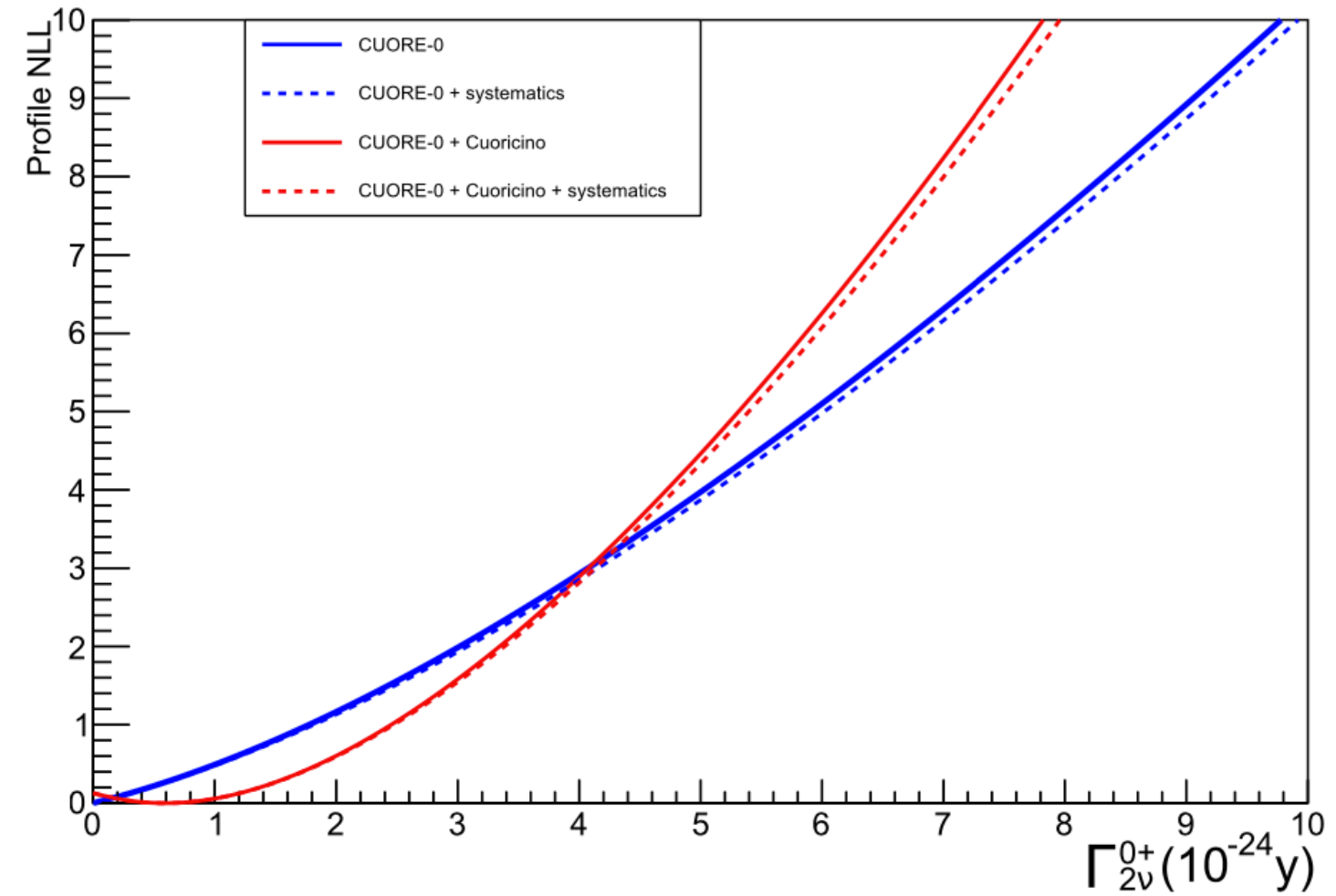
Systematics

Nuisance Parameter	Prior	$0\nu\beta\beta$ $\Delta T_{1/2}^{90}$	$2\nu\beta\beta$ $\Delta T_{1/2}^{90}$
Detector response	multivariate	10.1%	17.6%
Cut efficiency	gaussian	-0.1%	< 0.1%
PSA efficiency	uniform	-0.7%	-0.2%
Accidental coincidences	gaussian	-0.4%	0.1%
Containment efficiency	gaussian	-0.6%	-0.4%
Isotopic abundance	gaussian	-0.1%	-0.2%
Combined	multivariate	10.1%	17.2%

[G. Fantini *et al.*, paper in preparation]



Excited states analysis



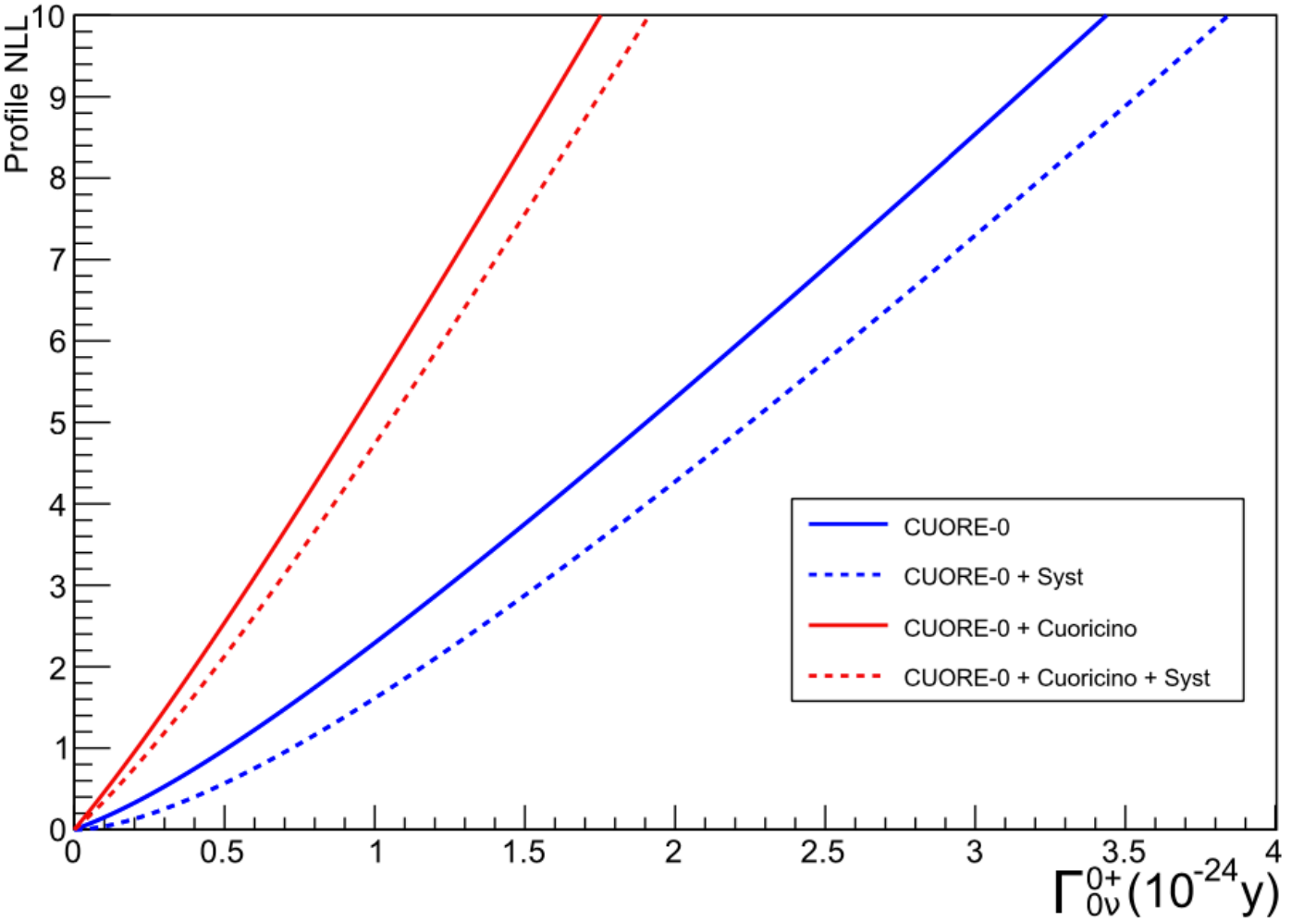
$T_{1/2}^{2\nu} > 2.5 \times 10^{23}$ yr, 90 % C . L .

$T_{1/2}^{2\nu} > 1.3 \times 10^{24}$ yr (90 % C . I.)

$T_{1/2}^{2\nu} = (7.2 - 16) \times 10^{24}$ yr QRPA

$T_{1/2}^{2\nu} = 2.2 \times 10^{25}$ yr

IBM-II + experimental input



$T_{1/2}^{0\nu} > 1.4 \times 10^{24}$ yr, 90 % C . L .

$T_{1/2}^{0\nu} > 5.9 \times 10^{24}$ yr (90 % C . I.)

[C. Alduino et al., Eur. Phys. J. C 79, 795 (2019)]

This work: [G. Fantini et al., paper in preparation]

[P. Pirinen, J. Suhonen, Phys. Rev. C 91, 054309 (2015)]

[B. Lehnert, 10.1051/epjconf/20159301025]

Summary

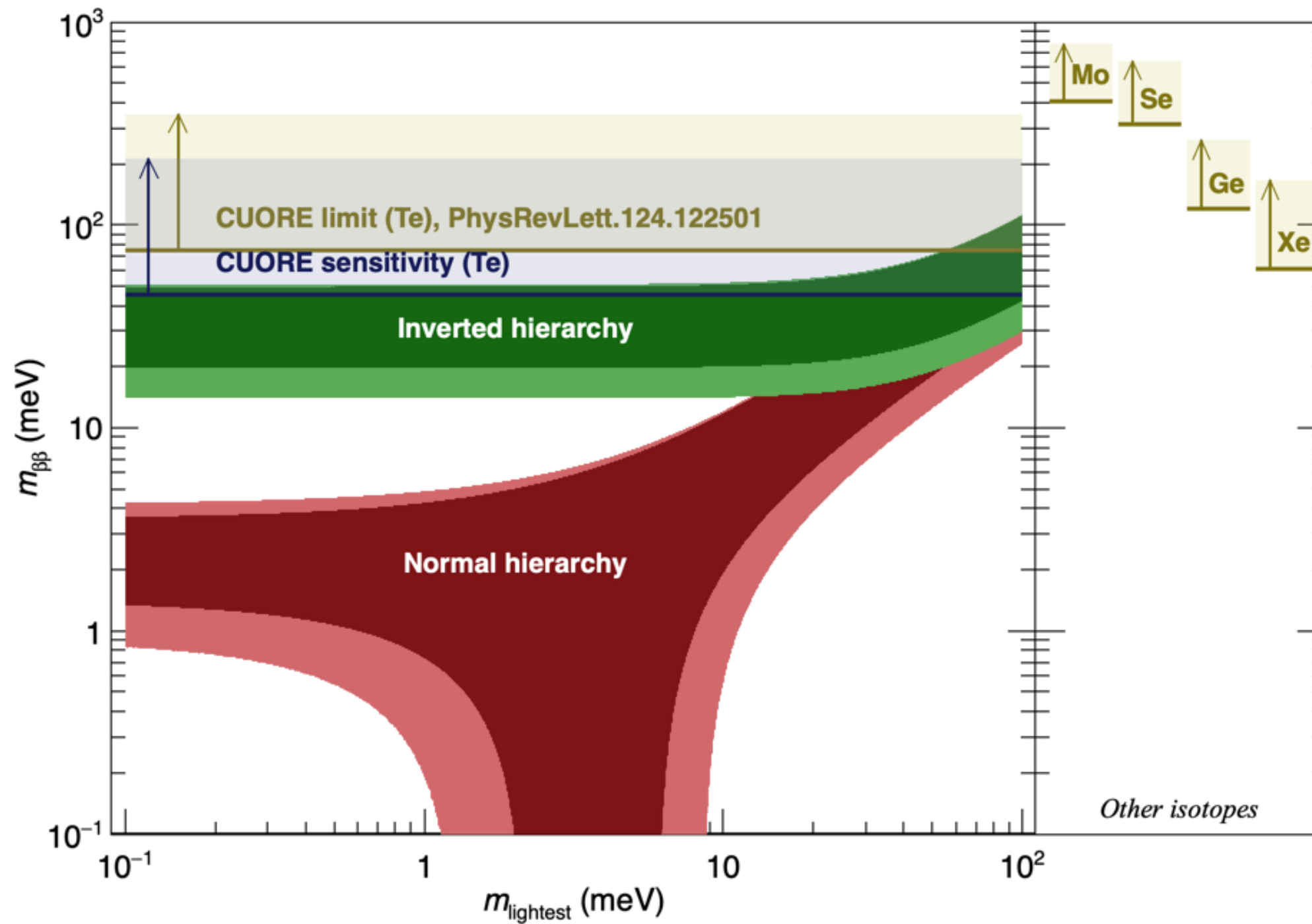
- Original contributions to the CUORE analysis
- New result on the double beta decay to excited states both in the neutrino-less and Standard Model mode
- No evidence for signal in either mode
- A factor 5 more stringent Bayesian limit with respect to the current most sensitive search (CUORE-0)

G S
S I

G S
S I

Backup

Effective Majorana Mass Interpretation



$$m_{\beta\beta} < 75 - 350 \text{ meV}$$

NMEs Used

- [57] J. Engel and J. Menéndez, *Rept. Prog. Phys.* **80**, 046301 (2017).
- [58] J. Barea, J. Kotila, and F. Iachello, *Phys. Rev.* **C91**, 034304 (2015).
- [59] F. Šimkovic *et al.*, *Phys. Rev.* **C87**, 045501 (2013).
- [60] J. Hyvärinen and J. Suhonen, *Phys. Rev.* **C91**, 024613 (2015).
- [61] J. Menéndez *et al.*, *Nucl. Phys.* **A818**, 139 (2009).
- [62] T. R. Rodriguez and G. Martinez-Pinedo, *Phys. Rev. Lett.* **105**, 252503 (2010).
- [63] N. López Vaquero, T. R. Rodríguez, and J. L. Egido, *Phys. Rev. Lett.* **111**, 142501 (2013).
- [64] J. M. Yao *et al.*, *Phys. Rev.* **C91**, 024316 (2015).
- [65] M. T. Mustonen and J. Engel, *Phys. Rev.* **C87**, 064302 (2013).
- [66] A. Neacsu and M. Horoi, *Phys. Rev.* **C91**, 024309 (2015).
- [67] A. Meroni, S. T. Petcov, and F. Simkovic, *JHEP* **02**, 025 (2013).

See-saw mechanism

$$\mathcal{L}_{D+M} = -\bar{N}_L^c M N \quad N_L = \begin{bmatrix} \nu_L \\ \nu_R^c \end{bmatrix} \quad M = \begin{bmatrix} m_L & m_D \\ m_D & m_R \end{bmatrix}$$

Assuming $SU(3)_C \times SU(2)_L \times U(1)_Y$ gauge invariance and renormalizability $m_L = 0$

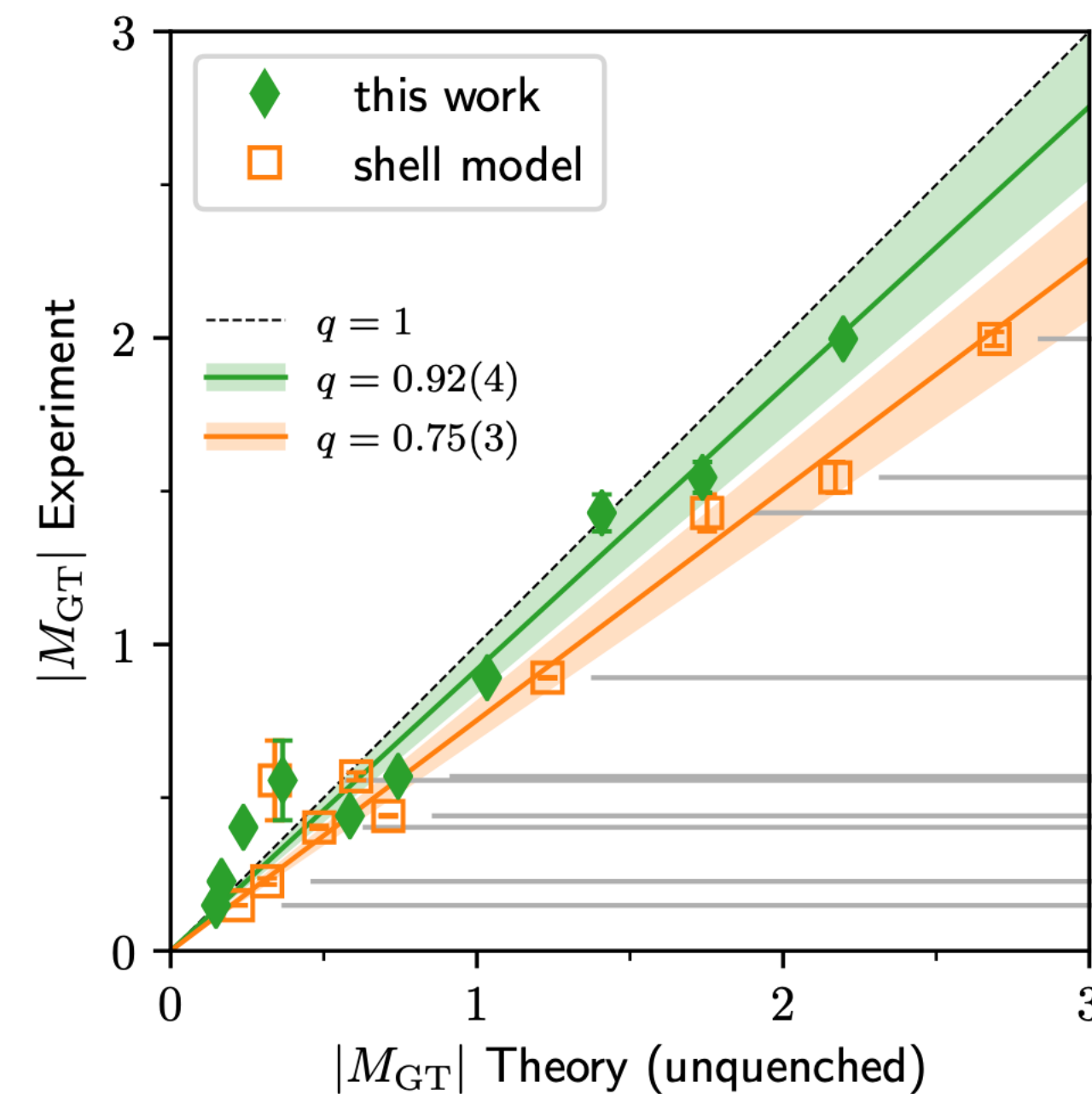
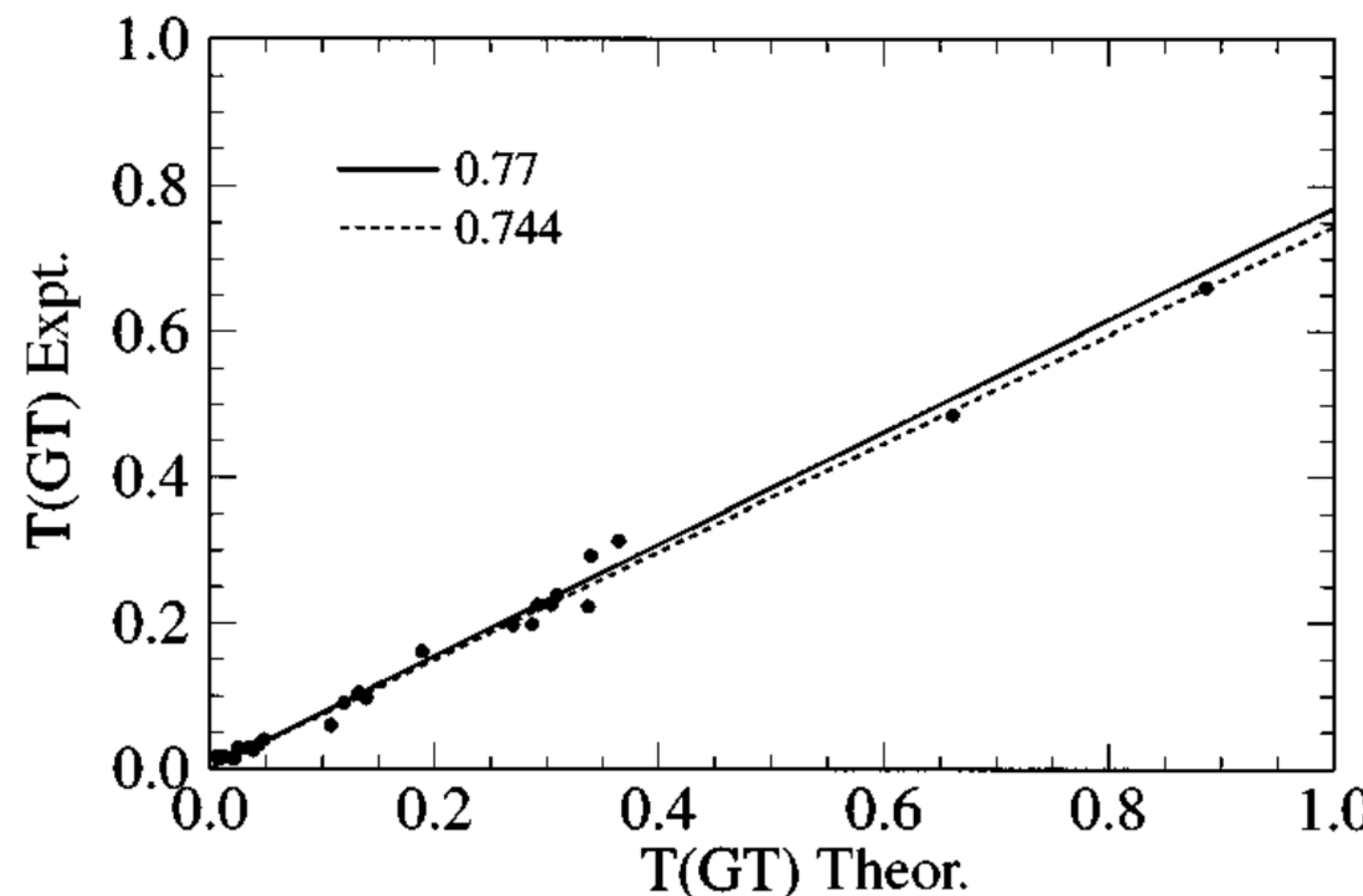
m_D of the order of the Higgs v.e.v., m_R arbitrarily large

$$m_{\pm} = \frac{m_R}{2} + \frac{m_R}{2} \sqrt{1 + \frac{4m_D^2}{m_R^2}} \xrightarrow{m_R \gg m_D} m_+ \sim m_D^2/m_R \quad m_- \sim m_R$$

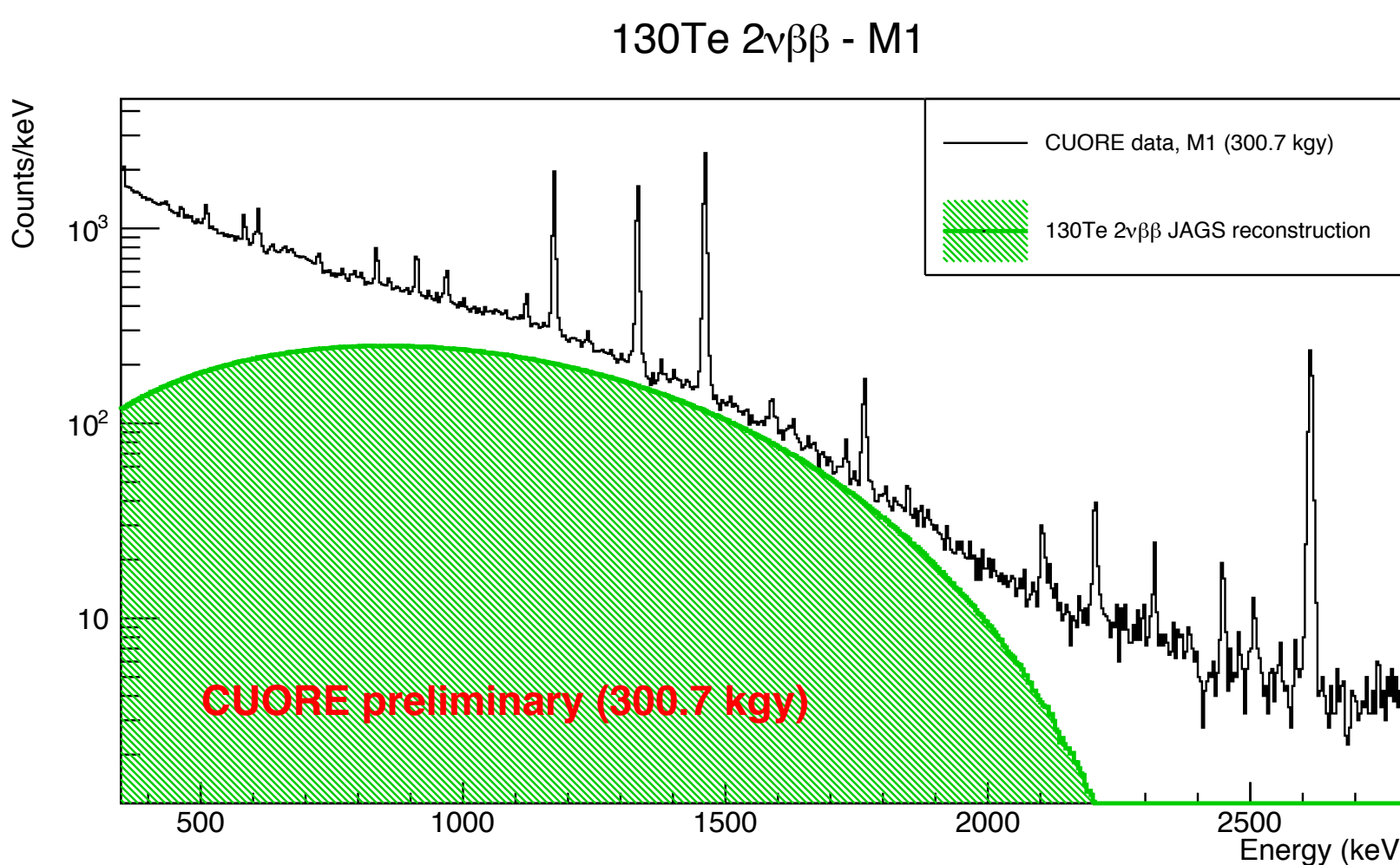
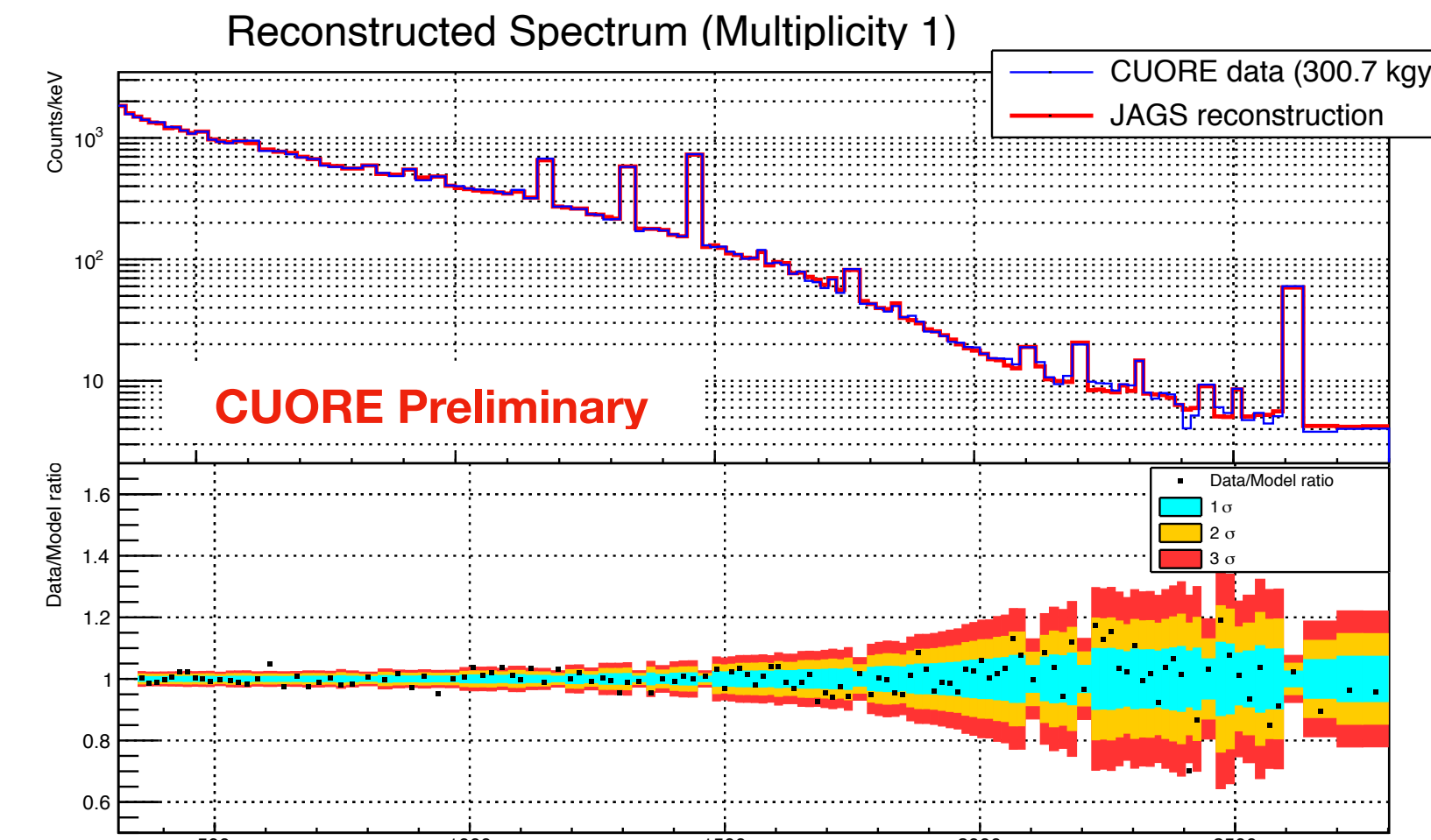
g_A quenching

- Parameterization of theory vs experiment mismatch
- Difference between the Gamow-Teller calculation and experimental results in beta-decay motivates quenching

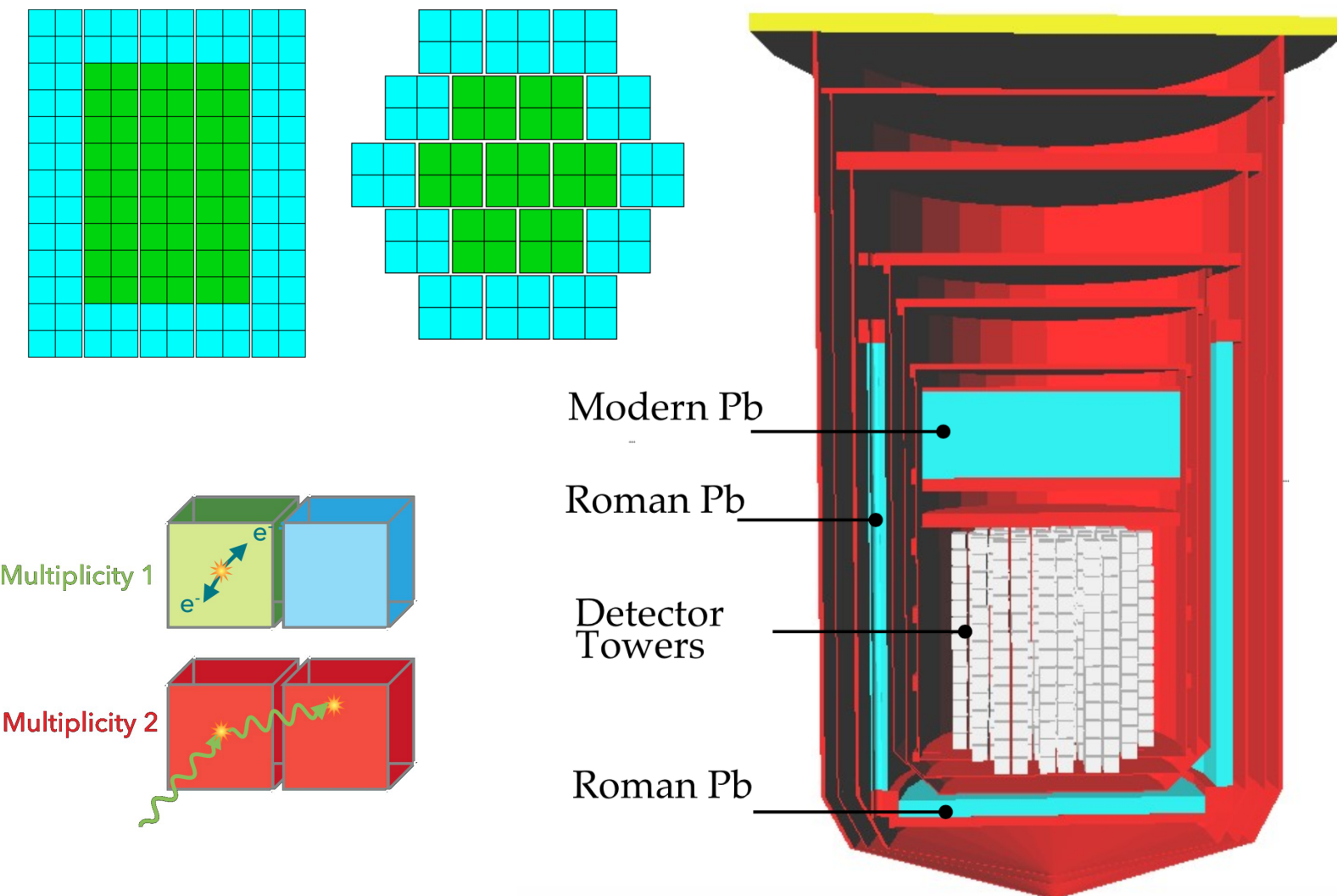
$$g_A^{eff} = q g_A$$
- Important uncertainty in neutrino-less double beta decay NME
- Ab-initio calculations including two-body / meson-exchange currents and additional nuclear correlations do not need any “quenching”



Background model



$$T_{1/2}^{2\nu} = [7.71^{+0.08}_{-0.06}(\text{stat.})^{+0.17}_{-0.15}(\text{syst.})] \times 10^{20} \text{ yr}$$



- GEANT4 simulation + detector response function to produce expected spectra
- 62 sources considered, Bayesian fit flat priors (except muons)
- Coincidences and self-shielding exploited to constrain source position

Baryon Asymmetry in the Universe

Sakharov Conditions

- Baryon number violation
- C-symmetry and CP symmetry violation
- Interactions out of thermal equilibrium

CP violation in the quark sector is not enough to explain the observed asymmetry

Baryogenesis via leptogenesis is a possibility

$$\eta = \frac{n_B - \bar{n}_B}{n_\gamma} \sim 10^{-10}$$

$$\frac{D_{CKM}}{T_{sph}^{12}} \sim 10^{-20} \ll \eta$$